

Spring 5-12-2018

Development of a Bacteriophage-based Portable Biosensor for the Detection of Shiga-toxin Producing Escherichia coli (STEC) Strains in Food and Environmental Matrices

Irwin A. Quintela

University of Maine Orono, irwin.quintela@maine.edu

Follow this and additional works at: <https://digitalcommons.library.umaine.edu/etd>

 Part of the [Biotechnology Commons](#), [Food Microbiology Commons](#), [Other Life Sciences Commons](#), and the [Other Nutrition Commons](#)

Recommended Citation

Quintela, Irwin A., "Development of a Bacteriophage-based Portable Biosensor for the Detection of Shiga-toxin Producing Escherichia coli (STEC) Strains in Food and Environmental Matrices" (2018). *Electronic Theses and Dissertations*. 2842.
<https://digitalcommons.library.umaine.edu/etd/2842>

This Open-Access Dissertation is brought to you for free and open access by DigitalCommons@UMaine. It has been accepted for inclusion in Electronic Theses and Dissertations by an authorized administrator of DigitalCommons@UMaine. For more information, please contact um.library.technical.services@maine.edu.

**DEVELOPMENT OF A BACTERIOPHAGE-BASED PORTABLE BIOSENSOR
FOR THE DETECTION OF SHIGA-TOXIN PRODUCING
ESCHERICHIA COLI (STEC) STRAINS IN FOOD
AND ENVIRONMENTAL MATRICES**

By

Irwin A. Quintela

B.S. University of the Philippines Los Banos, 2003

M.S. University of Maine, 2014

A DISSERTATION

Submitted in Partial Fulfillment of the

Requirements for the Degree of

Doctor of Philosophy

(in Food and Nutrition Sciences)

The Graduate School

The University of Maine

May 2018

Advisory Committee:

Vivian CH. Wu, Professor of Food Safety and Microbiology, Advisor

Benildo de los Reyes, Professor of Plant Genomics

Chih-Sheng Lin, Professor of Biological Science and Technology

Paul Millard, Associate Professor of Chemical Engineering

Jianjun Hao, Assistant Professor of Plant Pathology

© 2018 Irwin Quintela

**DEVELOPMENT OF A BACTERIOPHAGE-BASED PORTABLE BIOSENSOR
FOR THE DETECTION OF SHIGA-TOXIN PRODUCING
ESCHERICHIA COLI (STEC) STRAINS IN FOOD
AND ENVIRONMENTAL MATRICES**

By Irwin A. Quintela

Dissertation Advisor: Dr. Vivian C.H. Wu

An Abstract of the Dissertation Presented
in Partial Fulfillment of the Requirements for the
Degree of Doctor of Philosophy
(in Food and Nutrition Sciences)

May 2018

A fast and reliable on-site foodborne pathogens screening can reduce the incidence of foodborne illnesses, hospitalizations and economic loss. It can also circumvent conventional laboratory-based tests with minimal sample treatments and shorter turnaround time. Rapid detection of biological hazards has been largely dependent on immunological agents (ie antibodies). Antibodies are expensive to manufacture and experience cross-reactivity, instability with shorter shelf life. Our aim was to improve the screening process of Shiga-toxin producing *Escherichia coli* (STEC) strains in food and environmental matrices by developing a novel, inexpensive handheld bacteriophage-based amperometric biosensor that can directly detect live STEC cells.

This biosensor development began by isolating STEC-specific bacteriophages from natural environmental samples (ie cow manure and surface water) hence, constructing a comprehensive bacteriophage isolates collection targeting an array of significant STEC serogroups. As an alternative to antibodies, purified bacteriophages could be easily and

inexpensively propagated in a standard laboratory. Isolated bacteriophages were morphologically characterized while its physiologic behavior and specific host interactions were also investigated. The results indicated that majority of STEC-specific bacteriophages belong to Myoviridae and Siphoviridae families. Suitable bacteriophages for biosensor purposes were selected on the basis of the presence of head and tail and absence of virulence genes (*stx1/stx2*).

Chemical modification via site-specific biotinylation of bacteriophage heads was performed prior to its biosensor incorporation. The results showed that biotinylation of bacteriophages did not reduce biofunctionality. Representative STEC O26, O157, and O179-specific biotinylated bacteriophages were immobilized onto the surface of streptavidin-modified screen-printed carbon electrodes (SPCE) to capture their target STEC cells. After STEC cells were bound to the capture elements, another set of biotinylated bacteriophages labeled with streptavidin-horseradish peroxidase were added forming stable binding complexes which were then subjected to amperometric detection.

The sandwich-type bacteriophage-based detection approach allowed live STEC cells rapid detection in microvolume samples (50 μ L) via amperometric readouts (Δ current) between target and non-target bacteria in pure culture setup and complex matrices. With its simplicity and reliability, this technology can immensely assist the food industry and regulatory inspectors to efficiently maintain food safety in a fraction of the cost of traditional method.

ACKNOWLEDGEMENTS

I am thankful to my advisor, Dr. Vivian Wu, for her trust, technical guidance and untiring support. Her encouragement is truly appreciated especially during the most challenging part of the conduct of this project.

To my committee members who are experts in their own fields, Dr. Benildo de los Reyes, Dr. Chih-Sheng Lin, Dr. Paul Millard and Dr. Jay Hao, I am sincerely grateful for their feedback, flexibility and understanding.

I would also like to acknowledge the funding sources, USDA NIFA Grant Award #2015-68003-23410 and the School of Food and Agriculture Teaching Assistantship. Dr. Pina Fratamico of USDA provided the bacterial strains and the Produce Safety and Microbiology (PSM) Unit of the USDA-WRRC-ARS shared their environmental water samples for this project.

To the Pathogenic Microbiology Laboratory staff of the University of Maine, Bingbing Li and Shravani Tadepalli, your assistance in one way or another has made the initial part of this project easier and less stressful. I am also thankful to Dr. Gary Anderson, Don Valentine and Rong Zhang for their patience and contribution during the isolation of the bacteriophages.

To Kimberly Nguyen, Alexandra Salvador, Bhargavi Rane, Margo Lockwood, Dr. Alison Lacombe and Dr. Yen-Te Liao, their assistance during the transition, meaningful conversations and feedback are also appreciated.

To my family in the Philippines, you are my inspiration since the beginning.

TABLE OF CONTENTS

ACKNOWLEDGEMENTS	iii
LIST OF TABLES	ix
LIST OF FIGURES	xi
Chapter	
1. INTRODUCTION	1
2. LITERATURE REVIEW	5
2.1. Shiga-toxin Producing <i>Escherichia coli</i> (STEC)	5
2.2. Foodborne Pathogen Detection.....	9
2.2.1. Conventional Methods of Detecting Foodborne Pathogen	9
2.2.2. Rapid and Portable Screening and Detection Methods.	10
2.2.2.1. Current Biosensors in Foodborne Pathogen Screening and Detection.....	11
2.2.2.1.1. Portable Biosensors Classified Based on Bioreceptors or Capture Elements	12
2.2.2.1.1.1. Antibodies-based Biosensors	19
2.2.2.1.1.2. Aptamer-based Biosensors.....	23
2.2.2.1.1.3. Amino Acid-based Biosensors.....	25
2.2.2.1.1.4. Antimicrobial Peptides-based Biosensors.....	29
2.2.2.1.1.5. Bacteriophage-based Biosensors	31
2.2.2.1.1.6. Cell-based Biosensors	39
2.2.2.1.1.7. Biomimetic-based Biosensors.....	40

2.2.2.1.2. Other Types of Portable Biosensors and New	
Trends in On-Site Pathogen Screening	41
2.2.2.1.2.1. Lab-on-chip	41
2.2.2.1.2.2. Portable Phone-based Biosensors	43
3. ISOLATION AND CHARACTERIZATION OF STEC-SPECIFIC	
BACTERIOPHAGES FROM THE NATURAL ENVIRONMENT	47
3.1. Introduction	47
3.2. Materials and Methods	49
3.2.1. Bacterial Strains and Growth Conditions	49
3.2.2. Isolation, Purification and Enrichment of Bacteriophages	
from Environmental Samples	50
3.2.3. Host Range, Lytic Capability and Virulence Genes	51
3.2.4. Potential Biocontrol Capability of Isolated Bacteriophages	53
3.2.5. Transmission Electron Microscopy	54
3.3. Results	55
3.3.1. Isolated STEC Bacteriophages, Host Range and Susceptibility	55
3.3.2. Biocontrol Potential of Isolated Bacteriophages Against STEC Strains	56
3.3.3. Morphological Features of the Isolated Bacteriophages	59
3.4. Discussion	63
3.5. Conclusions	67

4. DEVELOPMENT AND OPTIMIZATION OF SHIGA TOXIN-PRODUCING <i>ESCHERICHIA COLI</i> (STEC)-SPECIFIC BACTERIOPHAGE-BASED AMPEROMETRIC BIOSENSOR.....	69
4.1. Introduction.....	69
4.2. Materials and Methods.....	71
4.2.1. Reagents and Apparatus	71
4.2.2. STEC Strains and Bacteriophages.....	73
4.2.3. Chemical Modification of Bacteriophages	74
4.2.4. Electrochemical Behavior and Characterization of SPCEs.....	75
4.2.5. Surface Modification and Biofunctionalization of SPCEs.....	76
4.2.6. Development of Bacteriophage-based Detection Elements and Substrate	77
4.2.7. Amperometric Tests and Limit of Detection (LOD).....	78
4.2.8. Determination and Quantification of Sources of Background Noise	79
4.2.9. Statistical Analysis	80
4.3. Results.....	82
4.3.1. Chemical Modification of Bacteriophages	82
4.3.2. Electrochemical Characterization of SPCEs	85
4.3.3. Surface Modification and Biofunctionalization SPCEs	87
4.3.4. Viability and Stability of Capture and Detection Elements	90
4.3.5. Determination of Background Noise.....	91
4.3.6. Amperometric Tests	93
4.4. Discussion	98
4.5. Conclusions.....	106

5. APPLICATION OF SHIGA TOXIN-PRODUCING <i>ESCHERICHIA COLI</i> (STEC)	
BACTERIOPHAGE-BASED BIOSENSOR ON FOOD AND ENVIRONMENTAL	
SAMPLES	107
5.1. Introduction.....	107
5.2. Materials and Methods.....	110
5.2.1. Reagents and Apparatus	110
5.2.2. Bacterial Strains and Biotinylated STEC-bacteriophages.....	111
5.2.3. Fabrication of the Bacteriophage-based Biosensor	112
5.2.4. Food Samples	113
5.2.5. Environmental Water Samples	114
5.2.6. Amperometric Test.....	117
5.2.7. Statistical Analysis	118
5.3. Results.....	118
5.3.1. Food Matrices- Fresh Ground Beef.....	118
5.3.2. Food Matrices-Pasteurized Apple Juice	123
5.3.3. Environmental Water Samples	128
5.4. Discussion	134
5.5. Conclusions.....	137

6. COST ANALYSIS OF THE NEWLY-DEVELOPED BACTERIOPHAGE- BASED STEC BIOSENSOR	138
6.1. Introduction.....	138
6.2. Methodology	140
6.2.1. Material Cost	140
6.2.2. Basic Process Cost.....	140
6.2.3. Manufacturing Cost.....	141
6.3. Results.....	142
6.4. Discussion.....	143
6.5. Conclusion	145
7. CONCLUSIONS.....	146
REFERENCES	149
APPENDIX. Optimization, cost calculation and analysis of the bacteriophage-based STEC biosensor	167
BIOGRAPHY OF THE AUTHOR.....	176

LIST OF TABLES

Table 2.1.	Comparisons of commercially-available products for STEC detection.....	7
Table 2.2.	Biosensors classified according to the types of its capture elements (CEs)	13
Table 3.1.	Primers for <i>stx</i> genes	53
Table 3.2.	Primers and probes for RT-PCR	54
Table 3.3.	Isolation of STEC bacteriophages from environmental cow manure samples.....	56
Table 3.4.	The specificity and potential biocontrol capability of isolated bacteriophages on its STEC hosts from cow manure samples.....	58
Table 5.1.	STEC-specific bacteriophages used in this study and their host bacteria	112
Table 5.2.	Primers for <i>stx</i> genes	115
Table 5.3.	List of environmental water samples from Pescadero, CA.....	115
Table 5.4.	Reference signal threshold [Δ current (μ A)] optimized from pure culture study	128
Table 6.1.	General rules for computing fixed costs	141
Table 6.2.	Estimated material cost incurred during the development cycle	142
Table 6.3.	Immunoassay-based commercial products for STEC serogroup (O157) detection	144
Table 7.1.	Calculation for estimating Material Cost (C_{mt}) (all values are in USD ₂₀₁₈).....	174

Table 7.2.	Calculation for estimating Total Process Cost (P_c) (all values are in USD ₂₀₁₈)	175
Table 7.3.	Calculation for estimating Manufacturing Cost (M_t) (all values are in USD ₂₀₁₈)	175
Table 7.4.	Calculation for estimating the cost of functionalized-screen printed carbon electrode (SPCE) (all values are in USD ₂₀₁₈).....	175

LIST OF FIGURES

Figure 1.1. Project goal and primary objectives.....	4
Figure 2.1. Schematic presentation of DNA aptamer selection by cell-SELEX technique.....	24
Figure 2.2. Schematic representation of microcontact imprinting	27
Figure 2.3 Schematic representation of self-assembly technique for SIP synthesis	28
Figure 2.4. Representation of AMP (Magainin I) immobilization on beads.....	30
Figure 2.5. Representation of PEI-functionalized CNT on electrode surface.....	33
Figure 2.6. Representation of T4-bacteriophage-based biosensors with electrochemical impedance spectroscopy (EIS) and loop-mediated isothermal amplification (LAMP).....	34
Figure 2.7. An example of a lab-on-chip (microfluidics).....	41
Figure 2.8. Schematic representation of a smartphone-based biosensor with <i>S. aureus</i> aptamer (Sap)-conjugated FMNPs.....	44
Figure 2.9. Schematic representation of the smartphone-based device for STEC O157:H7 detection.....	46
Figure 3.1. TEM images of various STEC-specific bacteriophages isolated from cow manure samples	60
Figure 3.2. The ultrastructures of STEC O121:H19 SJ18 bacteriophage from cow manure samples	61
Figure 3.3. The ultrastructures of STEC O103 bacteriophage isolated from cow manure samples	62
Figure 3.4. The ultrastructures of STEC O179 bacteriophage from water samples.....	62

Figure 4.1. Screen-printed carbon electrode (SPCE)	74
Figure 4.2. The newly-developed STEC-specific bacteriophage-based electrochemical biosensor	81
Figure 4.3 Biotinylation of O179 bacteriophage	84
Figure 4.4. Cyclic voltammetry of 0.5 mM K ₃ [Fe(CN) ₆] in various supporting electrolytes conducted on unmodified SPCE.....	86
Figure 4.5. Bar graph representation of the electrochemical characterization of unmodified SPCEs.....	88
Figure 4.6. Cyclic voltammetry (CV) of chemically-modified SPCE.	88
Figure 4.7. Cyclic voltammetry of 0.5 mM K ₃ [Fe(CN) ₆] in 1X PBS on both unmodified and modified SPCEs.....	89
Figure 4.8. Agar diffusion test of bacteriophage-modified SPCE.....	90
Figure 4.9. TEM image of detection element solution.	91
Figure 4.10. Determination of background noise.	92
Figure 4.11. Amperometric test of STEC O26.....	95
Figure 4.12. Amperometric test of STEC O179.....	96
Figure 4.13. Amperometric test of STEC O157	97
Figure 5.1. Location of the sampling sites where water samples were collected.....	116
Figure 5.2. Map of the specific sampling sites (starred) where water and sediment were collected.....	116
Figure 5.3. Amperometric test of artificially-inoculated fresh ground beef (STEC O26)	120

Figure 5.4. Amperometric test of artificially-inoculated fresh ground beef (STEC O157)	121
Figure 5.5. Amperometric test of artificially-inoculated fresh ground beef (STEC O179)	122
Figure 5.6. Amperometric test of artificially-inoculated pasteurized apple juice (STEC O26).....	125
Figure 5.7. Amperometric test of artificially-inoculated pasteurized apple juice (STEC O157).....	126
Figure 5.8. Amperometric test of artificially-inoculated pasteurized apple juice (STEC O179).....	127
Figure 5.9. Amperometric test of environmental samples using STEC O26-specific bacteriophage biosensor	130
Figure 5.10. Amperometric test of environmental samples using STEC O157-specific bacteriophage biosensor	131
Figure 5.11. Amperometric test of environmental samples using STEC O179-specific bacteriophage biosensor	132
Figure 5.12. Gel image showing four environmental samples after conventional PCR targeting <i>stx1</i> gene	133
Figure 5.13. Gel image showing four environmental samples after conventional PCR targeting <i>stx2</i> gene	134
Figure 6. Multiplicity of infection (MOI) of STEC representative strains determined by spectrophotometric data	167

Figure 7. Gel electrophoresis from conventional PCR of STEC bacteriophage DNA targeting <i>stx1</i> and <i>stx2</i>	168
Figure 8.1. Amperometric test of STEC O26 and blocking reagent optimization using Protein-free Blocking Reagent and TBS-T20 washing buffer.....	169
Figure 8.2. Amperometric test of STEC O26 and blocking reagent optimization using Protein-free Blocking Reagent and TBS-T20 washing buffer.....	169
Figure 9.1. Amperometric test of STEC O26 and blocking reagent optimization using 10% BSA and TBS-T20 washing buffer.....	170
Figure 9.2. Response current of STEC O26 with 10% BSA and TBS-T20 washing buffer.....	170
Figure 10.1. Amperometric test of STEC O26 and blocking reagent optimization using PEG (Polyethylene glycol) and TBS-T20 washing buffer.....	171
Figure 10.2. Response current of STEC O26 with PEG (Polyethylene glycol) and TBS-T20 washing buffer.....	171
Figure 11.1. Amperometric test of STEC O26 and blocking reagent optimization using 30% Casein and TBS-T20 washing buffer.....	172
Figure 11.2. Response current of STEC O26 with 30% Casein and TBS-T20 washing buffer.....	172
Figure 12.1. Amperometric test of STEC O179 and blocking reagent optimization using 30% Casein and TBS-T20 washing buffer.....	173
Figure 12.2. Response current of STEC O179 with 30% Casein and TBS-T20 washing buffer.....	173

CHAPTER 1

INTRODUCTION

Rapid and accurate screening of foodborne pathogens using highly selective and easy-to-operate tools is one of the most efficient approaches to reduce or prevent the incidence of illnesses and hospitalizations caused by infection of significant foodborne pathogens (ie. Shiga-toxin producing *Escherichia coli* or STEC) through contaminated food products. The ability to precisely screen pathogens in foods or food processing sites is important to maintaining safe food commodities (Bhunja, Kim et al. 2014).

Traditional foodborne pathogens detection methods employ time consuming procedures which take 5-7 days for confirmed positive results (Gracias and McKillip 2004, Jasson, Jacxsens et al. 2010). Laboratory-based assays require highly-trained staff and are often complicated and costly. Thus, automated, easy-to-operate, and on-site detection methods that can circumvent the limitations of conventional laboratory-based culture tests are needed. On-site and portable biosensors provide food processors and food safety authorities the capabilities to quickly screen and detect foodborne pathogens and potential contaminants with shorter turn-around time (Pérez-López and Merkoçi 2011, Wiedmann, Wang et al. 2014).

Antibodies are routinely used as recognition elements in the diagnostics and foodborne pathogen biosensing applications. Monoclonal and polyclonal antibodies provide selectivity and specificity when they are integrated onto the systems as bioreceptors. However, in terms of manufacturing costs, monoclonal antibodies are expensive to produce rendering it to be impractical for routine testing. On the other hand, polyclonal antibodies are less expensive but can experience high batch-to-batch variability. In addition, its heterogeneity towards other species or strains can contribute to the background signal. Antibodies are also prone to

environmental instabilities and degradation when exposed to high temperatures, extreme pHs and contaminants. These drawbacks ultimately influence antibodies-based biosensors to achieve relatively higher detection limits. Therefore, there is a need to explore other materials as alternatives to antibodies which can be efficiently utilized as bioreceptors or biorecognition elements and coupled it onto various detection platforms such as screen-printed electrodes (SPEs) for rapid screening of foodborne pathogens in various matrices.

Shiga-toxin producing *Escherichia coli* (STEC) serogroups are normally found in the gastrointestinal tract of cattle and other ruminants. STEC can also co-habitate bacteriophages as part of its microbiota. Bacteriophages are small viruses that are obligate parasites of bacteria which can be utilized as biosensors recognition elements due to its ability to attach and infect bacteria with high specificity via host-receptors recognition (Shabani, Zourob et al. 2008, Velusamy, Arshak et al. 2010). Bacteriophage infection cycle commences when it recognizes and binds to specific receptors displayed on bacterial cell surface. It is followed by either lytic or lysogenic cycle depending on the metabolic state of the bacterial host cells as well as the environmental conditions during the time of infection. Bacteriophages pose no direct harm or threat to humans and have changed the ways pathogens are identified. Bacteriophages host ranges can span across bacterial strains, species and genera but can also be highly specific, infecting only a single bacterial serotype, all depending on bacterial surface receptors that are uniquely identified by bacteriophages (Smartt and Ripp 2011). Their resistance to external stresses and high specificity toward its target hosts make them a superior molecular probe for the detection of pathogenic bacteria (Balasubramanian, Sorokulova et al. 2007).

The goal of this study is directed to the development of a novel bacteriophage-based detection technology for rapid screening of various STEC strains. The four primary objectives

(Figure 1) are to (1) isolate and characterize environmental STEC-specific bacteriophages from the natural environment, (2) develop and optimize STEC bacteriophages-based biosensor, (3) apply the biosensor to screen for the presence of STEC strains in food and environmental samples, and (4) conduct cost analysis and evaluate its commercial potential. The integration of bacteriophages onto antibodies-free biosensing systems as biorecognition and capture elements can allow rapid detection of significant foodborne pathogens at low-cost with high reliability that would ultimately improve the traditional screening of significant foodborne pathogens.

Development and optimization of a novel STEC-bacteriophage based electrochemical biosensor

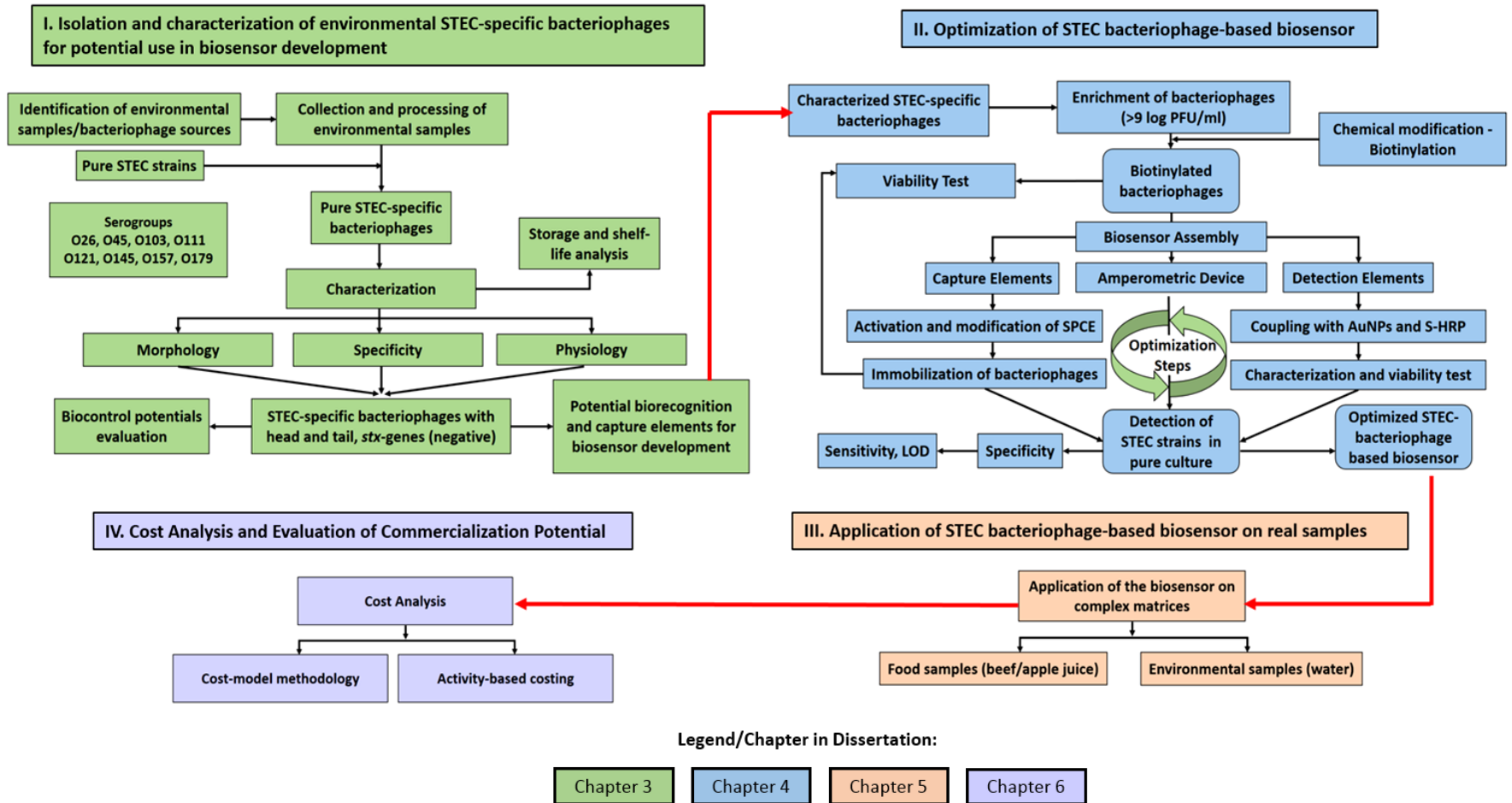


Figure 1.1. Project goal and primary objectives. The four primary objectives behind the development and optimization of the novel STEC-bacteriophage based electrochemical biosensor. (I) to isolate and characterize STEC-specific bacteriophages from the natural environment, (II) to develop and optimize bacteriophage based biosensor, (III) to apply the biosensor to screen for the presence of STEC strains in food and environmental samples, and (IV) to conduct cost analysis and evaluate commercial potential. For the purpose of this dissertation, each objective was written as a stand-alone chapter.

CHAPTER 2

LITERATURE REVIEW

2.1. Shiga-toxin Producing *Escherichia coli* (STEC)

Shiga toxin-producing *Escherichia coli* (STEC) is a group of foodborne pathogens that can cause serious human diseases such as acute kidney failure-hemolytic uremic syndrome (HUS) and hemorrhagic colitis (Brooks, Sowers et al. 2005, Trachtman, Austin et al. 2012). HUS is a combination of thrombocytopenia, renal failure and hemolytic anemia especially in children (Newell, Koopmans et al. 2010, Krüger and Lucchesi 2014). According to the Centers for Disease Control and Prevention (CDC), there were 4,437 cases of culture confirmed STEC infections in 2014 from 51 states and regional public health laboratories (CDC 2017). Though the infection incidence of STEC O157 declined in 2014, the incidence of infection of non-O157 serogroups continued to rise during the same year at around 0.79 cases per 100,000 population (CDC 2017). The food commodities that are usually routinely involved in outbreaks include beef, cheese, milk, juice, and produce (Esseili, Wang et al. 2012). It has been more than a decade ago since the CDC identified serogroups O26, O45, O103, O111, O121 and O145 as the “big six” non-O157 causative agents in human illnesses (Brooks, Sowers et al. 2005).

Shiga toxin (Stx - Stx1 and Stx2 classes) is the main virulence factor of STEC strains. Stx is an AB₅ cytotoxin; its B pentamer targets glycolipid globotriaosylceramide (Gb₃) expressing cells and also transports A-subunit into the cytoplasm. Enzymatically active A-subunit cleaves the N-glycosidic bond of adenine 4324 in 28S rRNA, thus preventing tRNA binding that ultimately inhibits protein synthesis (Fuller, Pellino et al. 2011). Stx1 and Stx2 are encoded by

stx1 and *stx2* genes, respectively, and each STEC pathotype produces at least one or both Stx toxins (Gyles 2007, Etcheverría, Padola et al. 2010, Fratamico, Bagi et al. 2011).

Cattle are the natural reservoir of various STEC strains. Cross-contamination occurs at different segments and levels of food chain primarily due to consumption of focally-contaminated water and food (Imamovic and Muniesa 2011). The presence and prevalence of STEC strains, specifically O157, are vigorously monitored in bovine fecal shedding (Durso and Keen 2007). Non-O157 STEC-linked diseases are rising in the United States and worldwide, indicating that some of these bacteria are emerging pathogens (Junillon, Vimont et al. 2012).

The current enrichment and isolation procedures for both STEC O157:H7 and non-O157 strains involve the use of modified tryptone soya broth supplemented with novobiocin (8.0 mg/L) plus casamino acids (mTSB+n), tellurite cefixime–sorbitol MacConkey agar (TC-SMAC), Levine’s eosin methylene blue (L-EMB), and Rainbow agar O157. These traditional methods may take up to 5-7 days followed by biochemical and serological testing (Tillman, Wasilenko et al. 2012). Alongside traditional culture methods, commercially available products are also used to screen for the presence of STEC strains in food and environmental samples which include those immunoassay-based and molecular-based methods (**Table 2.1**).

Immunoassay-based methods are relatively expensive and usually require concentration or enrichment of samples prior to the actual testing. These assays are prone to cross-reactivity and degradation of immuno-component over time. Similarly, molecular-based methods are also expensive and require trained staff. Though PCR-based assays have high sensitivity, the detection platform often cannot distinguish viable from non-viable microorganisms. Therefore, an alternative technology which inexpensive, simple and portable is necessary to meet the current needs.

Table 2.1. Comparisons of commercially-available products for STEC detection. Screening and detection of STEC serogroups from various food matrices can be conducted by using various commercially-available products. All values are in USD₂₀₁₈.

Assay		Description	Sensitivity ¹	Cost
Method	Product			
1. Traditional culture-based	Sorbitol-MacConkey	Presumptive STEC O157:H7 is differentiated by its inability to ferment sorbitol, appearing colorless (March and Ratnam 1986)	85.2%-100% (March and Ratnam 1986)	\$1.20/20 mL
	CHROM Agar™	STEC target cells are differentiated by chromogenic substrates (Parsons, Zelyas et al. 2016)	96.3% (Church, Emshey et al. 2007)	\$1.00/20 mL
	Rainbow Agar®	Typical <i>E. coli</i> O157 strains grow and form distinctive charcoal grey or black colonies (Manafi and Kremsmaier 2001)	91.1% (Manafi and Kremsmaier 2001)	\$1.20/20 mL
2. Immunoassay-based	Singlepath® <i>E.coli</i> O157	Immunochromatographic rapid test based on gold-labeled antibodies	< 99%	\$199/test

Table 2.1. Continued.

	TRANSIA® AG EHEC	Enzyme Immunoassay (EIA) technology relying on complex, proprietary antibody formulations	95%	\$5.28/well
	VIP® Gold – EHEC	Single-step visual immunoassay	90%	\$340/pack
	ProSpect™ Shiga Toxin <i>E. coli</i>	Direct, qualitative enzyme immunoassay	83.9% (Gerritzen, Wittke et al. 2011)	\$16.69/well
3. Molecular-based	FilmArray® GI Panel	Multiplex Polymerase Chain Reaction (mPCR)	100%	\$883.87/reactions
	Seeplex® Diarrhea ACE Detection	Multiplex Polymerase Chain Reaction (mPCR)	100%	\$155/test
	TaqMan® in-house STEC	Real-time polymerase chain reaction (RT-PCR)	100%	\$838/96 reactions

¹ – Sensitivity in percentages = $\frac{\text{True Positives}}{\text{True Positives} + \text{False Negatives}} \times 100$

Reliable monitoring that can detect harmful chemical compounds, toxins and pathogens are significant for the prevention, reduction of these chemical and biological hazards to acceptable limits or even elimination as mandated by the food safety regulatory authorities. Therefore, a rapid and accurate STEC strains detection method is needed for a quick implementation of countermeasures to resolve contamination events especially when food processing facilities and distribution networks are affected.

2.2. Foodborne Pathogen Detection

Microbiological analysis of foods is an integral part of food safety management. Food producers and processors, and food safety regulatory authorities use microbial analysis for surveillance and trend analysis in order to detect emerging risks (Jasson, Jacxsens et al. 2010). Due to the limitations of conventional methods, many researchers recently have shifted their focused and efforts on the development of highly sensitive, selective and reliable rapid foodborne pathogen detection methods.

2.2.1. Conventional Methods of Detecting Foodborne Pathogen

In general, traditional foodborne pathogen detection methods rely on enrichment and selective microbiological plating prior to performing immunological (ie antigen and antibody reactions), biochemical assays and nucleic acid-based amplifications (ie conventional polymerase chain reactions (PCR) or quantitative PCR and loop mediated isothermal amplification (LAMP)). Standardized classical culture methods are still in use because they are harmonized methods and viewed at as the “gold standards” in food diagnostics. Although culture methods can be conducted with inexpensive infrastructures and consumables, they are tedious to perform, demand large volume usage of both liquid and solid media and reagents, and involve time-consuming procedures both in operation and data collection. The PCR methods are

sensitive and quick (3-6 hr), but require nucleic acid extraction procedures coupled with relatively costly equipment while immunological assays have lower detection sensitivities (10^3 - 10^5 CFU/mL) (Wang, Chen et al. 2017). Conventional method is not the best option in terms of high-throughput screening of large food samples for the presence of one or more foodborne pathogens (Jasson, Jacxsens et al. 2010, Hegde, Cote et al. 2012). Therefore, a robust, low cost and efficient detection system, such as an on-site and portable biosensor, is needed to ensure safe food for consumers.

2.2.2. Rapid and Portable Screening and Detection Methods

Researchers are developing affordable and on-site systems that are aimed to move away sample processing and testing from centralized laboratory (Mustafa, Hassan et al. 2017). Recently, the World Health Organization (WHO) has indicated the vital characteristics of suitable rapid tests in areas and conditions with limited resource under the acronym, ASSURED (Affordable, Sensitive, Specific, User-friendly, Rapid and Robust, Equipment-free, Delivered to those who need it) (Ben Aissa, Jara et al. 2017). Rapid detection methods can be categorized into three groups namely (1) immunological-based, (2) nucleic acid-based methods and (3) biosensors (Vanegas, Gomes et al. 2017).

In the field of immunoassays, the common antibody-antigen interactions in enzyme-linked immunosorbent assay (ELISA) and agglutination kits for foodborne pathogen detection are relatively easier to perform but often generate false-positive results and are not capable of differentiating viable from non-viable cells (Bhardwaj, Bhardwaj et al. 2017, Wang, Chen et al. 2017). Though PCR-based method can improve the sensitivities of immunoassays (approx 100-fold) it requires thermocycling platforms, trained staff and reliable infrastructures which can be challenging in areas with scarce resources (Ben Aissa, Jara et al. 2017). Another drawback of

molecular or nucleic acid amplification techniques (ie PCR) is its destructive nature or the need to break up the cells in which in occasions when rare cells are encountered and would require more than single test to be carried out, then it becomes a limiting factor (Bole and Manesiotis 2016).

In terms of the biosensor technology which has been rigorously studied as a simple, rapid, sensitive and reliable tool, it can allow near real-time screening and detection of pathogens in complex matrices with minimal sample preparation steps (Valadez, Lana et al. 2009). It has been also found in published scientific literatures that biosensor ranks as the fourth most popular method and the fastest growing technology in the area of pathogen detection (Lazcka, Campo et al. 2007). Historically, biosensors originated from the integration of molecular biology and information technology (Zhao, Jiang et al. 2012). It is comprised of target or analytes-specific biorecognition or bioreceptor elements and a physio-chemical transducer that converts and relays signals to an amplifier and computer (Velusamy, Arshak et al. 2010, Deng, Xu et al. 2012).

However, it is important to note that the continuous emergence of rapid pathogen detection necessitates thorough understanding of the major differences among devices according to the molecular interactions between the target analyte and biorecognition agents for efficiency (Vanegas, Gomes et al. 2017).

2.2.2.1. Current Biosensors in Foodborne Pathogen Screening and Detection

Due to the inherently long turn-around time of conventional pathogen detection methods, biosensors are specifically designed to significantly reduce the processing time between sample uptake and test results at a fraction of the cost of conventional methods. As an analytical device, a biosensor is incorporated with recognition elements that can either be biological materials or its derivatives, and other molecules that can mimic natural bioactive molecules for recognition

(Lazcka, Campo et al. 2007). Recognition materials that are immobilized and anchored onto various platforms or transducers come in contact first with target analytes before the biosensing systems are able to generate signals. These molecules such as bioligands (antibodies, nucleic acids) and biocatalysts (enzymes, microorganisms, tissues and cellular materials) contribute to the sensitivity and specificity of the biosensors especially in the field of diagnostic applications.

2.2.2.1.1. Portable Biosensors Classified Based on Bioreceptors or Capture Elements

Biosensors may integrate nucleic acids, aptamers, antibodies, bacteriophages and whole cells as bioreceptors or capture elements. Conversion of the capture and binding events between the target analytes and its receptors (ie physical and chemical changes at the interface) into measurable signals via transducers is facilitated by various electrochemical techniques such as impedance spectroscopy (IS), cyclic voltammetry (CV), electronic field effects, potentiometry, amperometry as well as optical and thermal read-out principles (Eersels, Lieberzeit et al. 2016).

Table 2.2 shows the recently developed biosensors for foodborne pathogens detection and are grouped based on the six types of capture elements (CE); (1) antibody, (2) aptamer, (3) amino acid, (4) antimicrobial peptides, (5) bacteriophage, (6) cells and (7) biomimetic. The non-covalent interactions that exist between the recognition elements and ligands dictate the basis for a specific range of biosensing applications.

Table 2.2. Biosensors classified according to the types of its capture elements (CEs).

Biosensors		Target Pathogens/ Molecules	Sample Matrices	Time of Analysis	Detection Limit	Reference
Capture Elements	Transducer/Techniques					
1. Antibody	Poly-L-lysine (PLL) glass slide/Chemiluminescence	<i>E. coli</i> O157:H7, <i>Salmonella</i> spp.	Milk	1 h	7.5 x 10 ⁶ CFU/mL, 1.25 x 10 ⁷ CFU/mL	Karoonuthaisiri, Charlermroj et al. (2009)
	Electrochemiluminescence, fluorescence and cytometric bead assay	<i>E. coli</i> O157:H7, <i>S. aureus</i>	Spinach rinse and lysostaphin /nisin	6.5 h and 10 h	10 ³ CFU/mL	(Leach, Stroot et al. 2010)
	Quartz crystal microbalance (QCM) immunosensor	<i>E. coli</i> O157:H7	PBS/Milk	4h	23 CFU/mL and 53 CFU/mL	(Shen, Wang et al. 2011)
	(3-glycidoxypropyl) trimethoxysilane (GPTS)/ Surface acoustic wave (SAW)	<i>E. coli</i>	Pure culture	1 h	10 ⁶ bacteria /500 µL	(Moll, Pascal et al. 2007)

Table 2.2. Continued.

Screen -printed carbon electrode/Differential Pulse Voltammetry	<i>S. Typhimurium</i>	Skimmed milk	1.5 h	143 cells/mL	(Afonso, Pérez-López et al. 2013)
Evanescent waver fiber-optic assay	<i>Salmonella</i> spp.	Pure culture/egg, chicken breast	2-4 h	10 ³ CFU/mL/ 10 ⁴ CFU/mL	(Valadez, Lana et al. 2009)
Nitrocellulose/Lateral-flow assay	<i>E. coli</i> O157:H17 <i>S. Paratyphi</i> A <i>S. Paratyphi</i> B <i>S. Paratyphi</i> C <i>S. Enteritidis</i> <i>S. Typhi</i> <i>S. Choleraesuis</i> <i>V. cholera</i> O1 <i>V. cholera</i> O139 <i>V. parahaemolyticus</i>	279 food samples (dairy and marine products, beverages, snacks, and meats)	20 min (14 h enrichment)	10 CFU/0.6 mg	(Zhao, Wang et al. 2016)

Table 2.2. Continued.

	CM3 sensor chip/Surface plasmon resonance (SPR)	Calicivirus – norovirus surrogate	Purified cell culture lysates	15 min	10 ⁴ TCID ₅₀ FCV/mL	(Yakes, Papafragkou et al. 2013)
2. Aptamer	Chemoluminescence	<i>S. Paratyphi</i> A	Water	--	10 ³ CFU/mL	(Yang, Peng et al. 2013)
	Gold electrode/Differential Pulse Voltammetry	<i>E. coli</i> O111	Pure culture/milk	3.5 h	112 CFU/mL/ 305 CFU/mL	(Luo, Lei et al. 2012)
	Quartz Crystal Microbalance (QCM)	<i>E. coli</i> O157:H7	Pure culture	50 min	1.46 x 10 ³ CFU/mL	(Yu, Chen et al. 2018)
3. Amino acid	Gold sensor/Whole cell imprinting, Surface Plasmon Resonance (SPR) and Quartz Crystal Microbalance (QCM)	<i>E. coli</i>	Water	7 min and 20 min	1.54 x 10 ⁶ CFU/mL (SPR); 3.72 x 10 ⁵ CFU/mL (QCM)	(Yilmaz, Majidi et al. 2015)

Table 2.2. Continued.

	Gold electrode/ Microcontact imprinting, capacitive biosensing	<i>E. coli</i>	River water		70 CFU/mL	(Idil, Hedstrom et al. 2017)
4. Antimicrobial Peptides	Microfluidic chip/	<i>E. coli</i>	Pure culture	30 min	10 ³ cells/mL	(Yoo, Woo et al. 2014)
5. Bacteriophage	Polyethylenimine (PEI)- carbon nanotube (CNT)/ Impedimetric	<i>E. coli</i> B	Pure culture		10 ³ CFU/mL	(Zhou, Marar et al. 2017)
	Gold electrode/ Impedance spectroscopy (IS), LAMP, linear sweep voltammetry	<i>E. coli</i>	Pure culture	< 1 h	8 x 10 ² CFU/mL (IS), 10 ² CFU/mL (LAMP)	(Tlili, Sokullu et al. 2013)
	Interdigitated gold microelectrodes/Electroche mical Impedance Spectroscopy (EIS)	<i>E. coli</i>	Water		10 ⁴ CFU/mL	(Mejri, Baccar et al. 2010)

Table 2.2. Continued.

Magnetoelastic material/Resonance frequency	<i>S. Typhimurium</i>	Water and fat-free milk	5×10^3 CFU/mL	(Lakshmanan, Guntupalli et al. 2007)
Screen-printed carbon electrode microarrays/ Direct Impedance	<i>E. coli</i> K12	Pure culture	10^4 CFU/mL	(Shabani, Zourob et al. 2008)
Enzyme-linked immunosorbent assay (ELISA)	<i>Salmonella spp.</i> and <i>E. coli</i>	Pure culture	10^4 CFU/mL	(Galikowska, Kunikowska et al. 2011)
Screen-printed gold electrode/Electrochemical Impedance Spectroscopy (EIS)	<i>Listeria innocua</i> serovar 6b	Milk (2%)	10^5 CFU/mL	(Tolba, Ahmed et al. 2012)
Gold surface of SPREETA/Surface Plasmon-resonance	<i>Staphylococcus aureus</i>	Pure culture	10^4 CFU/mL	(Balasubramanian, Sorokulova et al. 2007)

Table 2.2. Continued.

6. Cell (encapsulated B lymphocyte)	Multi-well plate/colorimetric	<i>Listeria</i> spp. and <i>Bacillus</i> spp. and their toxins	Pure culture/toxins		(Banerjee, Lenz et al. 2007)
7. Biomimetic materials	Odorant binding protein mimicking <i>Drosophila</i> and Quartz Crystal Microbalance (QCM)	Volatile organic compounds (VOCs)/ <i>Salmonella</i> spp.	Packaged beef	< 5 ppm of VOCs	(Sankaran, Panigrahi et al. 2011)
	Colorimetric phage bundle nanostructures mimicking turkey skin	Explosive chemical (trinitrotoluene - TNT)	Chemicals	300 pbb of TNT	(Oh, Chung et al. 2014)

TCID₅₀/mL, 50% tissue culture infective dose per mL.

2.2.2.1.1.1. Antibodies-based Biosensors

Antibodies are commonly integrated as bioreceptors and CEs with biosensors due to their high affinities to specific targets (Ertürk and Lood 2018). Binding fragments are also relatively easy to modify using protein engineering and are widely utilized in nanotechnology applications (Trilling, Hesselink et al. 2014). Foodborne pathogens such as STEC O157:H7, *Salmonella* spp., *Vibrio* spp., and viruses have been detected by antibodies-based biosensors coupled with various transducers and techniques such as chemiluminescence (Karoonthaisiri, Charlermroj et al. 2009), electrochemiluminescence and fluorescence (Leach, Stroot et al. 2010), QCM immunosensor (Shen, Wang et al. 2011), SAW (Moll, Pascal et al. 2007), differential pulse voltammetry (Afonso, Pérez-López et al. 2013), evanescent wave fiber-optic assay (Valadez, Lana et al. 2009), lateral-flow assay (Zhao, Wang et al. 2016) and SPR (Yakes, Papafragkou et al. 2013).

An array of antibodies has simultaneously detected STEC O157:H7 and *Salmonella* spp. strains using a mini ELISA-like sandwich chemiluminescent approach in a poly-L-lysine (PLL) glass slide solid support (Karoonthaisiri, Charlermroj et al. 2009). Luminol-based chemiluminescent substrate was added to generate and detect HRP signals within one hour of assay time. However, the limit of detection (LOD) was very high; 7.5×10^6 CFU/mL for STEC O157:H7 while 1.25×10^7 CFU/mL for *Salmonella* spp in milk sample. An improved LOD (10^3 CFU/mL) for *E. coli* and *S. aureus* detection using antibodies was later reported by Stroot, Leach et al. (2012) by developing dual labeling method for fluorescence in situ hybridization (FISH) and capture antibody targeted detection (CAT-FIS). This technique had to be conducted with the aid of immunomagnetic capture and cytometric array biosensor which made the process cumbersome, less efficient and not economical.

Quartz crystal microbalance (QCM) is a mass-based piezoelectric biosensor that allows recognition and detection of slight mass changes even at the nanogram level causing resonance frequency disruption that is proportional to the deposited materials on the quartz surface (Deng, Xu et al. 2012, Guo, Lin et al. 2012, Yu, Chen et al. 2018). It utilizes quartz crystal resonator as a sensing material (Kimmel, LeBlanc et al. 2011). Mass changes can occur when the target analytes such as whole cells of foodborne pathogens are captured by the immobilized highly-specific ligands (Deng, Xu et al. 2012). Shen, Wang et al. (2011) reported QCM immunosensor targeting STEC O157:H7 based on beacon immunomagnetic nanoparticles (BIMPs), streptavidin-gold, and enrichment solution. O157:H7-BIMPs complex was loaded with O157:H7 polyclonal antibody (target antibody) and biotin-antibody (beacon antibody) to capture and separate STEC O157:H7 cells in the QCM setup. The LOD was 23 CFU/mL and 53 CFU/mL in phosphate buffer and milk, respectively. Some of the disadvantages that are routinely encountered in using QCM biosensor include relatively long incubation times of bacterial sample on the biosensor surface, difficulty with crystal surface regeneration, high packaging cost, and the implementation of related fluidic has been challenging (Rocha-Gaso, March-Iborra et al. 2009).

Surface acoustic wave (SAW) biosensor has been also developed with antibodies as its capture elements for the detection of whole *E. coli* strain cells (Moll, Pascal et al. 2007). SAW can produce and detect acoustic waves using interdigital transducers (IDT) found on the surface of piezoelectric crystals. In such condition, the acoustic energy is restricted at the surface of the device which is within the range of the acoustic wavelength. Thus, the wave becomes very sensitive to any variation on the surface such as mass loading, viscosity and changes in conductivity (Länge, Rapp et al. 2008). SAW devices can be used also to detect proteins, sugars,

DNA and viruses. Whole *E. coli* cells have been detected by shear horizontal guided SAW immunosensor consisting of grafting goat anti-mouse antibodies onto the sensor surface, 3-glycidoxypropyl trimethoxysilane (GPTS), before introducing it to anti-*E. coli* antibodies as reported by Moll, Pascal et al. (2007) which had a detection limit of 10^6 bacteria/ml in a 500 μ L chamber.

Afonso, López et al. (2012) developed an immunosensor for *S. Typhimurium* LT2 (S) detection using a magneto-immunoassay and AuNPs as labels for electrochemical detection. A permanent magnet underneath the screen-printed carbon electrode (SPCE) was also utilized. Pure *Salmonella* spp. samples were tested with anti-*Salmonella* magnetic beads (MBs-pSAb) as capture phase and sandwiching it afterward with AuNPs modified antibodies (sSAb-AuNPs) which were detected by differential pulse voltammetry (DPV). The LOD was 143 cells/mL and a linear range from 10^3 to 10^6 log cells/mL of *Salmonella* spp. was obtained, and a coefficient of variation of about 2.4%. Recoveries of the sensor by spiking skimmed milk with different quantities of *Salmonella* spp. of about 83% and 94% for 10^3 CFU/mL and 10^5 CFU/mL were obtained, respectively which were expected from immunosensors.

Valadez, Lana et al. (2009) developed a detection technique by immobilizing an anti-*Salmonella* polyclonal antibody onto the surface of an optical fiber via biotin-avidin interactions to capture *Salmonella* spp. Alexa Fluor 647-conjugated antibody (MAb2F-11) was used as the reporter. Detection occurred when an evanescent wave from a laser (635 nm) excited the Alexa Fluor and the fluorescence was measured by a laser spectrofluorometer at 710 nm. The biosensor was specific to *Salmonella* spp. and the LOD was 10^3 CFU/mL in pure culture and 10^4 CFU/mL when it was applied on egg and chicken breast samples. Food samples were spiked with 10^2 CFU/mL and had 2-6 hours of enrichment. The need for specialized reagents such fluorescent

probe or DNA-binding dye and the relatively costly instruments for monitoring fluorescence can be a critical factor in some environments with limited resource (Jung, Jung et al. 2010).

The sensitivity of an antibody-based lateral flow assay (LFA) has been improved recently by incorporating up-converting phosphor (UCP) particle (UPT-LFA) (Zhao, Wang et al. 2016). The UPT-LFA technique is based on the optical properties of anti-Stokes shift and the highly stable fluorescence of UCP (Yan, Zhou et al. 2006). UPT-LF strips were individually developed based on antibodies sandwich binding on the 10-channel UPT-LF that simultaneously detected 10 foodborne pathogens (*E. coli* O157:H17, *S. Paratyphi* A, *S. Paratyphi* B, *S. Paratyphi* C, *S. Enteritidis*, *S. Typhi*, *S. Choleraesuis*, *V. cholera* O1, *V. cholera* O139 and *V. parahaemolyticus*) from either natural or artificially-spiked food items (279 food samples). Without enrichment, the sensitivity of the technology was in the range of 10^4 CFU/mL- 10^5 CFU/mL while 10 CFU/0.6 mg with enrichment and 20 min turn-around time. However, some limitations were reported such as the position encoding that utilized multiple lanes in a single strip could increase false binding as well as the signal encoding would need several settings of the optical source, receiver and filter that directly contribute to the complexity of the system.

An immuno-based surface plasmon resonance (SPR) biosensor was developed by Yakes, Papafragkou et al. (2013) for the detection of norovirus surrogate (feline calicivirus, FCV). The antibody-based assay was initially constructed by immobilizing anti-FCV onto the SPR chip surface and then measured the virus interaction and subsequent secondary antibody binding. Results showed that the biosensor detected intact FCV particles with an LOD of approximately 10^4 tissue culture infective dose (TCID₅₀) FCV/mL (purified cell culture lysates). This sensitivity is more applicable for clinical samples; more studies are needed especially if the assay will be

implemented on foodborne viruses in combination with virus extraction and concentration procedures.

Antibody-based biosensors suffer cross-reactivity with other bacteria which may result in false positives (Shabani, Zourob et al. 2008). Immunosensors lack the ability to discriminate between viable and non-viable bacterial cells because antibodies can recognize and bind to the antigen that is present in the bacteria even if it is dead (Tlili, Sokullu et al. 2013). Antibodies require intermediate protein and rely on non-covalent protein-protein interactions that reduces the lifespan of the biosensor. In addition, the storage temperature of antibodies needs to be controlled to prevent its denaturation which can affect the reliability of antibody-based biosensors for on-site routine testing. Antibodies, specifically monoclonal, mainly require the use of live animals to stimulate immune response to produce the desirable antibodies, thus production is highly dependent on the environmental conditions of the host animals. More importantly, the production cost of antibodies is generally expensive, therefore inexpensive alternatives for capture and recognition elements of biosensors should be considered.

2.2.2.1.1.2. Aptamer-based Biosensors

Aptamers are synthetic receptors (ie. DNA or RNA sequences) that are evolved in vitro, usually by systematic evolution of ligands by exponential enrichment (SELEX), toward specific binding to target molecules such as proteins and cells (Balamurugan, Obubuafo et al. 2008).

Figure 2.1. shows the schematic presentation of DNA aptamer selection by cell-SELEX. In brief, target cells are incubated with single-stranded DNA (ssDNA) library pool. Unbound sequences are washed off while bound sequences are recovered. kControl cell line is incubated with the recovered pool for purification and removal of non-specific sequences, and then enriched for target binding. PCR with fluorescein isothiocyanate–labeled sense and biotin-

labeled antisense primers is used to amplify those binding sequences. Antisense strands are then removed to produce ssDNA for the next rounds of selection.

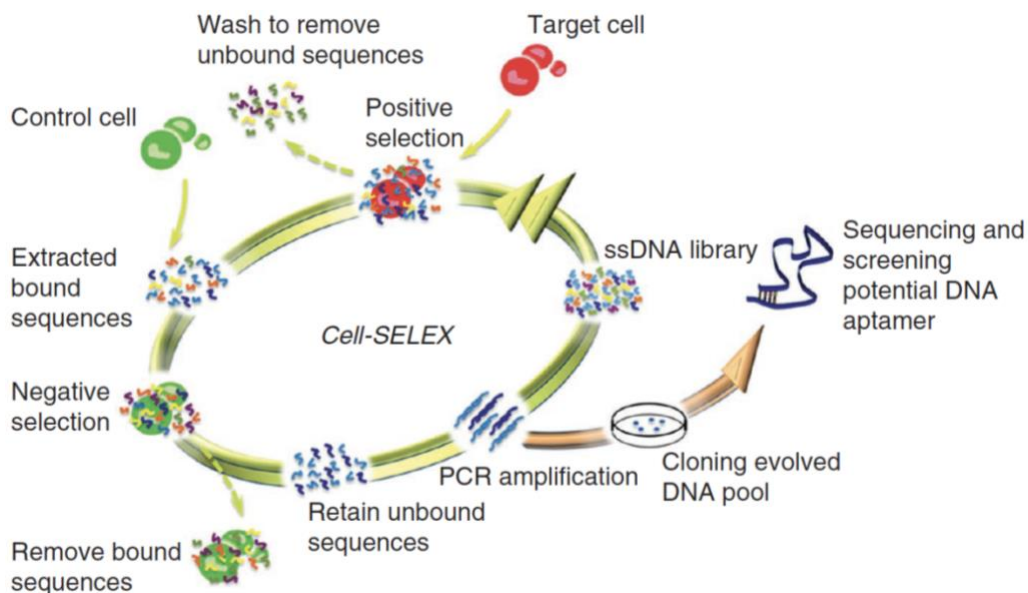


Figure 2.1. Schematic presentation of DNA aptamer selection by cell-SELEX technique. Highly-specific DNA sequences to its target cells are enriched, cloned and sequenced to identify the most appropriate aptamers. Image adapted from Sefah, Shanguan et al. (2010).

A set of highly-specific single-stranded DNA (ssDNA) aptamers against *S. Paratyphi A* was reported (Yang, Peng et al. 2013). These aptamers were selected from an amplified oligonucleotide pool which was initially generated by whole cell-SELEX. Aptamers were then labeled with DNase and acted as detection probes with single-walled carbon nanotubes (SWNTs). By monitoring the changes in the chemoluminescence intensity (420 nm), the authors were able to quantify *S. Paratyphi A* with a LOD of 10^3 CFU/mL.

Similarly, STEC O111 was directly detected by using a highly-sensitive and specific aptasensor which was based on target-induced aptamer displacement (Luo, Lei et al. 2012). Aptamers were hybridized with capture probes before immobilizing the complex onto the surface of gold electrode via Au-thiol binding. Dissociation of aptamers in the presence of target cell (STEC O111) occurred due to higher and stronger affinity which then allowed subsequent hybridization of the newly unhybridized capture probes with detection probes that generated an electrochemical response using DPV. The LOD of the study was 112 CFU/mL and 305 CFU/mL in saline solution and milk, respectively, within 3.5 hours testing time.

STEC O157:H7 was also detected using an aptamer-based biosensor coupled with QCM technique (Yu, Chen et al. 2018). The authors performed SELEX with 19 rounds of selection (O157:H7) and six rounds of counter-selection (*S. aureus*, *L. monocytogenes*, and *S. Typhimurium*) to generate highly selective aptamers against STEC O157:H7. This QCM aptasensor had a LOD of 1.46×10^3 CFU/mL for STEC O157:H7 and a detection time of 50 min.

Though ELISA can be improved in terms of its sensitivity when aptamers replaced its antibodies biorecognition elements, aptamers are rapidly degraded by nucleases, thus limiting its practical use (Lakhin, Tarantul et al. 2013). In addition, production of aptamers in reality is time consuming and labor-intensive. When suboptimal SELEX procedures are performed, the final aptamer products tend to have weak affinity against its target molecules.

2.2.2.1.1.3. Amino Acid-based Biosensors

Synthetic amino acid has been studied and tested as a recognition element in developing micro imprinting-based biosensors. Synthetic amino acid such as the polymerizable form of histidine, N-methacryloyl l-histidine methylester (MAH), can recognize whole cells of generic *E. coli* (model microorganism) similar to natural antibodies as reported by Yilmaz, Majidi et al.

(2015). A detection method using a micro contact imprinting of whole *E. coli* cell on mass (QCM) and optical (SPR) sensitive devices was developed as shown in **Figure 2.2**. Imprinted polymeric film for *E. coli* was formed on the surfaces of SPR and QCM sensors. *Bacillus* spp. and *Staphylococcus* spp. were also tested to challenge the specificity of the method. In brief, a monomer solution was dropped onto SPR and QCM surfaces where *E. coli* attached surfaces were also added and pressed to polymerize using UV light under nitrogen atmosphere. Micro imprinting technology complementary cavities were then formed which allowed chemical recognition of *E. coli* on the sensor surface upon functionalization using MAH. The cavities or bacterial stamps created on the electrodes of both SPR and QCM devices, captured and detected *E. coli* cells in real-time. These coupling of QCM and SPR techniques provided a LOD of 3.72×10^5 CFU/mL and 1.54×10^6 CFU/mL, respectively. Additional information is shown in **Figure 2.3** presenting a schematic flow of a surface imprinting approach (SIP) which is a classic molecular imprinting wherein a template solution is assembled on top of the substrate. After which, extraction of template creates binding cavities where specific targets that perfectly fit into those microcavities can rebind (Eersels, Lieberzeit et al. 2016). Molecular imprinting technology builds artificial recognition sites which match the size, shape and spatial orientation of its template such as bacterial cells which then incorporated with various transducer platforms.

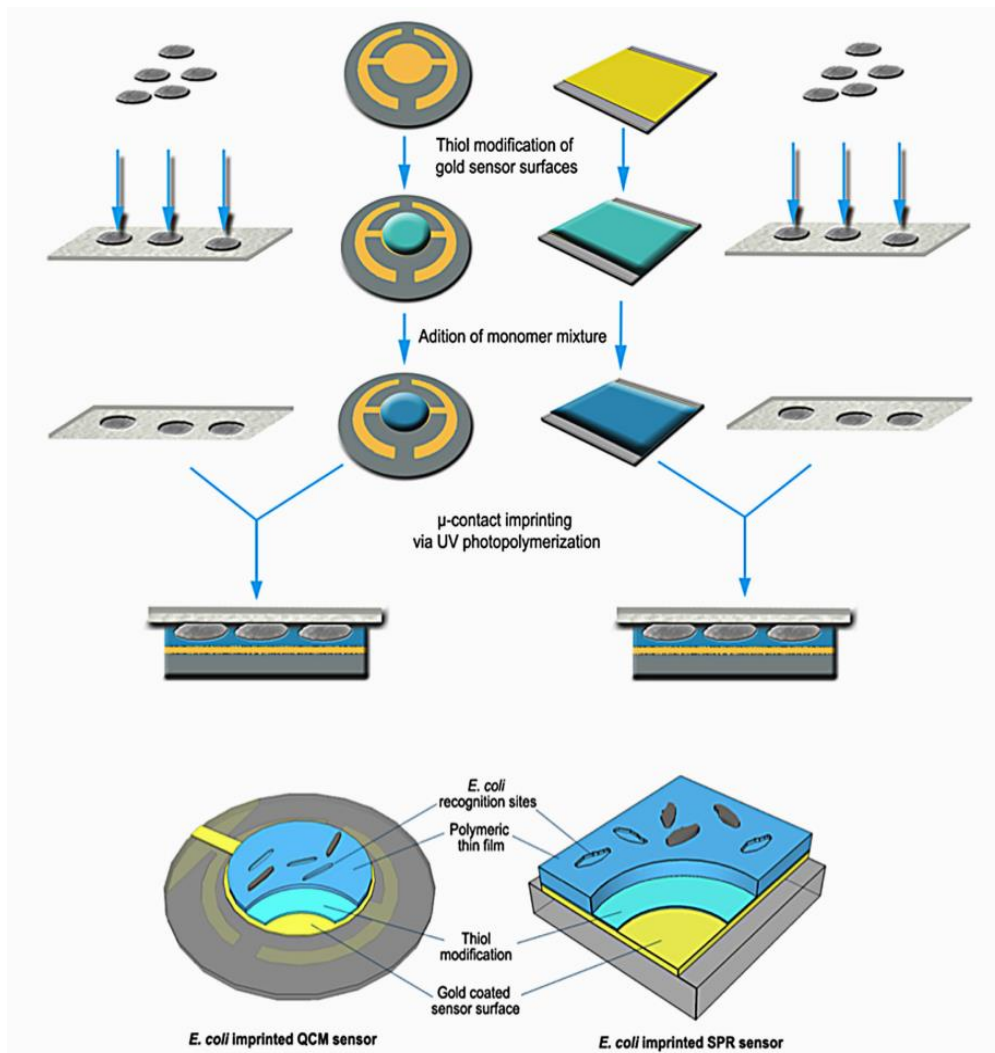


Figure 2.2. Schematic representation of microcontact imprinting. Microcontact imprinting of *E. coli* on QCM and SPR sensor surfaces. Image adapted from Yilmaz, Majidi et al. (2015).

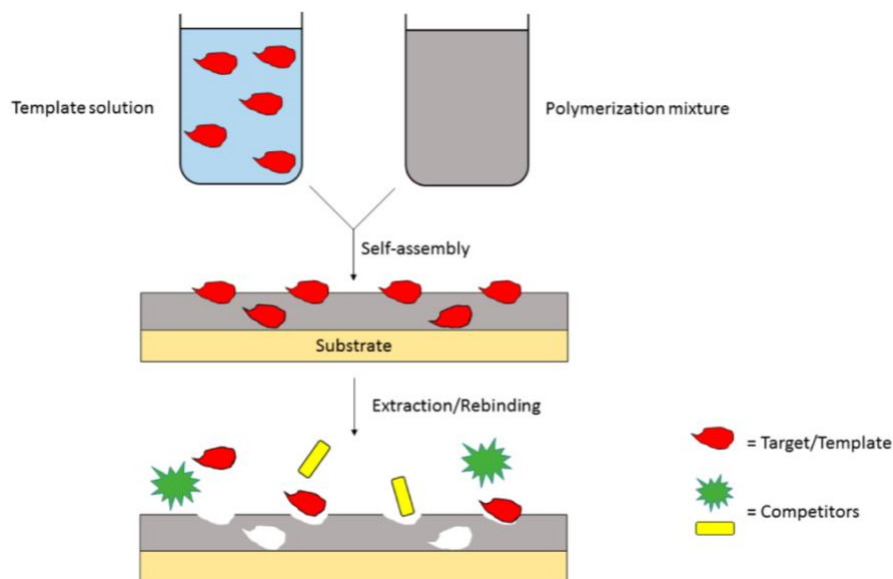


Figure 2.3. Schematic representation of self-assembly technique for SIP synthesis. Template is mixed with polymer, cross-linker(s), and initiators which forms microcavities where target selectively rebinds. Image adapted from Eersels, Lieberzeit et al. (2016).

Similarly, another amino acid-based biosensor was developed by Idil, Hedstrom et al. (2017) in which they used MAH in combination with 2-hydroxyethyl methacrylate (HEMA) as monomers and ethyleneglycol dimethacrylate (EGDMA) as crosslinker under UV polymerization. Instead of conducting QCM and SPR techniques with micro imprints, they utilized capacitive sensor for real-time recognition and monitoring of *E. coli* cells. The LOD was 70 CFU/mL and was able to distinguish target from non-target bacterial strains with similar morphology.

Based on the current literatures, amino-acid based biosensors are mainly comprised of molecular imprinted polymers (MIPs) and MAH. Artificial recognition pockets-like regions in polymeric matrices are made by imprinting to complement the morphological features such as

size and spatial arrangement of target analytes or functional groups (Ertürk and Mattiasson 2017). MIPs and its integration onto various biosensor platforms pose great promise.

The drawback of this “molecular key and lock” approach for the detection of whole bacterial cells is its high LOD that can be attributed to the low binding capacity and relatively long equilibration time of the target analyte and binding molecules. In addition, the complicated cross-linking network prevents the diffusion of target molecules for specific recognition. Further studies and thorough investigation should be conducted to determine the applicability, sensitivity and specificity of MAH with other significant foodborne pathogens.

2.2.2.1.1.4. Antimicrobial Peptides-based Biosensors

Antimicrobial peptides (AMPs) have been recently proposed as an alternative to antibodies for bacterial detection. Yoo, Woo et al. (2014) developed a biosensing technique that targeted *E. coli* by utilizing a microfluidic chip with AMP (Magainin I)-labeled microbeads embedded on its channels as shown in **Figure 2.4**. The beads were initially modified with NH₂ group and N-[γ -maleimidobutyryloxy] succinimide ester (GMBS) for AMP attachment.

Recognition and binding of propidium iodide (PI)-stained *E. coli* via its teichoic acid (TA) and lipopolysaccharide (LPS) are also shown in the figure 2.4 below.

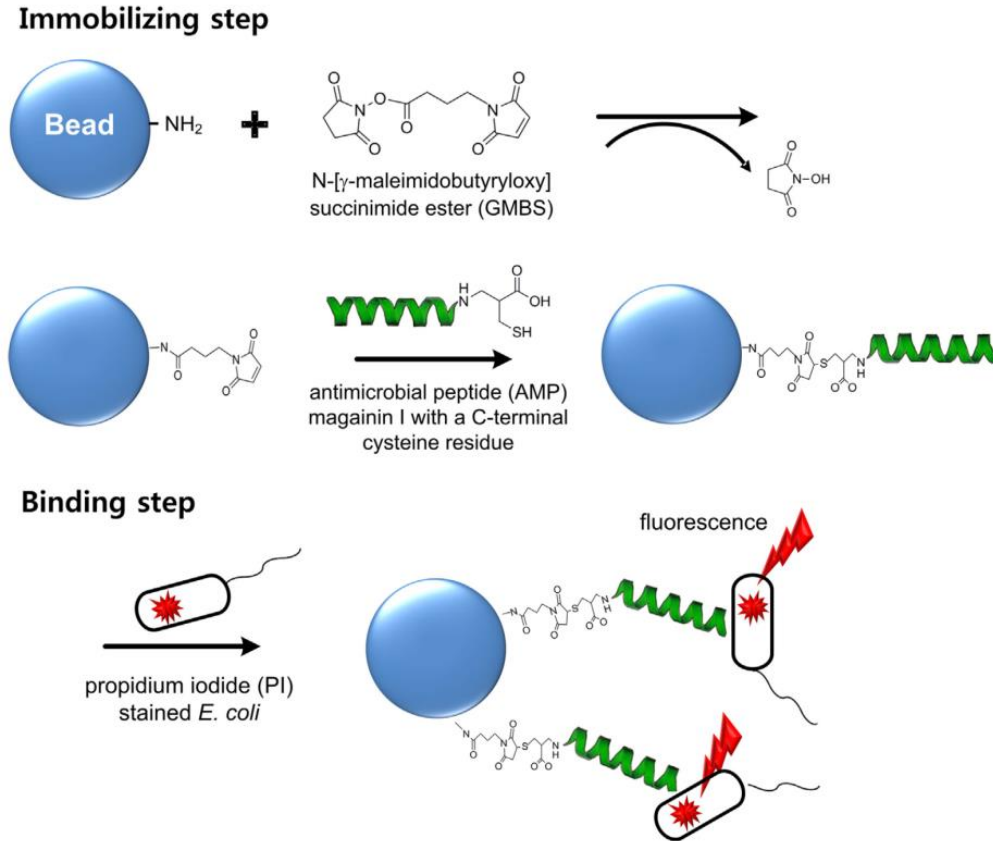


Figure 2.4. Representation of AMP (Magainin I) immobilization on beads. Immobilization and binding of propidium iodide-stained *E. coli* to the AMP-functionalized bead. Image adapted from Yoo, Woo et al. (2014).

Magainin I is an antibiotic peptide that specifically binds to TA and LPS of *E. coli*. Yoo, Woo et al. (2014) designed the technology by allowing propidium iodide-stained *E. coli* suspension to flow into a microfluidic chip that was attached to a fluorescence microscope. Increased flow of bacterial suspension caused a shorter time (30 mins) to reach a saturation level suggesting a rapid detection of *E. coli* cells. Cumulative changes in fluorescence intensity determined the LOD of the biosensor, approximately 10^3 CFU/mL. The specificity of magainin I and other AMPs needs to be further evaluated as it has been found that magainin I does not readily bind to Gram-positive bacteria due to absence of LPS. Its sensitivity and specificity to its

target when applied to heterogenous samples (ie mixed with Gram-negative and other enterobacter) requires more investigation to establish stability and reliability. It is also important to evaluate the potential health risks that AMPs pose to humans, animals and the environment.

2.2.2.1.1.5. Bacteriophage-based Biosensors

There has been a significant progress in the past years in the biosensor development that utilize bacteriophage or bacteriophage-derived affinity molecules as recognition elements (Schmelcher and Loessner 2014). Bacteriophages are unique and natural biological materials that feature excellent host selectivity which is highly useful as recognition probes for pathogen detection (Singh, Poshtiban et al. 2013). As recognition elements, bacteriophages can recognize and distinguish live target bacterial cells which is more rapid than conventional cultivation techniques (Hagens and Loessner 2007). Propagation of bacteriophages is relatively easy and inexpensive due to its abundance in nature.

Like other biosensing systems, the efficient and stable immobilization of bacteriophages either by physical absorption, covalent, chemical functionalization and oriented immobilization by genetic modification plays a crucial role on the performance and robustness of the biosensors. In addition, the successful immobilization of bacteriophages for target recognition, capture and binding due to strong inherent affinity to various receptors should be coupled with the most appropriate biosensor techniques to generate the strongest signal with minimal background noise. Bacteriophages can be utilized with various transducers and techniques such as impedimetric spectroscopy (Mejri, Baccar et al. 2010, Tolba, Ahmed et al. 2012, Tlili, Sokullu et al. 2013, Zhou, Marar et al. 2017), LAMP and linear sweep voltammetry (Tlili, Sokullu et al. 2013), SPR (Balasubramanian, Sorokulova et al. 2007) and other electrochemical approaches.

A new impedimetric biosensing based on carbon nanotube (CNT) with T2 bacteriophages for detection of *E. coli* B was developed by Zhou, Marar et al. (2017) as shown in **Figure 2.5**. In brief, bacteriophage T2 was immobilized on the surface of polyethylenimine (PEI)-modified carbon nanotube transducer on a glassy carbon electrode to act as the biorecognition element of the biosensor.

First, the surface was charge-enhanced to render it more suitable for the oriented immobilization of bacteriophages via covalently linking its capsid. A positive potential of +0.5 V vs Ag/AgCl was then applied to the working electrode (1 hr) in order to facilitate the charge-directed immobilization process. Tailed bacteriophages have net-negative charge, where head is more negative due to the presence of nucleic acid while its tail fibers are positively charged and this difference allowed bacteriophage immobilization using electrostatic interaction and electrophoretic deposition. The target bacterial cells (*E. coli* B) were then added and monitored by EIS and its interfacial impedance changes as a result of capturing *E. coli* B cells by T2 bacteriophages. In pure culture setup, the LOD of this method was relatively high, 10^3 CFU/mL.

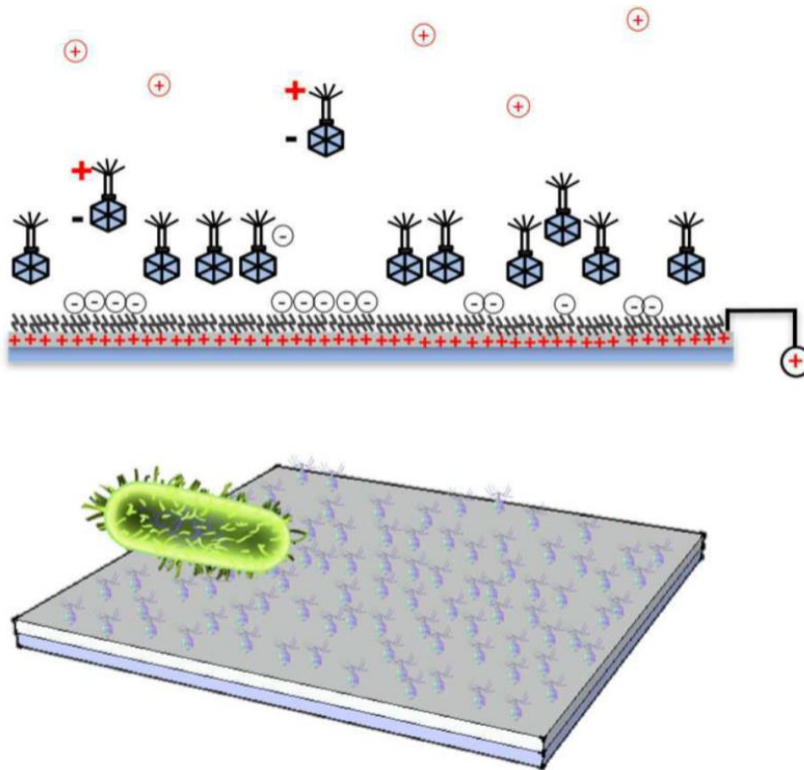


Figure 2.5. Representation of PEI-functionalized CNT on electrode surface. CNT with charge-directed and orientation and immobilization of T2 bacteriophage. Image adapted from Zhou, Marar et al. (2017).

Two complimentary bacteriophage-based approaches were combined by Tlili, Sokullu et al. (2013) for the rapid detection of *E. coli*. By immobilizing bacteriophage T4 on gold electrodes, it acted as the recognition element of electrochemical impedance spectroscopy (EIS) before coupling it with loop-mediated isothermal amplification (LAMP) technique for amplification of *Tuf* gene of lysed *E. coli* cells. Linear sweep voltammetry (LSV) monitored the LAMP amplification of *Tuf* gene (**Figure 2.6**). The authors successfully detected the target cells and achieved an LODs of 8×10^2 CFU/mL (15 min) for EIS and 10^2 CFU/mL (40 min) for LAMP during the confirmatory test. The study suggested that bacteriophage T4 is highly useful

and viable as a recognition element for screening significant foodborne pathogens. However, this study also presented complex multilayer detection techniques that are not suitable for on-site routine testing.

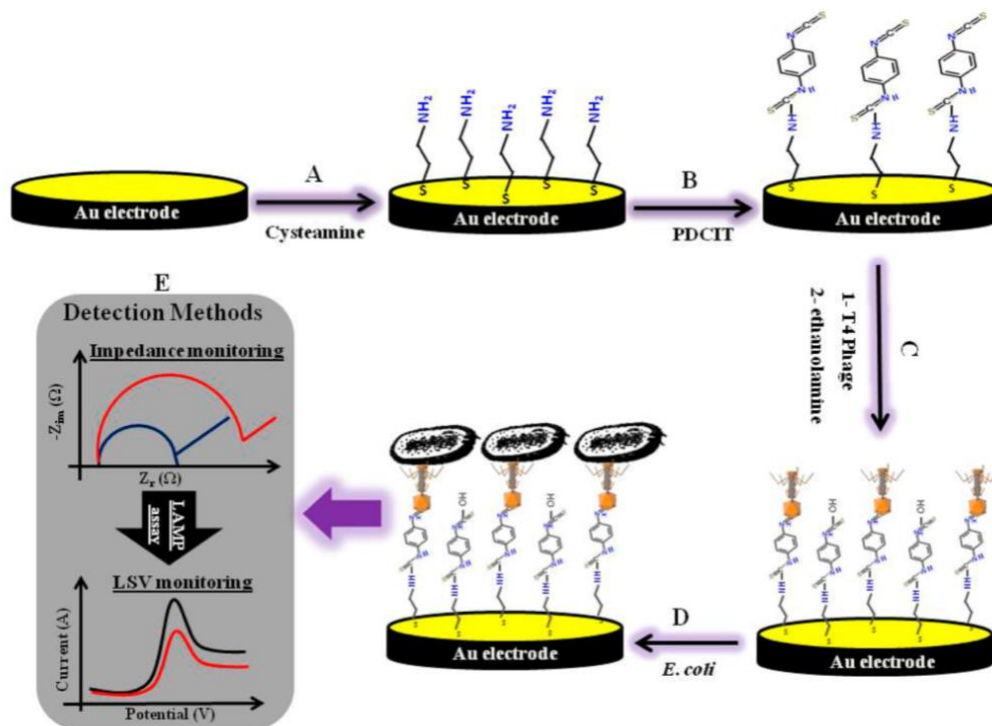


Figure 2.6. Representation of T4-bacteriophage-based biosensors with electrochemical impedance spectroscopy (EIS) and loop-mediated isothermal amplification (LAMP). (A) Cysteamine-assembly on gold electrode before activation with 1,4- dithiocyanate (PDCT) cross-linker (C) Immobilization of the T4 phage (D) Capturing of the *E. coli* cells and (E) Detection steps of *E. coli* cells based on EIS and LSV. Image adapted from Tili, Sokullu et al. (2013).

Bacteriophages have been utilized as bioreceptors for EIS detection of *E. coli* and were compared to its antibody counterpart (Mejri, Baccar et al. 2010). Both bioreceptors were immobilized in parallel onto interdigitated gold microelectrodes. The capture and lysis of target bacteria produced successive dual signals of opposite patterns. These two signals allowed

detection of target bacteria from non-target as well as from non-specific adsorption and cross-reactivity which were not observed when target cells were applied on antibody bioreceptors. This *E.coli* detection technology had an LOD of 10^4 CFU/mL.

Filamentous bacteriophages in magneto elastic sensor have been utilized for the detection of *Salmonella* spp. in fat free milk (Lakshmanan, Guntupalli et al. 2007). Bacteriophages replaced antibodies as probes that allowed quantification of target pathogen upon recognition and binding on the sensor's surface via the shift of resonance frequency. The LOD was 5×10^3 CFU/mL with a sensitivity of 159 Hz/decade in water samples as compared to 159 Hz/decade in fat free milk. The authors immobilized the filamentous bacteriophages on the surface of the sensors chips via physical adsorption by modifying the sensor surface with sugars (dextrose and sucrose) and amino acids (histidine and cysteine) which in earlier reports resulted in poor bacteriophage coverage (Singh, Glass et al. 2009).

E. coli-specific bacteriophage T4 was immobilized on the surface of screen-printed carbon electrode (SPCE) before coupling it with impedance measurements (Shabani, Zourob et al. 2008). The generated Nyquist plots in this study showed the binding of target bacterium, *E. coli*, shifted the impedance in the order of $10^4 \Omega$ and no significant response was observed when non-target and control were tested. Immobilization of bacteriophage T4 was conducted by 1-ethyl-3-(3-dimethylaminopropyl) carbodiimide (EDC)-bacteriophage interaction, specifically via EDC-amide (capsid) bond formation. The high LOD of 4 log CFU/mL for 50 μ L samples can be attributed to the induced-lysis of target bacteria after capturing by the immobilized bacteriophages. This single target-binding event and release of cellular components from induced-bacterial lysis were the basis of impedance measurements which was highly-prone to

signal interference that contributed to high LOD which also made the reproducibility of the method to be very challenging.

A similar study was conducted by Galikowska, Kunikowska et al. (2011) where they employed bacteriophages instead of antibodies in an ELISA-based detection of *Salmonella* spp. and *E. coli* strains. Bacteriophages (10^8 /well) were adsorbed onto the polystyrene surface of ELISA plate wells before subsequently adding bacterial samples and biotinylated anti-rabbit secondary antibodies. Signal measurement determined the sensitivity of the assay, 10^6 /mL, which was comparable to ELISA in terms of detecting target bacterial cells without enrichment but still relatively poor if the technology will be applied on routine food analysis.

Researchers have also explored utilizing not the entire bacteriophage structures but only bacteriophage-derived affinity molecules as recognition elements. Tolba, Ahmed et al. (2012) developed a biosensor with a cell wall binding domain (CBD) of bacteriophage-encoded endolysin before immobilizing it on the surface of gold-screen printed electrode (SPE) and employing EIS for *Listeria* spp. detection. By using the EDC/NHS interaction, the endolysin was coupled onto the gold (SPE) for capturing and detecting *Listeria innocua* serovar 6b. The integration of CBD-encoded endolysin with EIS allowed the direct detection of target bacterial cells with an LOD of 1.1×10^4 CFU/mL for pure culture samples and 10^5 CFU/mL for 2% milk. Endolysin is a peptidoglycan hydrolase encoded by bacteriophages (Heselpoth, Yin et al. 2015). As an enzyme, its stability in various conditions such as relatively high temperature and pH may cause its denaturation especially after its integration onto the biosensing system.

Surface plasmon resonance (SPR) is a direct technique that allows the measurement of the refractive index (RI) caused by biospecific interactions such as antibody-antigen binding at or close to a thin metal film surface of an assay (Nanduri, Bhunia et al. 2007, Velusamy, Arshak

et al. 2010, Yakes, Papafragkou et al. 2013). Refractive index (RI) can also be used to determine binding kinetics and thermodynamics (Nanduri, Bhunia et al. 2007). It also measures the change of angle of the reflected light as a function of change of density of medium against time (Velusamy, Arshak et al. 2010). The amount of shift in SPR angle can be related to the concentration of the bound molecules (Narsaiah, Jha et al. 2012). SPR technique with *S. aureus*-specific lytic bacteriophage was used by Balasubramanian, Sorokulova et al. (2007). Initially, the bacteriophage was immobilized on the surface of SPREETA™ sensor gold chip via physical adsorption before employing SPR measurements with target and non-target samples.

SPREETA™ is a sensor which is integrated with SPR system (light emitting diode of 840 nm and Si-photodiode array), a flow cell and control box. The SPR platform had an LOD of 10^4 CFU/mL in pure culture. Since the bacteriophages were immobilized on the surface via physical adsorption, it was expected to cover less area and had weak attachment. It has been found that bacteriophage detachment from the surface was reduced when they were covalently linked (Hosseinidou, Van de Ven et al. 2011). Thus, a stronger immobilization approach is needed to improve the sensitivity of this bacteriophage-based biosensor.

Rapid screening and detection assays for spoilage organisms and foodborne pathogens have been widely accepted by the food industry but improved testing methods that would permit reproducible same-day detection of initial low-level contaminants are needed (Leach, Stroot et al. 2010, Wiedmann, Wang et al. 2014). With this, bacteriophages have shown great viability and excellent features as an alternative that can also improve the currently used biorecognition elements due to its abundance in nature, high specificity, require inexpensive procedures during modification and have high resistance to extreme conditions that most recognition elements do not possess.

However, most of the current bacteriophage-based biosensors have not attained low LOD, and the majority of the reported methods achieved 10^3 CFU/mL LOD, even in pure culture setup. This phenomenon can be attributed to the design of the detection system and the platforms that were utilized. Many of these detection systems employed single-binding event between the biorecognition or capture element of the biosensors and target analyte. Though bacteriophages have shown high-specificity toward its bacterial, incorporating it onto the detection system as the biorecognition elements may need a secondary binding event to enhance sensitivity, specificity and reliability. Secondary binding event is often employed in dual-site binding assay or known as sandwich assay. The first element captures the target analyte while the second one acts as the reporter probe. The capture molecules are normally immobilized onto the surface of solid supports. Most of bacteriophage-based biosensors are coupled with screen-printed electrodes (SPE). SPEs are advantageous to use because it is a disposable device that can be discarded after carrying out single analysis. This property is due to its low-cost production, thus preventing cross-contamination and erroneous read-outs during analysis. More importantly, SPE offers great flexibility by allowing customization and modification of its surface depending on the composition and assembly required for the electrochemical system. SPE has rapid results capability, easy to use and practical which provide substantially wide applications in the field of development of selective and sensitive biosensing.

The reporter probes are often conjugated with signaling compounds and moieties which generate signals that can be correlated to the amount of target analytes present in the samples. Bacteriophages are highly-flexible in terms of its biocompatibility with most signaling moieties (ie. enzymes, fluorophores and nanoparticles). With these two layers of recognition, the

performance of bacteriophage-based can be greatly improved even when used in more complicated setup and testing various complex matrices.

2.2.2.1.1.6. Cell-based Biosensors

Cell-based biosensors (CBB) are integrated with live cells and transducers for cellular physiological parameter detection, pharmaceutical effects, toxicity test and rapid diagnostics in food microbiology (Banerjee, Lenz et al. 2007, Liu, Wu et al. 2014). Cell culture, silicon microfabrication and genetic technologies have promoted extensive investigation of CBB (Wang, Xu et al. 2005). Cell-based biosensors are consisted of two main parts: the living cells which act as the sensing element that receive and produce signals and the second is the transducer that converts the physiological signals to quantifiable electrical signals. Similar to other biosensors, CBBs requires isolation and immobilization of the living cells on the surface of its transducer (Liu and Wang 2009).

Banerjee, Lenz et al. (2007) developed a multi-well plate biosensor containing B-cell hybridoma, Ped-2E9, encapsulated in type I collagen matrix for the detection of *Listeria* spp and *Bacillus* spp and their toxins, listeriolysin O and enterotoxin, respectively. The principle behind this study was to colorimetrically quantify the released alkaline phosphatase from infected Ped-2E9 cells. *L. monocytogenes* or *B. cereus* cells and its toxins showed cytotoxicity ranging from 24 to 98% at 3-6 h after infection which were significantly lower (0.4-7.6%) as compared to its non-pathogenic counterparts, *L. innocua* (F4247) and *B. subtilis*. CBB can rapidly detect pathogenic bacteria and their toxins with high sensitivity though moving it into a portable and on-site detection system can be very challenging.

2.2.2.1.1.7. Biomimetic-based Biosensors

Materials science and chemistry are increasingly focusing on generating artificial matrices using the biomimetic approach. Artificial receptor strategies in chemical and biological sensing for large biological entities, such as bacteria, viruses, proteins are currently developing towards a mature discipline (Hussain, Wackerlig et al. 2013).

In a study described by Sankaran, Panigrahi et al. (2011), they developed odorant-binding protein based quartz crystal microbalance (QCM) sensors for detecting alcohols, 3-methyl-1-butanol and 1-hexanol. These volatile organic compounds (VOCs) are bacterial gaseous metabolites trapped in the headspace of packaged products that are also specific indicators of *Salmonella* contamination in packaged beef. The olfactory sensors mimicked insect (*Drosophila*) odorant binding protein (LUSH) sensitive to alcohols and was used as the sensing material by initially depositing it into the QCM through self-assembly. This newly-developed sensor was sensitive to alcohols with estimated lower detection limits of < 5 ppm. However, these sensors did not generate high sensitivity to other VOCs tested and the specificity and applications to real food samples were not conducted.

Another biomimetic-based biosensor was reported by Oh, Chung et al. (2014). Volatile organic compounds and explosive chemical (trinitrotoluene - TNT) were detected using this newly-developed colorimetric biosensor (Phage Litmus) which was composed of phage-bundle nanostructures and possess viewing-angle independent color, similar to collagen structures in turkey skin. Phage Litmus responded to changes in humidity upon exposure to TNT and to changes of polarity index of different volatile organic compounds. The biosensor quickly swells and goes through distinct color changes. The phage displaying TNT-binding peptide motifs can selectively distinguish TNT down to 300 ppb over similar chemicals by using handheld camera

such as iPhone coupled iColour Analyser software. Application to non-gaseous matrices still needs to be explored.

2.2.2.1.2. Other Types of Portable Biosensors and New Trends in On-Site Pathogen Screening

2.2.2.1.2.1. Lab-on-chip

Lab-on-chip is one of the interesting technologies that promise to bring detection assay in the field for application. It is a tool that integrates multiple laboratory functions onto a portable platform (approx 1 mm or cm) with highly manipulative microfluidics system to build mini laboratories as shown in **Figure 2.7** (Yoon and Kim 2012).

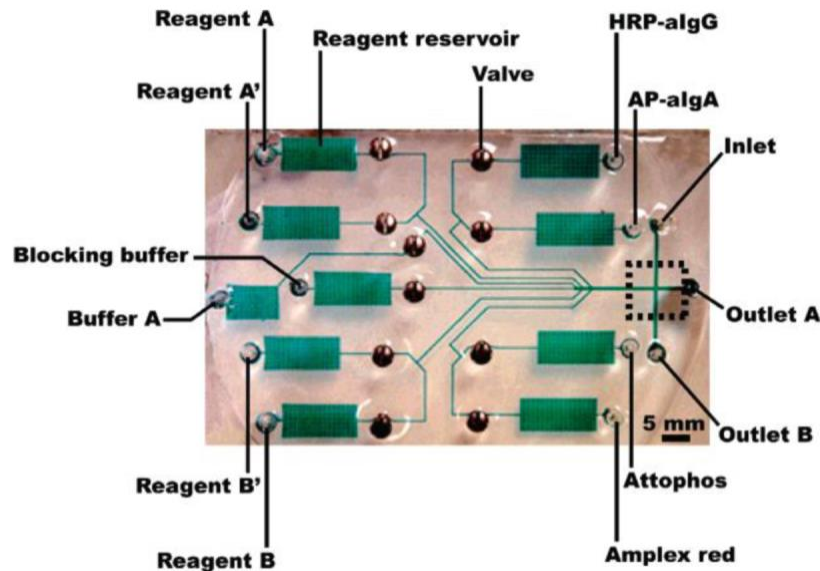


Figure 2.7. An example of a lab-on-chip (microfluidics). The extensive network of channels and wells of a microfluidic system. Image adapted from Yoon and Kim (2012).

Some of the advances in lab-on-a-chip technologies are presented here. Rapid detection of *S. Enteritidis*, *Streptococcus pneumoniae* and *E. coli* O157:H7 by using the Culture–Capture–Measure (CCM) approach “on a chip” coupled with SPR has been recently reported by

Bouguelia, Roupioz et al. (2013). Micro total analysis system (μ TAS) (Birnbaumer, Lieberzeit et al. 2009) capable of continuously monitoring viral contamination (Tobacco Mosaic Virus TMV and the Human Rhinovirus serotype 2, HRV2) with high sensitivity and selectivity by microfluidics containing integrated native polymer and molecular imprinted polymer with contact-less dielectric microsensors shows promising potentials for screening foodborne viruses. Lab-on-chip as a carbon nanotubes based immunoassay for detection of *Staphylococcal* Enterotoxin B (SEB) as described by Yang, Peng et al. (2013) is a versatile approach aimed to aid end-users to conduct testing outside the laboratory.

A simultaneous detection STEC O157 and *L. monocytogenes* with a novel microfluidic duplex droplet digital PCR (ddPCR) platform that used a mineral oil-saturated polydimethylsiloxane (OSP) chip was reported by Bian, Jing et al. (2015). They coupled it with TaqMan-MGB fluorescent probes which exhibited a single molecule resolution level (10 CFU/mL) when artificially inoculated drinking water sample was tested (2 h). A microfluidic lab-on-a-disc which was integrated with LAMP for *Salmonella* spp detection was also reported by Sayad, Ibrahim et al. (2016). It was a miniaturized system that allows reagent preparation, LAMP, and pathogen detection all integrated onto a single microfluidic compact disc (CD) within 70 min. The LOD was 0.005 ng/ μ L DNA when tomatoes were artificially spiked with *Salmonella* spp. Both of these technologies provide the opportunity to test samples in the field using highly-compact hand-held devices. However, it is important to note that PCR-based detection technologies that are employed in some of the lab-on-a-chip mentioned here are not capable of discriminating live from dead cells which is a major consideration in the food safety area.

These are some of the newest development and trend in the field of on-site screening of STEC serogroups and other significant foodborne pathogens. Though further improvements are needed, the technologies that are presented here have high potentials in assisting the food industry and food safety regulators in the onsite monitoring and screening foodborne pathogens and other health hazards to maintain safe and healthy foods.

2.2.2.1.2.2. Portable Phone-based Biosensors

Mobile diagnostics has been attracting attention in food and agriculture, environmental monitoring and healthcare sectors, thus providing opportunities for rapid and on-site screening of target analytes (Ratani, Dario et al. 2017). Specifically, smartphones which are essential communication tools can also be deployed for detection and measurement of various targets due to the availability of its useful components such as battery, camera, display and intuitive user interface as well as wireless connections (ie Wi-fi, Bluetooth and cellular data service) (Kanchi, Sabela et al. 2017, Ratani, Dario et al. 2017). However, to be able to fully utilize and convert smartphones into diagnostic instruments, it has to be augmented with the necessary accessories and software or applications (Apps).

A smartphone-based biosensor was recently reported by Shrivastava, Lee et al. (2018) for detecting *S. aureus* in processed liquid samples using functionalized fluorescent magnetic nanoparticles (**Figure 2.8**). In brief, fluorescent magnetic nanoparticles (FMNPs) were utilized to capture and detect the target bacterium via smartphone imaging. A customized cassette was built to mix the samples with aptamer-conjugated FMNPs. The FMNP-tagged bacteria cells were then imaged using a smartphone camera integrated with white light-emitting diode (LED). The minimum detectable concentration of the system was 10 CFU/mL by counting individual cells of *S. aureus* from peanut milk sample. One of the major drawbacks of aptamers is its stability due

to rapid degradation. Though the technology was tested on peanut milk sample, complex matrices with high protein and enzyme contents can have a direct adverse effect on the function and recognition capabilities of aptamers.

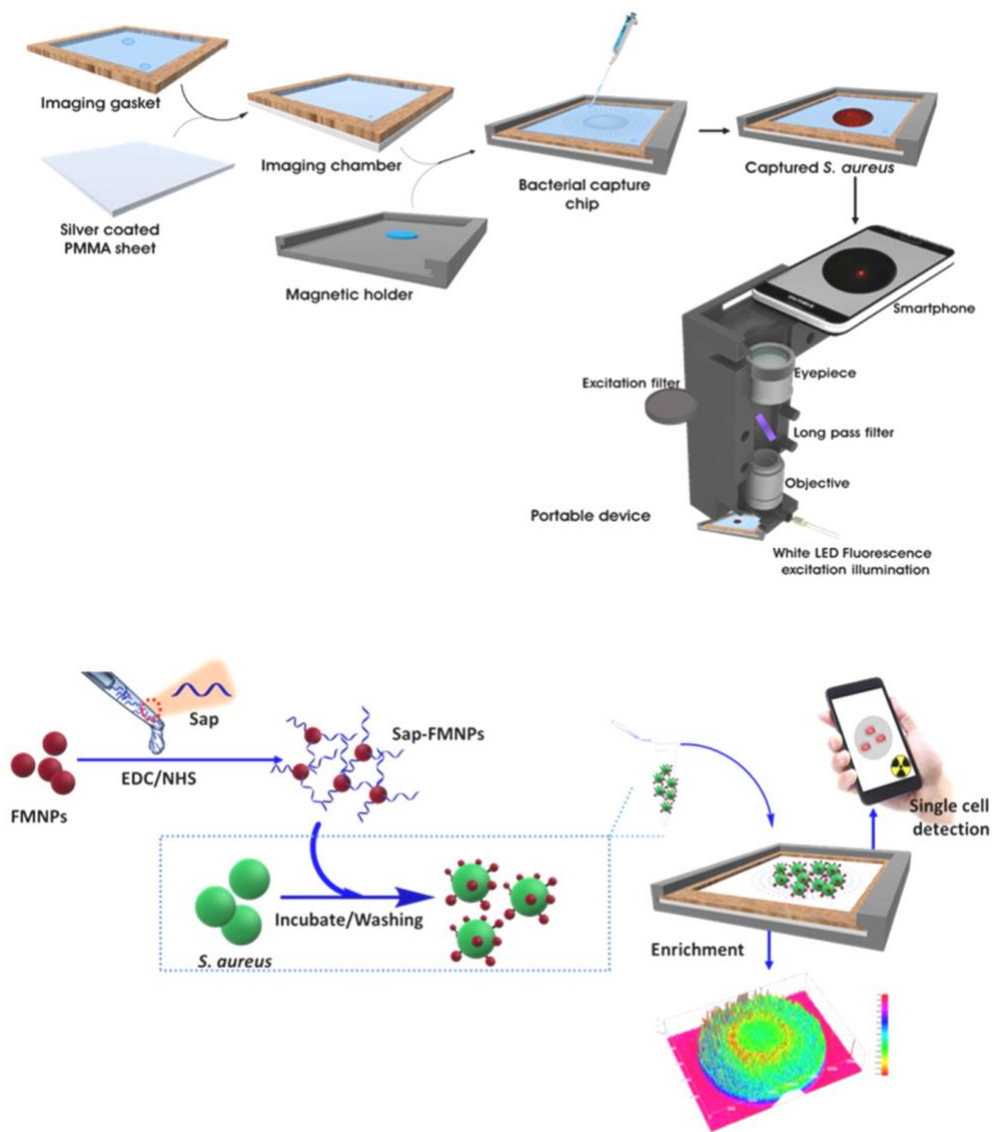


Figure 2.8. Schematic representation of a smartphone-based biosensor with *S. aureus* aptamer (Sap)-conjugated fluorescent magnetic nanoparticles (FMNPs). A reflective polycarbonate sheet and a gasket with magnet comprised a sealed chamber forming a cassette for sample testing. Captured target pathogen was washed and imaged with a smartphone fluorescence microscope for detection and quantification. Image adapted from Shrivastava, Lee et al. (2018).

Another smartphone-based biosensor was reported by Zeinhom, Wang et al. (2018) for the detection of STEC O157:H7 using sandwich ELISA with fluorescent imager and compact laser-diode-based photosource attached to the smartphone (**Figure 2.9**). In brief, an excitation light resource that illuminated the sample chamber (cuvette) with a signal collection system were assembled with the smartphone. Based on sandwich ELISA, fluorescein isothiocyanate (FITC)-labeled rabbit polyclonal antibody and magnetic beads labeled monoclonal antibody were conjugated with the target *E. coli* O157:H7 and formed a sandwich structure. The fluorescent imager on the smartphone had a laser-diode-based photosource with interference filter and insert lenses. Fluorescent signal emission from the samples was captured and recorded by a sensor chip and built-in lens embedded on smartphone for detection. The mean fluorescence intensity was then analyzed by picture processing program. The LOD of the new method for both milk and egg was around 10 CFU/mL. However, due to the dependence of the system on sandwich detection with antibodies (both polyclonal and monoclonal), the assay is highly prone to cross-reactivity as well as high-cost of manufacturing which is not the best option for routine testing and screening of target bacteria on various food or environmental samples.

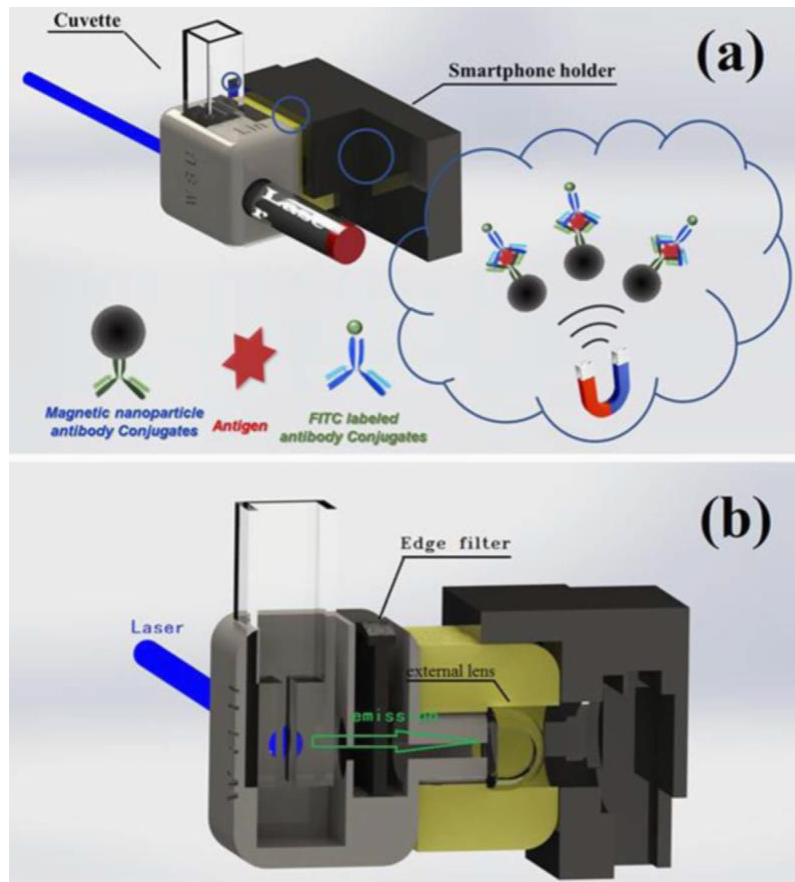


Figure 2.9. Schematic representation of the smartphone-based device for STEC O157:H7 detection. Sandwich immunosensing was employed using fluorescein isothiocyanate (FITC)-labeled rabbit polyclonal antibody and magnetic beads labeled monoclonal antibody for STEC O157:H7 detection. Image adapted from Zeinhom, Wang et al. (2018).

Biosensors provide rapid screening and measurements of foodborne pathogens on complicated matrices within hours and allow on-site screening instead of conducting laboratory-based assays. Although there have been numerous materials available to use for biorecognition purposes, the cost, sensor performance, sensitivity, specificity and the ability to detect live or viable cells are important considerations. Bacteriophages are unique entities that can provide superior selectivity and high compatibility with various detection platforms even after its integration with the biosensing systems.

CHAPTER 3

ISOLATION AND CHARACTERIZATION OF STEC-SPECIFIC BACTERIOPHAGES FROM THE NATURAL ENVIRONMENT

3.1. Introduction

Bacteriophages are considered as the most abundant biological entities on Earth, approximately 10^{31} and can be found almost everywhere including soil, water, even within human and animal bodies (Callaway, Edrington et al. 2008, Shahrabak, Khodabandehlou et al. 2013, Liu, Niu et al. 2015, Jurczak-Kurek, Gąsior et al. 2016). Bacteriophages are obligate bacterial parasite that subvert bacterial host resources (Hagens and Loessner 2007, Singh, Arutyunov et al. 2012). Specifically, it infects and colonizes susceptible bacterial host by binding to highly-specific receptors that are expressed on the cell surface, injects its DNA and control local cellular machineries for the production and release (cell lysis) of its progeny. Bacteriophage also integrates its DNA into the host bacterial genome during its lysogenic phase and continuously carried by host daughter cells during replication.

In its natural environment, bacteriophages can inhabit mammalian gastrointestinal tract (GIT) where they become part of the microbial ecosystem (Callaway, Edrington et al. 2008). Microbial composition across bacterial ecology system of the ruminants GIT has shown high heterogeneity (Mao, Zhang et al. 2015). Specifically, cattle are asymptomatic carriers and natural reservoirs of Shiga-toxin producing *Escherichia coli* (STEC), a group of foodborne pathogens that has been attributed to major food outbreaks (O'flynn, Ross et al. 2004). It has been found that 30% of feedlot cattle in North America shed O157:H7 strains in its feces (Niu, Stanford et al. 2012). In addition, cattle have also been shown to shed approximately 10^7 bacteriophages per

gram of manure (Callaway, Edrington et al. 2008, Niu, McAllister et al. 2009). Considering bacteriophages life cycle and its relationship with its bacterial hosts, researchers have found its potential to mitigate O157:H7 in ruminants (Wang, Niu et al. 2015).

Bacteriophages have become a promising approach as biocontrol agents due to the continuous unraveling of new information about its biology, host specificity, impacts on normal microflora and mammalian cells as well as ease of propagation (Shahrbabak, Khodabandehlou et al. 2013). Advanced technologies can ensure absence of virulence or antibiotic resistance genes increasing its efficacy and level of safety in phage therapy. In addition, bacteriophages that are highly-infective over a range of target groups and possess lytic life cycle that prevents recombination of its DNA with bacterial chromosome are key characteristics of excellent agents for biocontrol use. Because bacteriophages are bacterial predator, they can provide natural and non-antibiotic options that can reduce the incidence of foodborne pathogen contamination such as STEC serogroups from food supply.

Specific and rapid detection of foodborne pathogens in the food system is significant for containment and prevention of human, animal and plant diseases (Singh, Arutyunov et al. 2012). Biosensors overcome the limitations of traditional foodborne pathogen detection such as tedious and time consuming by providing reliable, specific and highly sensitive platforms with shorter turnaround time. More importantly, biosensors circumvent the limitations of the traditional laboratory microbial screening by its hand-held features and portability for on-site rapid analysis and detection of significant groups of foodborne pathogens and toxins. Bacteriophages possess excellent host selectivity attributes and have been used as biorecognition elements for pathogen detection (Singh, Poshtiban et al. 2013). Rapid detection technologies can take advantage of each

bacteriophage-host recognition stage and infection pathway to cover a wider range of foodborne pathogens targets.

The aim of this study was to isolate and characterize STEC-specific bacteriophages from environmental cow manure and water samples for potential biosensor and biocontrol use.

3.2. Materials and Methods

3.2.1. Bacterial Strains and Growth Conditions

All bacterial strains used in this study were part of the University of Maine-Pathogenic Microbiology Laboratory, Orono, ME and USDA-Agricultural Research Services (ARS) Centers (Produce Safety and Microbiology Unit, Albany, CA and Wyndmoor, PA) strain collections. Representative strains of each top six STEC serogroups (O26, O45, O103, O111, O121, and O145), O157 ATCC (ATCC 43888), and non-O157 (O179) were included. For isolation, purification, enrichment and quantification of bacteriophages, STEC O26:H11 HH8, O26:H11 SJ1, O26:H11 SJ2, O26:H2 TB285, O45:H2 SJ7, O45:H2 05-6545, O45:H2 96-3285, O103:H2 GG7, O103:H25 SJ11, O103:H11 SJ12, O111:H8 EE5, O111:NM SJ13, O111:H- 94-0961, O121:H19 SJ18, O121:H19 96-1585, O145:NM SJ23, O145:H28 07865, O145:H- 94-0491, O179 were used individually or in cocktail, as hosts. All other non-STEC strains, *Salmonella* Typhimurium ATCC 14028, *S. Typhimurium* ATCC 6962 and *Listeria monocytogenes* ATCC 19115 and generic *E. coli* were used to assess host range and lytic capabilities of the environmentally isolated bacteriophages. Frozen bacterial strains in cryogenic beads (CryoSavers; Hardy Diagnostics, Santa Maria, CA, USA) were initially activated then revived in Brain Heart Infusion (BHI) broth (Neogen, Lansing, MI, USA) at 37°C. Viability of strains was confirmed using appropriate selective agar media, MacConkey Agar with Sorbitol (Neogen) for

STEC strains, Xylose lysine deoxycholate (XLD) agar (Neogen) for *Salmonella* spp. strains and Palcam agar (Neogen) for *L. monocytogenes*.

3.2.2. Isolation, Purification and Enrichment of Bacteriophages from Environmental Samples

Cow manures collected from twenty-one cows (steer and heifer) located in five different sites in the state of Maine were used for bacteriophage isolation. Sampling was conducted five times from February 2015 to October 2015. Each fresh manure sample (300 g approx) was freshly picked and placed in sterile Whirlpak bags (Fisher Scientific, Wilmington, DE, USA) before transporting to the laboratory in an iced container within 6 h of collection. Since cow manure samples originated from various sources, pH of each sample was measured and recorded prior to storage at -20°C. WRRRC-PSM had an in-house collection of environmental water samples from California and other neighboring states. In this study, one trough water sample from crop-growing areas in Salinas, California was also used to isolate bacteriophages from the natural environment.

In brief, 10 g or ml of environmental sample was mixed with modified 90 mL Tryptic Soy Broth (mTSB) containing 8 mg/L novobiocin and casamino acids (Neogen) and then pulsed twice at a medium speed oscillation (30 sec/sample). Homogenized samples were centrifuged at medium speed (4000 × *g*) for 15 min before collecting the supernatant, followed by mixing with a cocktail of seven overnight representative STEC pure culture strains (300 µL each) and CaCl₂ (10 mmol/L, final concentration). Mixtures were incubated overnight (37°C). To kill all bacterial cells, chloroform (4% v/v, final concentration) was added and kept at room temperature for 30 min. Medium speed centrifugation (4000 × *g*) was conducted for 15 min to collect the supernatant where potential bacteriophages were suspended.

To determine the specific susceptible STEC host strain, a 10,000-fold diluted supernatant (with potential bacteriophages) was spotted (10 μ L) on various Tryptic Soy Agar (TSA) (Neogen) plate with overnight lawn of individual STEC strains. Formation of spots after an overnight incubation at 37°C confirmed bacteriophage specificity and STEC host susceptibility. Spots were picked and mixed with the corresponding STEC host (300 μ L, overnight) for enrichment in 50 ml Tryptic Soy Broth (TSB) with CaCl₂ (10 mmol/ L, final concentration) under the same incubation conditions (37°C, overnight) as used previously.

For the initial enrichment of bacteriophage isolates, supernatant (100 μ L) was mixed with CaCl₂ (10 mmol/L, final concentration) and overnight STEC cultures (500 μ L) at 37°C for 24 hours. Only those STEC cultures which had spots and zones of clearing were used for this enrichment. Soft agar overlay technique as previously described by Kropinski, Mazzocco et al. (2009) was then conducted in three cycles to purify individual bacteriophages before the final enrichment. In brief, bacteriophage suspension (100 μ L) was mixed with its host bacterium (200 μ L, overnight culture) and distributed evenly to solidify on a bottom agar plate (TSA). After an overnight incubation at 37°C, a zone of clearing that showed in the overlay was sliced, picked and resuspended in 100 μ L 1X PBS.

Last, enriched bacteriophage samples were filtered using a 0.2 μ m membrane (Millipore, Billerica, Massachusetts, USA) before performing plaque assay on Tryptic Soy Agar (TSA) for titer level (PFU/mL) evaluation. All enriched bacteriophages were stored in Tryptic Soy Broth (TSB) at 4°C until further use.

3.2.3. Host Range, Lytic Capability and Virulence Genes

Bacteriophages that formed clear plaques during the spot assay were re-tested against non-STEC strains to determine specificity, host range, host susceptibility and lytic capability. In

brief, non-STEC overnight cultures were mixed with molten TSA (Neogen), incubated overnight at 37°C to create a lawn of bacteria. High titer bacteriophages stock solution was spotted on the agar and also incubated overnight at 37°C. Representative STEC bacteriophages were also tested for multiplicity of infection (MOI) (Niu, Stanford et al. 2012).

Bacteriophage stocks with $> 8 \log$ PFU/mL titer level (10^0 - 10^7) were serially diluted and mixed with overnight cultures of STEC strains (8 log CFU/mL) for 5 h at 37°C in 96-well microplate for spectrophotometric reading and analysis. The MOI of the bacteriophage was measured, $MOI = \text{titer level (log PFU/mL)}_f / \text{STEC (log CFU/mL)}$ where $(\text{PFU/mL})_f$ is the lowest bacteriophages concentration that nearly or completely lysed STEC based on the turbidity (least turbid).

Conventional PCR was also performed to determine the presence of STEC virulence genes, *stx1* and *stx2*. In brief, bacteriophage genomic DNA was extracted from purified bacteriophages using Phage DNA Isolation Kit (Norgen Biotek Corp, Ontario, Canada) following manufacturer's extraction. Extracted DNA was kept at -20°C until further use. Specific primers (**Table 3.1**) and amplification conditions as previously reported were used. The conventional PCR conditions were as follow, denaturation at 95°C for 2 min; 35 cycles of 30 sec denaturation at 95°C, annealing at 56°C for 30 sec, elongation at 72°C for 30 sec and final extension at 72°C for 5 min (Quintela, de los Reyes et al. 2015).

Table 3.1. Primers for stx genes (Quintela, de los Reyes et al. 2015).

Name	Sequence
<i>stx1</i> For(<i>stx1</i> -1-F)	5' - CATCGCGAGTTGCCAGAATG - 3'
<i>stx1</i> Rev(<i>stx1</i> -1-R)	5' - AATTGCCCCCAGAGTGGATG - 3'
<i>stx2</i> For(<i>stx2</i> -5-F)	5' - GTATAC GATGACGCCGGGAG - 3'
<i>stx2</i> For(<i>stx2</i> -5-R)	5' - TTCTCCCCACTCTGACACCA - 3'

3.2.4. Potential Biocontrol Capability of Isolated Bacteriophages

Aside from isolating bacteriophages, the same cow manure samples were also processed, screened and tested for the presence of STEC strains following the previous published study of Cooley, Jay-Russell et al. (2013). In brief, 1 g of samples was enriched in 9 mL TSB (Neogen) and processed for plating using Washed Blood Agar with novobiocin (Hardy Diagnostics, Springboro, OH), O-antigen serotyping and real-time (RT) PCR. Then, 1 mL of enrichment was centrifuged for 2 min at $10000 \times g$. Genomic DNA was extracted by boiling method (100 μ L, 80°C for 5 min and 100°C for 20 min) using PCR thermocycler (Biorad, Hercules, CA) and cleared out the cellular debris by centrifugation at $5000 \times g$. RT-PCR was performed by mixing 5 μ L of the extracted DNA (template), 0.3 μ M of primer and 0.2 μ M of probes as listed on **Table 3.2**. MX3000P RT-PCR machine (Stratagene Agilent, Santa Clara, CA) was set at 95°C for 10 min, 40 cycles of 95°C for 20 sec, and 60°C for 45 sec. The Cycle threshold (C_t) value below 27 was considered positive STEC strains.

Table 3.2. Primers and probes for RT-PCR (Cooley, Jay-Russell et al. 2013).

Name	Sequence
Stx1 forward	CATCGCGAGTTGCCAGAAT
Stx1 reverse	TCCCACGGACTCTTCCATCT
Stx1 probe	Q670-ATCTGATGATTTCTTCTATGTGTCCG-BHQ2
Stx2abc forward	GGACCACATCGGTGTCTGTTATT
Stx2abc reverse	CCCTCGTATATCCACAGCAAAT
Stx2abc probe	CFO560-CCACACCCACCGGCAGT-BHQ1
Stx2ex forward	GAAACTGCTCCTGTTTATACGATGAC
Stx2ex reverse	CCGGAAGCACATTGCTGAT
Stx2ex probe	FAM-CCCCCAGTTCAGAGTGAGGTCCACG-BHQ1
Stx2f forward	CGCTGTCTGAGGCATCTCC
Stx2f reverse	TCCTCTGTACTCTGGAAGAACATTAC
Stx2f probe	CFR610-TTATACAATGACGGCTCAGGATGTTGACCTTACC-BHQ2

3.2.5. Transmission Electron Microscopy

For morphological characterization of isolated bacteriophage, transmission electron microscopy was used. In brief, 4 mL of purified bacteriophage stock solution was ultracentrifuged for 2 h at $18000 \times g$ using Optima MAX-XP (Beckman Coulter Inc., Brea, CA). Samples were washed in 1X PBS buffer before dropping (2 μ L) onto carbon-coated Formvar films on copper grids. TEM samples on grids were negatively stained using 1.5% uranyl acetate (pH 4 - 4.5) air-dried and before viewing under FEI Tecnai transmission electron microscope (Tecnai G2 F20 model FEI, USA) at 200 kV. Negative staining was the most appropriate electron microscopy technique which allowed gross morphology, dimensions and ultrastructure investigation of bacteriophages with excellent contrast in a lighter background.

3.3. Results

3.3.1. Isolated STEC Bacteriophages, Host Range and Susceptibility

Fresh cow manures collected from heifers and steers that were raised in five different farms in the state of Maine were the primary sources of environmental samples. The recorded average pH was 7.24 ± 0.14 . In total, 21 bacteriophages were isolated, all of which lysed representative bacterial strains of various STEC serogroups and displayed no biological activities (ie no cell lysis and plaques formation) against non-STEC strains (*S. Typhimurium*, *L. monocytogenes* and generic *E. coli*) (**Table 3.3**). Site 3 had the most number of bacteriophage isolates (13 isolates) in which bacteriophage specific to STEC O26 was the most prevalent. Plaque morphologies were very similar among the isolates; most of it formed clear plaques which was common for virulent or lytic bacteriophages. The average diameter was in the range of 1-1.5 mm in TSA (Neogen) plates. In addition, STEC bacteriophages showed similar infective patterns against STEC strains. Relative to host susceptibility, MOI value was used as a parameter to classify host-bacteriophage interaction and infection. It is the lowest ratio of bacteriophage and STEC bacteria that resulted to complete lysis or lowest absorbance (least turbid) of an overnight STEC culture during 5 h of incubation with serially diluted bacteriophages (Niu, McAllister et al. 2014). STEC O26 and O45 representative strains were highly susceptible bacterial hosts based on MOI, 0.5 - 0.875 range (**Appendix -Figure 6**). Molecular characterization showed selected STEC bacteriophages were devoid of *stx1* or *stx2* gene; only one bacteriophage isolate specific to STEC O26 generated an amplicon (**Appendix-Figure 7**).

Table 3.3. Isolation of STEC bacteriophages from environmental cow manure samples. Cow manures were collected from five different locations in the state of Maine. The table shows the number susceptible STEC hosts to bacteriophages per site.

STEC and non-STEC host cells (Number of strains used)	Isolated bacteriophages per site (based on STEC host susceptibility)					Total
	Site 1 (n=5)	Site 2 (n=4)	Site 3 (n=1)	Site 4 (n=10)	Site 5 (n=2)	
STEC O26 (3)	2	2	2	1	1	8
STEC O45 (3)	0	0	3	0	1	4
STEC O103 (3)	0	0	3	0	1	4
STEC O111 (3)	0	0	1	0	0	1
STEC O121 (2)	0	0	2	0	0	2
STEC O145 (3)	0	0	1	0	0	1
STEC O157 (3)	0	0	1	0	0	1
<i>E. coli</i> (1)	0	0	0	0	0	0
<i>S. Typhimurium</i> (1)	0	0	0	0	0	0
<i>L. monocytogenes</i> (1)	0	0	0	0	0	0
Total bacteriophage isolate/site	2	2	13	1	3	
Total Isolated bacteriophages						21

n = sample size

3.3.2. Biocontrol Potential of Isolated Bacteriophages Against STEC Strains

In this study, characterization of STEC bacteriophages was conducted in conjunction with its potential biocontrol capability against STEC strains in the natural environment. As shown in **Table 3.4**, STEC strains were screened and detected from cow manure samples where STEC-specific bacteriophages were previously isolated. Presumptive STEC colonies from Washed Blood Agar were also evaluated by O-antigen typing which had negative results for all samples. These results were not conclusive; therefore RT-PCR analysis was further conducted.

Based on the C_t values of RT-PCR which targeted various *stx* variants, specific STEC host strains were not detected on three sampling sites (Sites 1, 3 and 5) but were present on the remaining two sites (Sites 2 and 5). C_t value below 27 was considered positive STEC strains.

Table 3.4. The specificity and potential biocontrol capability of isolated bacteriophages on its STEC hosts from cow manure samples. STEC strains were screened and detected from various cow manure samples where STEC-specific bacteriophages were previously isolated (Table 3.3).

Source	Bacteriophage-susceptible STEC host strains	STEC screening and detection assays		
		Washed Blood Agar with Novobiocin	Serotyping (O - antigen)	RT-PCR (C_t values \pm SD*)
Site 1 (n=5)	O26:H11 SJ11 O26:H11 SJ2	Negative (-)	Negative (-)	Non-detect
Site 2 (n=4)	O26:H11 SJ11 O26:H11 SJ2	Presumptive (+) colonies	Negative (-)	<i>stx1acd</i> 20.19 \pm 0.66 <i>stx2f</i> 19.22 \pm 0.81 <i>stx2ex</i> 18.99 \pm 0.64
Site 3 (n=1)	O26:H11 SJ11 O26:H11 SJ2 O45:H2 SJ7 O45:H2 05-6545 O45:H2 96-3285 O103:H2 GG7 O103:H25 SJ11 O103:H11 SJ12 O111:H8 EE5 O121:H19 SJ18 O121:H19 96-1585 O145:H28 07865 O157:H7 12900	Negative (-)	Negative (-)	Non-detect
Site 4 (n=10)	O26:H11 SJ11	Presumptive (+) colonies	Negative (-)	<i>stx1acd</i> 19.33 \pm 0.52 <i>stx2f</i> 17.66 \pm 0.60
Site 5 (n=2)	O26:H11 SJ11 O45:H2 05-6545 O103:H2 GG7	Negative (-)	Negative (-)	Non-detect

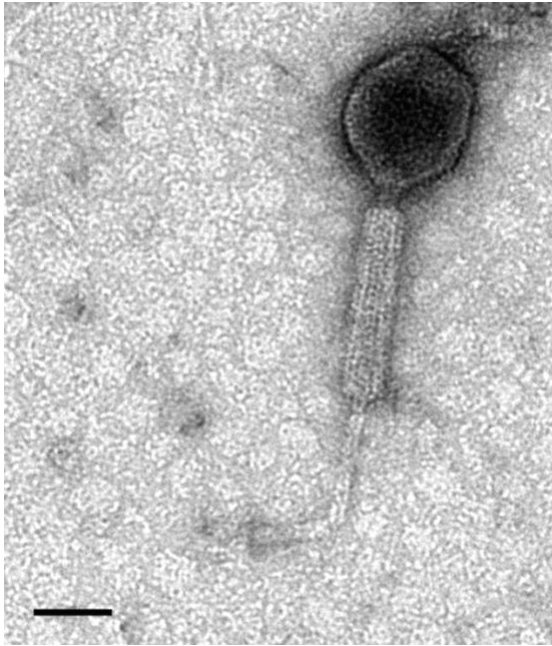
* C_t values ≤ 27 was indicative of strong positive reactions and abundance of target DNA;
n = sample size

3.3.3. Morphological Features of the Isolated Bacteriophages

Negatively-stained TEM samples provide a quick diagnosis to demonstrate structures in virology and basis to classify novel viruses into families (Ackermann 2012). In this study, negatively-stained bacteriophage both from cow manure and water environmental samples belonged to tailed-bacteriophage order *Caudovirales* based on the established parameters in published literatures. Published bacteriophage morphological dimensions have allowed grouping of the isolates into three families (*Siphoviridae*, *Myoviridae* and *Podoviridae*) under the order *Caudovirales* (Ackermann 1998, Jurczak-Kurek, Gąsior et al. 2016). TEM images in **Figure 3.1** show four bacteriophage isolates specific to STEC O157:H7, O121 and O103. Prominent morphological feature of STEC O157 bacteriophage was its contractile sheathed-tail that extended and covered more than half of its tail length, **Figure 3.1 (A)**. Other features such as collar, base plate and tail fibers were also observed in some isolates. The tail fibers that radiated from the baseplate of STEC O121:H19 SJ18 bacteriophage can be obviously seen on **Figure 3.1 (B)**. **Figures 3.2-3.4** show the ultrastructures of bacteriophages O121, O103, and O179 with dimensions, respectively. The diameter of icosahedral head (width perpendicular to the tail), head length (along the tail axis), tail length as well as tail diameter were all measured.

Based on the morphologies observed, the isolated bacteriophages were from families *Myoviridae* and *Siphoviridae*. According to Ackermann (1998) and Jurczak-Kurek, Gąsior et al. (2016), bacteriophages that exhibit tail length < 40 nm belong to *Podoviridae*. None of the isolates in this study had shorter tail length than 40 nm. For bacteriophages that possess tails longer than 40 nm, it can be classified either under *Myoviridae* or *Siphoviridae* based on tail diameter, specifically > 16 nm (*Myoviridae*) or < 16 nm (*Siphoviridae*).

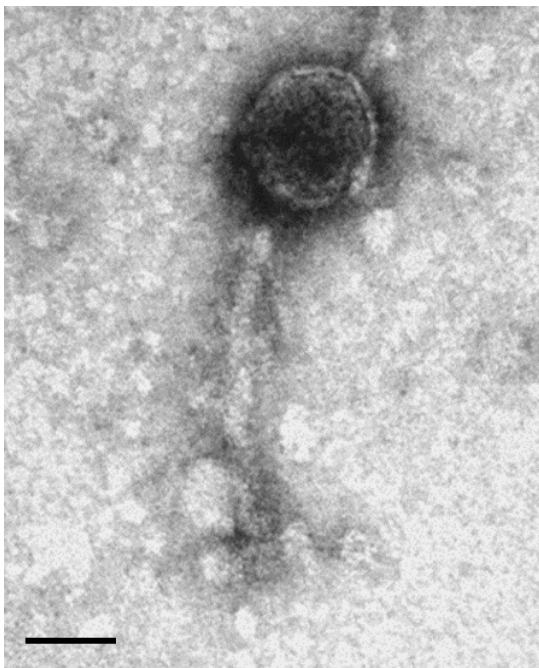
(A)



(B)



(C)



(D)

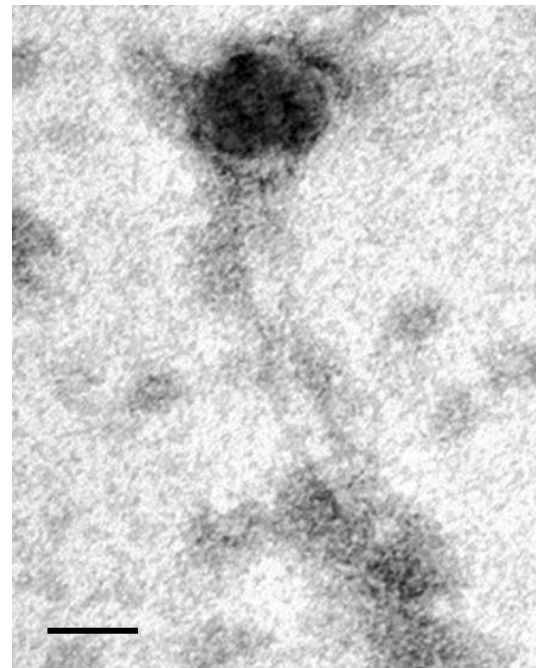


Figure 3.1. TEM images of various STEC-specific bacteriophages isolated from cow manure samples (A) STEC O157:H7 bacteriophage (B) STEC O121:H19 SJ18 bacteriophage (C) STEC 121:H19 96-1585 bacteriophage (D) STEC O103 bacteriophage. Scale bar: 50 nm

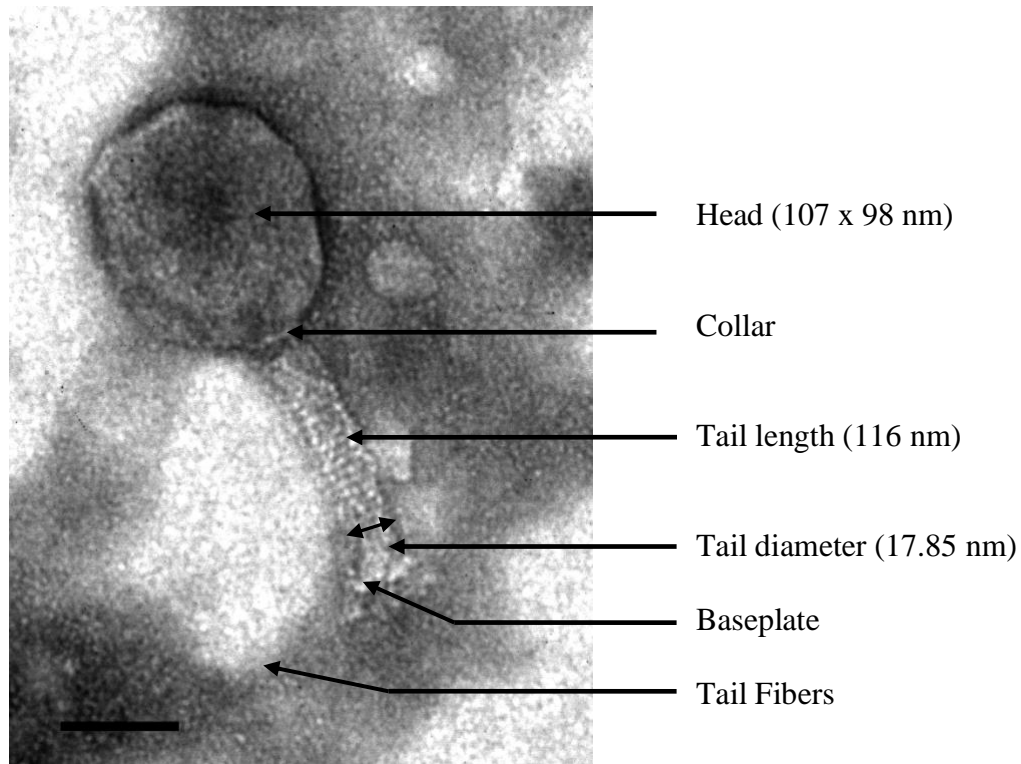


Figure 3.2. The ultrastructures of STEC O121:H19 SJ18 bacteriophage from cow manure samples. The TEM image shows the high-resolution morphological features of one of the environmental bacteriophage isolates having a complete icosahedral head and a long tail with appending tail fibers radiating from the base plate, suggesting that it belongs to *Myoviridae*. Dimensions: head = 107 x 98 nm, tail length = 116 nm and tail diameter = 17.85 nm Bar graph: 50 nm

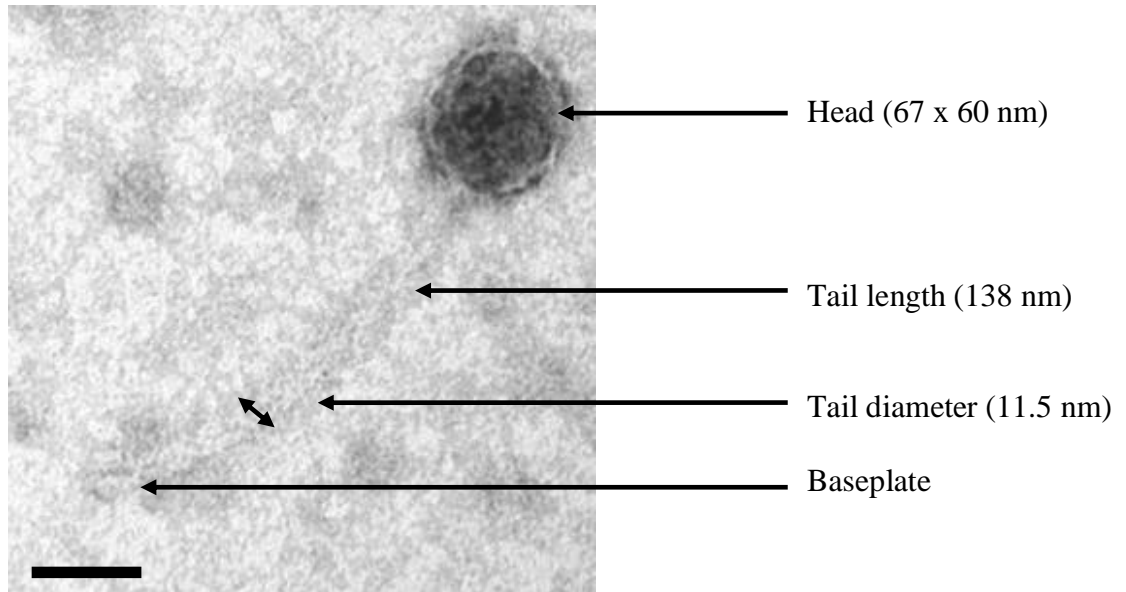


Figure 3.3. The ultrastructures of STEC O103 bacteriophage isolated from cow manure samples. The TEM image shows the high-resolution morphological features of STEC O103 bacteriophage but with longer tail as compared to other isolates. It has relatively smaller icosahedral head and baseplate which is typical STEC bacteriophage and suggesting that it belongs to *Siphoviridae*. Dimensions: head = 67 x 60 nm, tail length = 211 nm and tail diameter = 11.5 nm. Bar graph: 50 nm

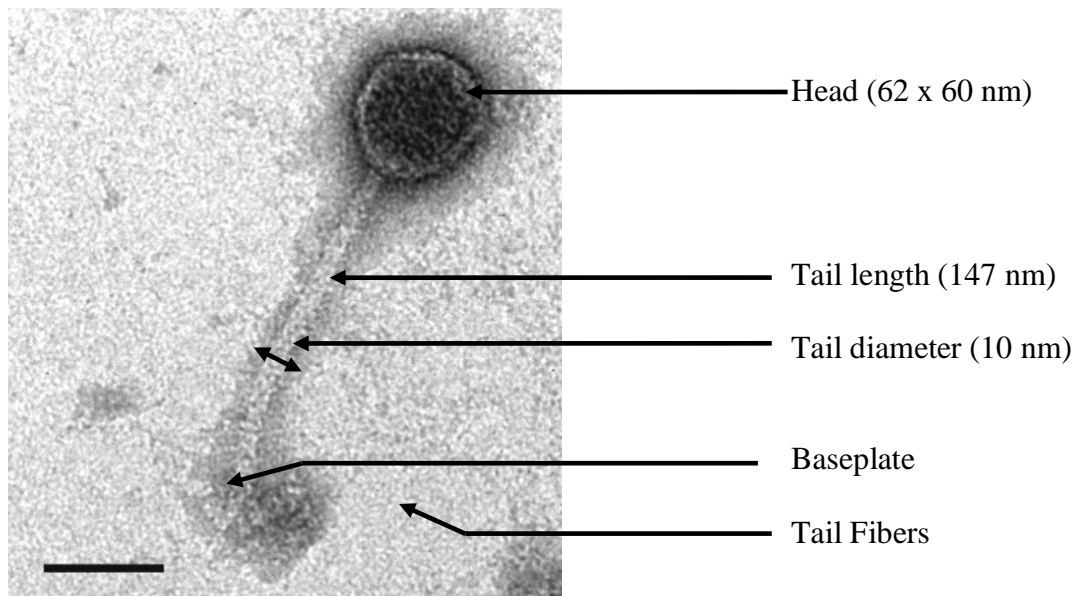


Figure 3.4. The ultrastructures of STEC O179 bacteriophage from water samples. The TEM image shows the high-resolution morphological features of STEC O179 under family *Siphoviridae*. Dimensions: head = 62 x 60 nm, tail length = 147 nm and tail diameter = 10 nm. Bar graph: 50 nm

3.4. Discussion

The intestines of healthy cattle are often colonized by STEC strains which then spread to the environment via fecal shedding and farm effluent on soil (Fremaux, Prigent-Combaret et al. 2008). It has been observed that the prevalence of STEC strains (ie O157:H7) in cattle herds fecal shedding has a seasonal pattern which peaks during summer months (Hancock, Besser et al. 1997, Niu, McAllister et al. 2009). Since bacteriophages are part of the microbial ecosystem of its bacterial host cells, it was expected to isolate bacteriophages that were specific not only to O157 serogroup but also to the other “top 6” non-O157 STEC serogroups from the manure samples.

In this study, a total of 21 STEC-specific bacteriophages were isolated from environmental fecal samples. Among these isolated bacteriophages, STEC O26-specific bacteriophage was the most prevalent. It was found in all five sampling sites with a total number of eight isolates or 38% of the total isolated bacteriophages. The wide distribution of STEC O26-specific bacteriophages was likely due to the prevalence of its host, STEC O26 serogroup. STEC O26 serogroup is the most common STEC host and dominant non-O57:H7 serogroup (Byrne, Vanstone et al. 2014). STEC O26:H11 was first identified in 1983 and has been detected both in meat and dairy products. It was the most commonly isolated non-O157:H7 serotype in Europe corresponding to 12% isolates in 2012 while in the US, it was around 22% of the clinical isolates from 1996 to 2013 (Bonanno, Petit et al. 2016). In addition, another surveillance study showed that STEC O26 serogroup was the most common serotype of the total STEC isolates (18%) from 1997 to 1999 (Hiramatsu, Matsumoto et al. 2002).

Bacteriophages specific to STEC O45 and STEC O103 serogroups had both four (19%) isolates each and tied as the second most prevalent isolated bacteriophage groups. In terms of the

distribution of STEC O45 serogroup, it was found to be the third most prevalent at 14.6% on summer months among the STEC serogroups though it was not detected on winter season (Dewsbury, Renter et al. 2015). For STEC O103 serogroup, it was revealed to be present in the cattle population during summer and winter seasons with a prevalence of 59% and 40.2%, respectively (Dewsbury, Renter et al. 2015).

This study has shown the prevalence and distribution of some STEC serogroups which agreed with the previous findings. This observational pattern also supported the hypothesis of bacteriophage and STEC host co-existence which was confirmed by the bacteriophage-STECHost interaction and susceptibility, and results of RT-PCR analysis. The diversity of the isolated STEC bacteriophages may have been influenced by the geographical sites where it originated from, as well as the diet and health conditions of cattle. Subsequently, the results also imply that non-O157 STEC bacteriophages (STEC O26, O45 and 103-specific bacteriophages) were more abundant in cattle as compared to STEC O157 bacteriophages. We hypothesized that the prevalent STEC bacteriophages must have possessed stable pathogenic properties that allow them to persist in the cattle reservoir as well as in the open environment. The average pH (7.24 ± 0.14) of the environmental samples may have also largely contributed to the persistence of STEC bacteriophages which was similar to the previous reports (Nyambe, Burgess et al. 2016). Bacteriophages are stable in the range of pH 5 - 9, coagulate at pH 2, loss its viability at pH 3 or lower, and precipitate at pH 3 - 4 though shaking would allow redispersion (Dini and De Urraza 2010, Jończyk, Kłak et al. 2011). In terms of its host bacteria, STEC serogroups can adapt and thrive under harsh conditions and consequently, the specific groups of bacteriophages can co-exist with them and take advantage of cellular machineries for survival and reproduction of bacteriophage progenies. Only one STEC bacteriophage was positive for *stx* gene among the

representative bacteriophages that were tested. *Stx*-negative bacteriophages do not pose threats of possible horizontal virulence genes transfer or transduction therefore can be potentially utilized as biocontrol agents against STEC strains.

Bacteriophage ecology influences the fecal shedding of STEC serogroup such as O157 in cattle and its environment (Wang, Niu et al. 2015). By utilizing several STEC screening and detection assays, this study has presented how the bacteriophage ecology played an important role in shaping the population of STEC serogroups in its natural environment. The data suggests that highly diverse bacteriophage populations (Sites 3 and 5), majority of which has lytic capability, are more likely effective in controlling the population of target STEC serogroups as compared to homogenous bacteriophage communities (Sites 2 and 4). When two or more groups of STEC bacteriophages were found in a single community, there was a decrease in the prevalence of STEC serogroups as shown by RT-PCR analysis which targeted variants of *stx* genes. Similar observations have been reported in studies where the effectiveness of individual bacteriophage was compared to bacteriophage cocktails in reducing STEC O157:H7 populations in the gastrointestinal tracts of sheep and ruminants (Bach, McAllister et al. 2003, Tanji, Shimada et al. 2004). Bacteriophages outnumber the coexisting bacteria in the natural environment and inflict significant reduction of its hosts bacteria population (Koskella and Brockhurst 2014). More specifically, bacteriophages compete for bacterial host cells as each bacterial strain could only be infected by up to two bacteriophage genotypes (Clokier, Millard et al. 2011). Hosts and bacteriophages coexistence often results in evolutionary arms race in order to sustain their abilities to survive (Shapiro, Kushmaro et al. 2009). This may be the highly plausible reason why STEC O26 serogroup was detected in the environmental samples where only a homogenous bacteriophage population was recovered. The dynamics of host-

bacteriophage coexistence and coevolution must have reduced the susceptibility of hosts to bacteriophage possibly by modulating the availability of receptors or blocking bacteriophage access to it, therefore allowing the host bacteria to persist and thrive (Samson, Magadán et al. 2013).

Most of the isolated bacteriophages belong to families *Myoviridae* and *Siphoviridae* under order *Caudovirales*. These families represent 96% of bacteriophages and share similar lifecycle, proteins and genes (Ackermann and Węgrzyn 2014). Members of these groups are tailed bacteriophages which were characterized and confirmed under TEM. Prominent isometric and elongated heads are some of its morphological features as well as the presence of crisscross sheath (Jurczak-Kurek, Gąsior et al. 2016). The receptor binding proteins (RBP) in bacteriophages are situated on the tail fibers and spikes which specifically bind to the receptors on the bacterial host surfaces (Samson, Magadán et al. 2013). Receptors include flagella, pilli, lipopolysaccharides (LPS), outer membrane and teichoic acids (Wang, Niu et al. 2015). Receptor localization, its amount and density determine the specificity of bacteriophage adsorption with its hosts (Rakhuba, Kolomiets et al. 2010).

The representative isolated STEC bacteriophages showed similar infective patterns against STEC strains. In terms of susceptibility, previous reports of Niu, McAllister et al. (2014) showed that MOI at 0.01 was extremely susceptible, MOI at 1 as highly susceptible while MOI at 10 as moderately susceptible. Both STEC O26:H2 and STEC O45:H2 have exhibited high level of sensitivities and susceptibilities with the isolated bacteriophages at MOI values within 0.5 - 0.875 range. The same trend was supported by the absence of STEC O45 strains from all the samples where STEC O45 bacteriophages were isolated. This suggests that in the natural environment, STEC O45 bacteriophage can effectively control and inhibit the population of its

host bacterium due to high susceptibility. Prevalence of other STEC serogroups (O103, O111, O121, O145 and O157) was also low as they were not detected from the screened samples where its infective bacteriophages were isolated. However, this susceptibility and sensitivity pattern did not extend to O26 bacteriophage based on the results of environmental screening for STEC O26. Two sampling sites (Site 2 and Site 4) had high STEC O26 serogroup prevalence while it coexisted with its infective bacteriophage. It is highly-likely that those bacteriophages may have successfully integrated its genome into its host's genome as it undergoes to the lysogenic phase of its life cycle. This may also suggest that in the natural environment, the susceptibility of STEC O26 serogroup to bacteriophage decreases or become non-susceptible at all due to coadaptation and coevolution via host-bacteriophage interaction. This can be one of the reasons behind its successful proliferation in the environment and considered as the most commonly encountered non-O157 STEC serogroup. Further investigation is needed to evaluate whether bacteriophage conversion from lytic (virulent) to lysogenic (temperate) has occurred during the course of its life cycle.

3.4. Conclusions

The newly isolated and characterized STEC specific bacteriophages were highly effective against major STEC serogroups. STEC O26 was the most prevalent bacteriophage group among the 21 isolated bacteriophages from the environmental cow manure samples that were collected from late winter to summer months. Most of the isolated bacteriophages were *stx*-negative, therefore do not pose threats of possible horizontal virulence genes transfer to its hosts. Isolated bacteriophages were under families *Myoviridae* and *Siphoviridae* with icosahedral head, sheathed-tail and fibers. In the natural environment such as in the cattle farms, heterogenous bacteriophage population is likely more effective in controlling and inhibiting its hosts

population as compared to its homogenous counterpart. The susceptibility of bacterial hosts to bacteriophages may either decrease or loss in the natural environment due to continuous coevolution and coadaptation through host-bacteriophage interaction. Purified bacteriophages were highly stable and infective (virulence genes-negative) for potential biocontrol and biosensor applications.

CHAPTER 4

**DEVELOPMENT AND OPTIMIZATION OF SHIGA TOXIN-PRODUCING
ESCHERICHIA COLI (STEC)-SPECIFIC BACTERIOPHAGE-BASED
AMPEROMETRIC BIOSENSOR**

4.1. Introduction

Shiga toxin-producing *Escherichia coli* (STEC) has been a significant cause of periodic and epidemic foodborne diseases such as gastroenteritis, hemorrhagic colitis (HC) and hemolytic-uremic syndrome (HUS) (Vallières, Saint-Jean et al. 2013, Beutin and Fach 2014, Quintela, de los Reyes et al. 2015). An estimate of 110,000 cases is reported each year, ranging from mild diarrhea to HUS (10%) and a recent multi-state prospective study showed 259 children had HUS as a complication of STEC O157:H7 infection (Fuller, Pellino et al. 2011, Mayer, Leibowitz et al. 2012). HUS is one of the primary causes of acute kidney injury (AKI) especially in pediatric patients (Trachtman, Austin et al. 2012, Vallières, Saint-Jean et al. 2013). Rapid and accurate screening of STEC using highly selective and easy-to-operate tools is one of the most efficient approaches to reduce the incidence of illnesses and hospitalizations caused by accidental ingestion of STEC cells through contaminated food products.

Cattles are identified as the natural reservoir of STEC and consumption of fecally-contaminated food or water is the primary route of STEC transmission to humans (Imamovic and Muniesa 2011, Beutin and Fach 2014). The gastrointestinal tracts of cattle and other ruminants may co-harbor STEC and bacteriophages as part of its microbiota. Bacteriophages are naturally-occurring infectious agents and predators of bacteria but pose no direct harm to humans. They are small viruses that can be utilized as recognition elements in bacterial biosensors due to its

ability to attach and infect bacteria with high specificity via bacterial receptors recognition (Shabani, Zourob et al. 2008, Velusamy, Arshak et al. 2010).

Biosensors are analytical devices that utilize and integrate biologically sensitive materials as recognition elements with a transducer to generate quantifiable signal proportional to the concentration of target molecules (Alonso-Lomillo, Domínguez-Renedo et al. 2010, Su, Jia et al. 2011). Coupling biocomponents with transducer techniques may involve electrochemical detection. Some of the important advantages of electroanalytical techniques include low limit of detection (LOD) and cost, relative simplicity, real-time and portable options (Alonso-Lomillo, Domínguez-Renedo et al. 2010). Most of these advantages have been fully utilized with the inclusion of screen-printing technology.

Screen-printing technology is applied to the manufacturing of inexpensive, sensitive and stable disposable electrochemical sensors (ie. electrodes) for the detection of significant compounds in trace amounts (Wring and Hart 1992). Screen-printed electrode (SPE), a planar electrode, is primarily based on a multilayer of printed inks on various substrates including polyimide, plastic, epoxy, or ceramic (Tangkuaram, Ponchio et al. 2007, Alonso-Lomillo, Domínguez-Renedo et al. 2010). For microbial biosensors, the effective conversion of biochemical response into a physical signal requires close association of the bioactive recognition element with its transducer via encapsulation, adsorption, cross-linking and covalent bonding (Su, Jia et al. 2011). Addition of analytes onto the functionalized transducer can result to a highly-specific interaction which is detected by several analytical sensing techniques such as amperometry, conductometry, potentiometry and voltammetry. The quantified signal is correlated with the analyte concentration (Su, Jia et al. 2011).

The use of antibodies as recognition elements is very common in diagnostics and foodborne pathogen biosensing applications due to its availability and high affinity (Kumar, Aaron et al. 2008, Karoonuthaisiri, Charlermroj et al. 2009). Monoclonal and polyclonal antibodies provide selectivity and specificity when incorporated as receptors. However, the major drawbacks of antibodies that are constantly met by end-users include high-cost of production, instability and high-prone to contamination and degradation rendering it very impractical and unreliable recognition elements. In addition, cross-reactivity towards other strains or species and interference are innate to polyclonal antibodies. With these drawbacks, bacteriophages that exist in nature and inexpensive to propagate are excellent alternative to antibodies as biological recognition receptors. More importantly, bacteriophages are highly-specific to its host bacteria and very stable that allows easy handling and storage.

The primary aim of this study was to develop and optimize an STEC-specific amperometric rapid biosensor integrated with novel bacteriophages as biorecognition and detection elements. Modification and incorporation of bacteriophages into antibodies-free recognition receptor systems would enable the development of highly sensitive and specific detection platforms for the detection of live cells of significant foodborne pathogens at low-cost with high reliability.

4.2. Materials and Methods

4.2.1. Reagents and Apparatus

Phosphate buffered saline 10X Solution (PBS), Pierce™ 20X TBS Tween™ 20 buffer (TBS-T20), biotin, sulfo-N-hydroxysulfosuccinimide (NHS), streptavidin, potassium ferricyanide $K_3[FeCN_6]$, 30% hydrogen peroxide (H_2O_2) solution, dimethyl sulfoxide (DMSO) solvent, sulfuric acid, ethyl alcohol as well as blocking reagents - Pierce Protein-Free blocking

buffer, polyethylene glycol (PEG), blocker-casein blocking buffer, Pierce™ BCA Protein Assay Kit, sulfosuccinimidobiotin (EZ-Link™ Sulfo-NHS-Biotin), Zeba™ Spin Desalting Columns, HABA (4'-hydroxyazobenzene-2-carboxylic acid), streptavidin-coated nanocrystals (Qdots) were all purchased from Thermofisher Scientific (Waltham, MA). N-(3-dimethylaminopropyl)-N'-ethylcarbodiimide hydrochloride (EDC), carboxymethyl dextran (CMD) sodium salt, horseradish peroxidase (HRP)-conjugated streptavidin (S-HRP) and bovine serum albumin (BSA) were from Sigma-Aldrich (St. Louis, MO) while the mediator, 1,1'-ferrocenedicarboxylic acid (FeDC) was purchased from Strem Chemicals (Newburyport, MA). Gold nanoparticles (AuNP) solution with an average diameter of 13 nm was synthesized following previous reports (Quintela, de los Reyes et al. 2015). Unmodified disposable screen-printed carbon electrodes (SPCEs, reference # DRP-110, DRP-C110) with three electrodes in ceramic substrate support (3.4 length x 1.0 width x 0.05 height cm) and silver contacts ideal for microvolumes (50 µL) were purchased from DropSens (Asturias, Spain) (**Figure 4.1**). These planar SPCEs were consisted of circular carbon working electrode (WE) (4 mm diameter), carbon counter electrode (CE) and silver reference electrode (RE). Electrochemical measurements were conducted with a PalmSens3 Electrochemical Portable Apparatus - Potentiostat/Galvanostat/Impedance Analyser (PalmSens Instrument BV, Houten, The Netherlands) which was wirelessly connected via Bluetooth™ and controlled by an Android™ device. The PalmSens3 instrument was used with three electrodes and its dynamic range allowed applications as microelectrodes such as SPCEs and supported by its software - PStace5 (Palm Instrument BV).

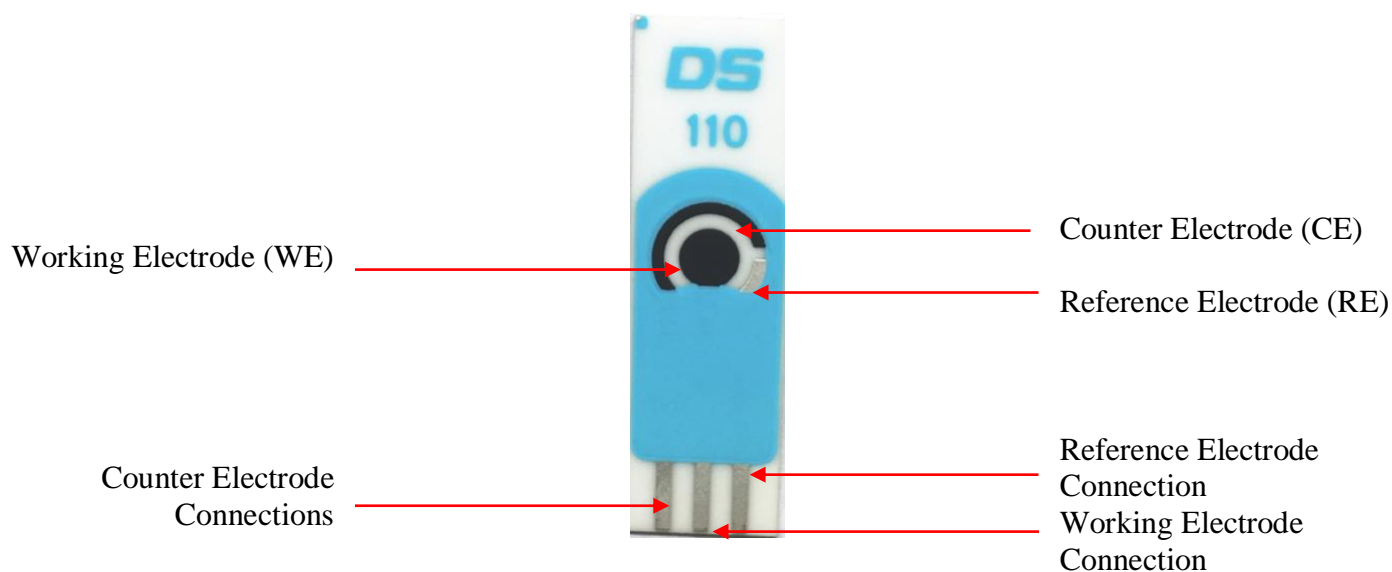


Figure 4.1. Screen-printed carbon electrode (SPCE). The general dimensions of SPCE: 3.4 x 1.0 x 0.05 cm. Working and counter electrodes are made of up of carbon. Silver is the main component of reference electrode and electric contacts in a ceramic substrate with cured carbon ink paste.

4.2.2. STEC Strains and Bacteriophages

All bacterial strains and STEC-specific bacteriophages (O26, O157, O179) used in this study were part of the University of Maine-Pathogenic Microbiology Laboratory, Orono, ME and USDA-Agricultural Research Services (ARS) Centers (Produce Safety and Microbiology Unit, Albany, CA and Wyndmoor, PA) collections. Representative strains of STEC serogroups (O26, O157 and O179) were utilized as target bacterial groups. These STEC strains have been fully-characterized in terms of its interactions with specific bacteriophages as discussed in the

previous chapter of this dissertation. All other non-STEC strains such as *Salmonella* Typhimurium ATCC 14028 and *Listeria monocytogenes* ATCC 19115 were tested as non-targets to evaluate the specificity and stability of the electrochemical detection system. In brief, frozen bacterial strains in cryogenic beads (CryoSavers; Hardy Diagnostics, Santa Maria, CA, USA) were initially activated and revived in Brain Heart Infusion (BHI) broth (Neogen, Lansing, MI, USA) at 37°C. Overnight cultures were washed in 10 mL 1X PBS by centrifugation at $5000 \times g$ for 10 mins. Pellets were resuspended in 1X PBS and serially diluted up to 10^{-7} . MacConkey Agar with Sorbitol (Neogen) for STEC strains, Xylose lysine deoxycholate (XLD) agar (Neogen) for *Salmonella* spp. strains and Palcam agar (Neogen) for *L. monocytogenes*. Plaque assay was performed to determine the titer level (PFU/mL) of bacteriophages while the viability of STEC strains were confirmed using appropriate selective agar media. In brief, diluted (10^{-5} , 10^{-6} , 10^{-7}) bacteriophage suspensions (100 μ L) were mixed with its overnight host bacterium culture (200 μ L) and molten TSA (5 mL) before pouring into plates. After an overnight incubation at 37°C, plaques were counted to calculate its titer level (PFU/mL).

4.2.3. Chemical Modification of Bacteriophages

The concentration (μ g/mL) of high-titer bacteriophage stocks (> 9 log PFU/mL) was determined using Pierce™ BCA Protein Assay Kit (Fisher Scientific, Wilmington, DE, USA) following manufacturer's instructions. In brief, a concentration standard curve of known protein - diluted bovine serum albumin (BSA), supplied in the kit was initially created as the basis for measuring the concentration of bacteriophage sample stock solution (400 μ L). Microplate reader was set at 562 nm to generate absorbance data and plotted the curve.

After measuring the concentration (μ g/mL) of purified bacteriophage stocks in 1X PBS, bacteriophages stocks were then biotinylated with increasing concentrations of

sulfosuccinimidobiotin (EZ-Link™ Sulfo-NHS-Biotin, Fisher) ranging from 1-20 mM. Bacteriophage-sulfosuccinimido-biotin sample mixtures were incubated at 4°C overnight and dialyzed using Zeba™ Spin Desalting Columns (Fisher) against 1X PBS to remove excess unbound biotin following manufacturer's protocol. Incorporated biotin was measured colorimetrically (500 nm) using HABA (4'-hydroxyazobenzene-2-carboxylic acid, Fisher) reagent following manufacturer's protocol. To monitor and investigate the effects of biotin on the morphology, biotinylated bacteriophages were coupled with streptavidin-coated nanocrystals (Qdots, Fisher) and viewed under the transmission electron microscope (TEM). In brief, 2 µL of biotinylated bacteriophage-nanocrystal solution was dropped onto carbon-coated formvar films on copper grids. Negative staining was performed using 1.5% uranyl acetate (pH 4 - 4.5) air-dried and viewed under FEI Tecnai transmission electron microscope (Tecnai G2 F20 model FEI, USA) at 200 kV. Last, to determine the optimum concentration of biotin, the maximum viability (titer level, PFU/ml) retention of bacteriophages was investigated by conducting plaque assays at pre and post biotinylation stages.

All modified bacteriophages were initially suspended in 1X PBS and stored at 4°C prior to their use. No activation was needed for all the modified bacteriophages (specific to STEC O26:H11, STEC O157:H7 and STEC O179) that were used to target host bacteria. However, as a quality check, occasional titer level evaluation was conducted throughout the experiment using plaque assay in TSA (Neogen).

4.2.4. Electrochemical Behavior and Characterization of SPCEs

Cyclic voltammetry (CV) is a robust and commonly-used electrochemical technique to investigate the reduction and oxidation processes of various molecular species as well as the electron transfer-initiated chemical reactions (Elgrishi, Rountree et al. 2017). Unmodified SPCEs

were electrochemically characterized with PalmSens3 system by recording cyclic voltammograms (CV) of 0.5 mM $K_3[Fe(CN)_6]$ in two separate supporting electrolytes, acid (0.1 M H_2SO_4) and salt (1X PBS) at increasing scan rates (50 mV/sec, 100mV/sec, 200mV/sec and 500 mV/sec) under the same potential step (-500 mV to $+500$ mV vs counter/reference electrode). SPCEs were previously rinsed with sterile distilled water (100 μ L) and further cleaned with ethyl alcohol (100 μ L) before air drying. Oxidation and reduction peak potentials during the scans were generated to identify the peak separation ($\Delta E_p = E_p^c - E_p^a$, where E_p^c is the cathodic peak and E_p^a is anodic peak) of the redox system for quality evaluation of the surface of SPCEs.

Last to characterize the behavior of SPCE when modified with various chemicals, all reagents involved in the modification of SPCEs were tested individually first using CV test with $K_3[Fe(CN)_6]$ as the probe. In brief, reagents (20 μ L) such as CMD-dextran, EDC-NHS, streptavidin, biotinylated bacteriophage, FeDC, AuNP, BSA, casein, protein-free blocking reagents and PEG were dropped individually onto the working electrode (WE) of single and clean SPCEs, air-dried and tested with 0.5 mM $K_3[Fe(CN)_6]$ for CV at 100 mV/sec scan rate.

4.2.5. Surface Modification and Biofunctionalization of SPCEs

To introduce carboxyl ($-COOH$) onto the clean WE surface, CMD-Dextran(Sigma-Aldrich) was added (20 μ L, 50 mg/mL) and incubated for 3 hr with shaking (300 rpm) at room temperature. Then, an equal volume of EDC (0.4M, Sigma-Aldrich) and NHS (0.1M, Thermofisher Scientific) were added to activate $-COOH$. After the activation, streptavidin (20 μ L, 50 μ g/mL, Thermofisher Scientific) which carried the amine, was transferred and incubated for 40 mins to allow carboxyl-to-amine crosslinking. Excess liquid was removed and the modified SPCEs were kept in humidified containers before adding biotinylated bacteriophages

(20 μL , $> 8 \log \text{PFU/mL}$), for overnight incubation at 4°C . Biofunctionalized SPCEs with immobilized biotinylated bacteriophages were blocked with 30% casein (20 μL) overnight at 4°C before washing them twice (100 μL) with TBS-T20 (Thermofisher Scientific) and once with 0.5 X PBS (100 μL). Selection and optimization of blocking reagents were presented in the Appendix section (**Appendix-Figures 8.1-12.2**). All biofunctionalized SPCEs were stored at 4°C until further use. For the purposes of this study, the term “capture elements” refers to biofunctionalized SPCEs and has been used here thereafter. The bioactivity of two-day old capture elements of modified-SPCE was evaluated using agar diffusion test with lawn of overnight host bacterium.

Successfully-modified and functionalized SPCE (capture element) was characterized by comparing its cyclic voltammogram with the unmodified form of SPCE. Individual reagents were serially added to the working electrode based on the previously determined optimized conditions. In brief, SPCE was initially activated with CMD-Dextran, then EDC-NHS and streptavidin were added prior to the immobilization of STEC O179-specific biotinylated bacteriophage. Blocking reagent (30% casein) and mediator (FeDC) were also applied before conducting CV testing at 100 mV/sec with 0.5 mM $\text{K}_3[\text{Fe}(\text{CN}_6)]$ in 1X PBS as the electrochemical probe.

4.2.6. Development of Bacteriophage-based Detection Elements and Substrate

To complete the detection system that would allow utilization of sandwich-type recognition of live STEC cells, the remaining integral component termed as “detection element” was constructed. Streptavidin-Horseradish peroxidase (S-HRP) (100 $\mu\text{g/mL}$) (Sigma-Aldrich) and AuNP solution (ave 13 nm diameter, 20 μM , 100 μL) were both added onto biotinylated bacteriophages (700 μL , $> 8 \log \text{PFU/mL}$) and incubated overnight at 4°C . The viability of

biotinylated bacteriophage/S-HRP/AuNP complex was evaluated using plaque assay with host bacterium and characterized by viewing TEM.

In brief, 2 μL of detection element solution was dropped onto carbon-coated formvar films on copper grids. Negative staining was performed using 1.5% uranyl acetate (pH 4 - 4.5) air-dried and viewed under FEI Tecnai transmission electron microscope (Tecnai G2 F20 model FEI, USA) at 200 kV.

4.2.7. Amperometric Tests and Limit of Detection (LOD)

The complete system architecture is shown in **Figure 4.2 (A)**. The configuration of the biosensor architecture included a PalmSens3 amperometric device which was wirelessly connected to an Android device via Bluetooth. A dongle that supported the connection was attached to one of the ports of PalmSens3 and the SPCE was inserted to its holder which was connected to PalmSens3 as well. To analyze the amperometric readouts, PSTrace5 app was installed in the Android device.

The principles behind the novel approach that features sandwich-type recognition by capture and detection of live bacterial cells via the highly-specific biotinylated bacteriophages and the subsequent redox reaction are presented in **Figure 4.2 (B)**. Modification and bioactivation of SPCEs which involved sequential addition of chemical reagents in microvolumes (20 μL) are detailed in the previous section (Section 4.2.5). These modification steps allowed stable immobilization of biotinylated bacteriophages to create the capture element structures for biorecognition and binding of live target bacterial cells.

Samples (50 μL) including controls were individually dropped onto each working electrode (WE) of biofunctionalized SPCEs and incubated for 12 min at room temperature before washing with 0.5 X PBS (100 μL). Once the target STEC cells were captured by the

immobilized biotinylated bacteriophages, the detection element (20 μL) was added for sandwich-type detection for 10 min before washing twice with 100 μL volume of TBS-T20 and 0.5 X PBS. The mediator (5 μL , 250 mM FeDC in DMSO) was also added. After 30 sec of incubation, 15 μL of hydrogen peroxide (40 mM H_2O_2) was also dropped also onto the WE. It was allowed to stand for another 30 sec prior to initiating amperometric tests. Amperometric detection was performed with a fixed potential of 0.5 V in all samples (triplicates) throughout the trials, 0.5 sec interval within 100 sec run time and an operating temperature around 25°C (room temp).

Amperometric test measured the response current (RC) that was generated by the substrate within a set of potentials over time and was used to calculate for the delta (Δ) current, [Δ current = response current of samples (target or non-target) – RC of control]. The delta (Δ) current was used to determine the specificity and sensitivity of the assay.

In this study, the signal threshold for positive detection was defined by the signal-to-noise (S/N) characteristics as $S/N > 3$, where the target could provide a signal a least three times greater than the signal from non-targets. The linear calibration curve ($y = mx + b$) assumed the response (y) is linearly related to the concentration (x)(Shrivastava and Gupta 2011, Tolba, Ahmed et al. 2012). The limit of detection (LOD) was determined by the statistical significance of signals (Δ current) between non-target bacteria and the lowest inoculum of target bacteria which had a calculated Δ current above signal threshold for positive detection.

4.2.8. Determination and Quantification of Sources of Background Noise

Key chemical reagents used for biosensing assembly were investigated to determine and quantify the noise that it may have contributed to the background signal of the system. Individual reagent was amperometrically tested for its RC to verify the specific sources of noise. In brief, 20 μL of reagent was added onto clean SPCEs and incubated for 30 sec before testing with the

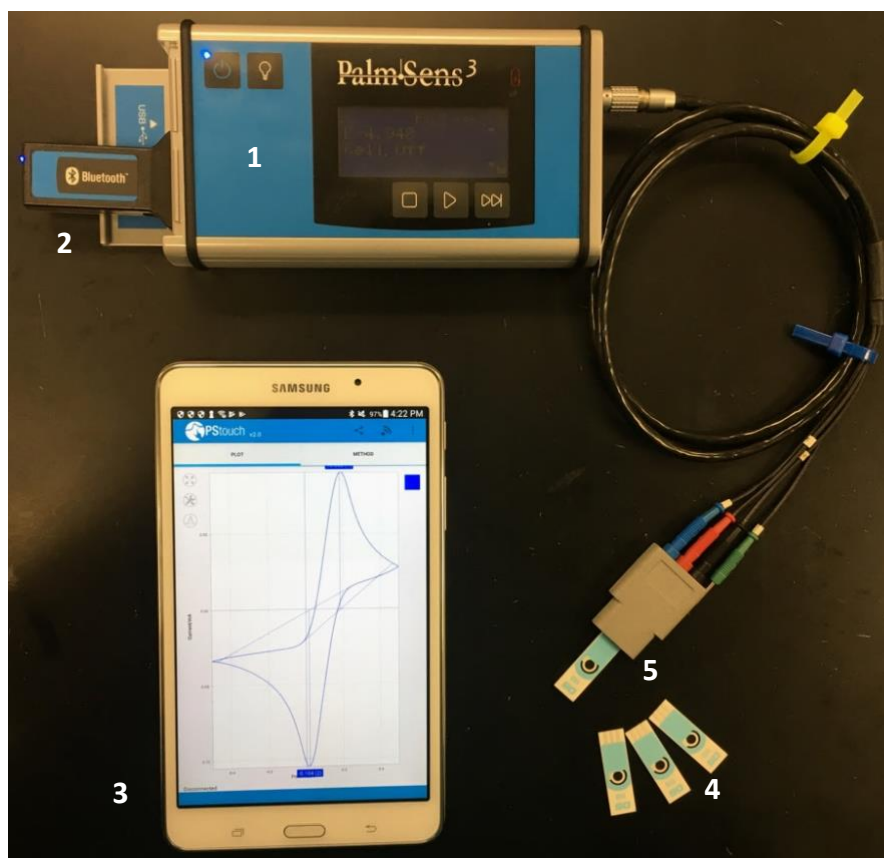
default amperometric measurement settings as mentioned in Section 4.2.6. RC was recorded.

Reagents were grouped as (1) reagents (2) detection elements (3) modified SPCEs.

4.2.9. Statistical Analysis

Three trials were performed per each experiment. To evaluate the assay's reproducibility, triplicates of disposable and modified SPCE per each sample were tested. The mean of the data \pm standard deviation (S.D.) was analyzed by JMP software using one-way ANOVA for significance ($P \leq 0.05$). Fisher's least significance difference (LSD) was then used for post-hoc analysis to confirm the significant differences between groups.

(A)



(B)

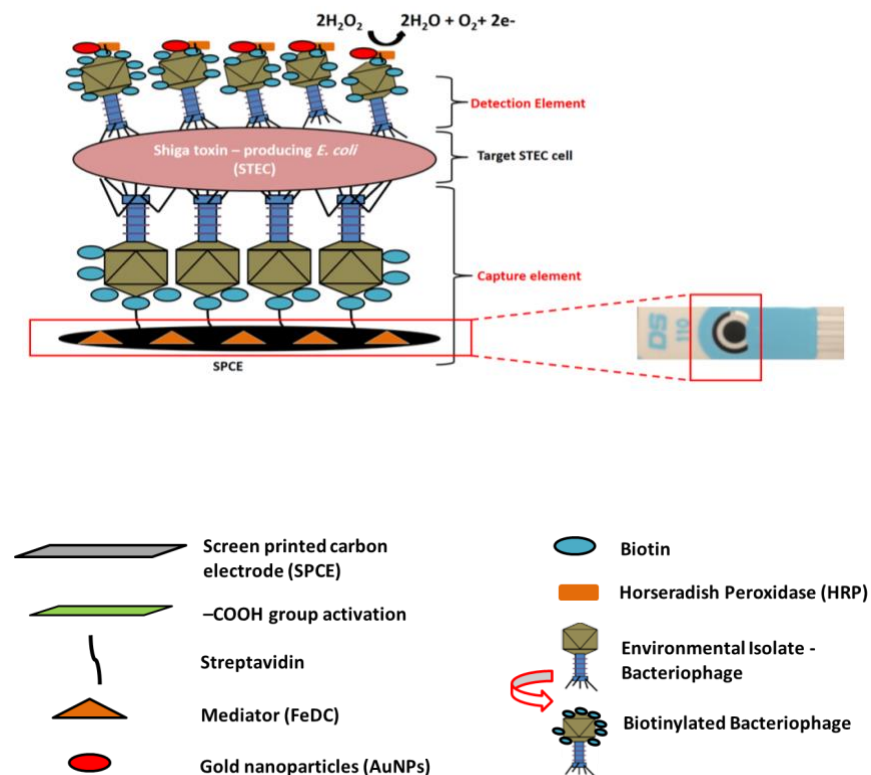


Figure 4.2. The newly-developed STEC-specific bacteriophage-based electrochemical biosensor. (A) The configuration of the biosensor architecture: 1-PalmSens3, 2-Bluetooth dongle, 3-Android device, 4-SPCEs, 5-SPCE holder and connector **(B)** The principle behind the novel approach that features sandwich-type recognition by capture and detection of live bacterial cells via the highly-specific biotinylated bacteriophages and the subsequent redox reaction.

4.3. Results

4.3.1. Chemical Modification of Bacteriophages

The concentration in $\mu\text{g/mL}$ of high-titer bacteriophage stocks ($> 9 \log \text{PFU/mL}$) was determined prior to chemical modification. Based on the standard curve, bacteriophages stock solutions at 9, 10, 10.4 and 10.85 $\log \text{PFU/ml}$ titer levels had the following concentrations, 550 $\mu\text{g/mL}$, 720 $\mu\text{g/mL}$, 900 $\mu\text{g/mL}$ and 950 $\mu\text{g/mL}$, respectively. Standard curve and other sample measurements are shown in Supplementary section.

The data that was recorded for the concentration ($\mu\text{g/mL}$) of bacteriophages was used to quantify incorporated biotin based on HABA (Fisher) dye absorbance as well as its avidin-binding properties at 500 nm. As shown in **Figure 4.3 (A)**, 10.85 $\log \text{PFU/ml}$ (initial) bacteriophage stock solution was biotinylated using five setups of increasing biotin concentrations 0, 1, 5, 10, 15, 20 mM and control. The effects of each concentration were assessed in relation to the retention of bacteriophage viability. Biotinylation of bacteriophage head by chemical modification was the lowest (49.37 biotin/mole protein) when 1 mM biotin was used. Detected biotin concentration almost doubled when 5 mM was used (95.71 biotin/mole) and remained around similar level even when 10 mM (98.15 biotin/mole) and 15 mM (103.02) were applied. The highest incorporated biotin was 121.92 biotin/mole when 20 mM biotin concentration was used.

The viability and infectivity of the bacteriophages remained superior even after chemical biotinylation in which the average % viability was around 94 % for the five setups and remained unchanged at 10 $\log \text{PFU/ml}$ titer level **Figure 4.3 (B)**. Morphological changes that occurred in bacteriophages were examined under the TEM. Quantum dots (QDots) or nanocrystals coated with streptavidin were used to monitor successful biotinylation of bacteriophage head in the

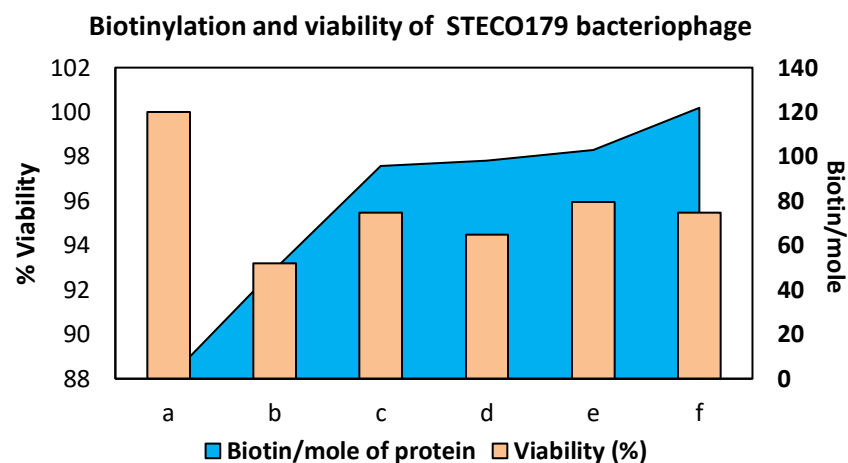
TEM via streptavidin-biotin binding. STEC O179 was used as a model bacteriophage for biotinylation of its head. It exhibited well-defined ultrastructures such as icosahedral head attached to a contractile tail, which perfectly fit in terms of showing morphological modification and analysis. **Figure 4.3 (C)** shows biotinylated STEC O179 bacteriophage coupled with QDots at increasing biotinylation levels (starred). The head of biotinylated bacteriophage can be seen as it bound with QDots. None of the QDots were seen bound to bacteriophage when control (i) and (ii) 1 mM were examined. However, on (iii), (iv) and (v) which corresponded to 5 mM, 10 mM and 15 mM, respectively, bound QDots can be easily observed with no major morphological changes on the bacteriophages. At 20 mM biotinylation level, (vii) shows thickening of bacteriophage capsid as well as accumulation of visible heavy mass structures along its periphery and toward the center.

(A)

Biotin (mM)	Log PFU/ml (O179) _i	Biotin/mole of protein	Log PFU/ml (O179) _f	Viability (%)
a. 0	10.85	0	10.85	100.00
b. 1	10.85	49.37	10.11	93.18
c. 5	10.85	95.71	10.36	95.48
d. 10	10.85	98.15	10.25	94.47
e. 15	10.85	103.02	10.41	95.94
f. 20	10.85	121.925	10.36	95.48

i = initial, *f* = final

(B)



(C)

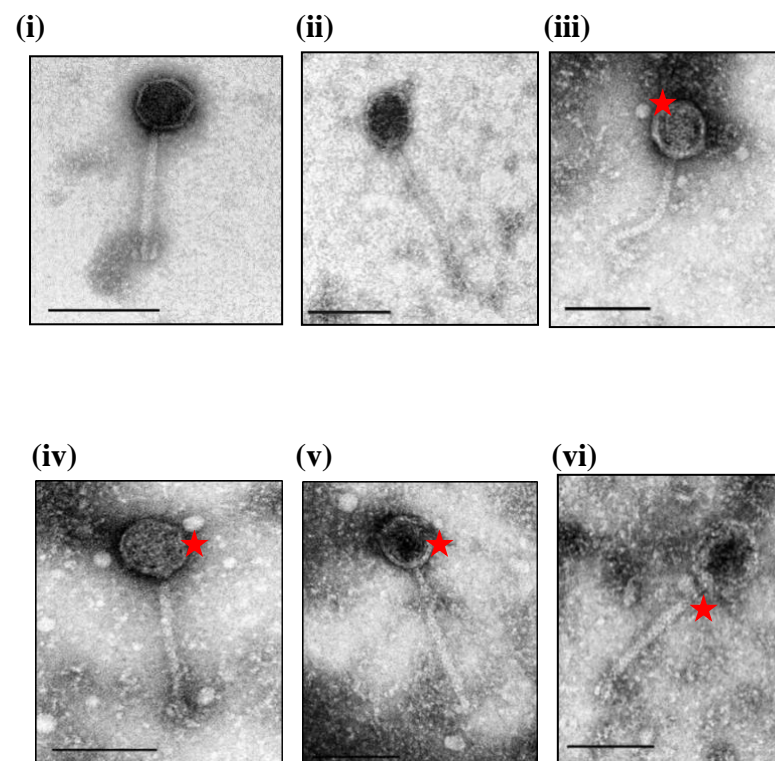


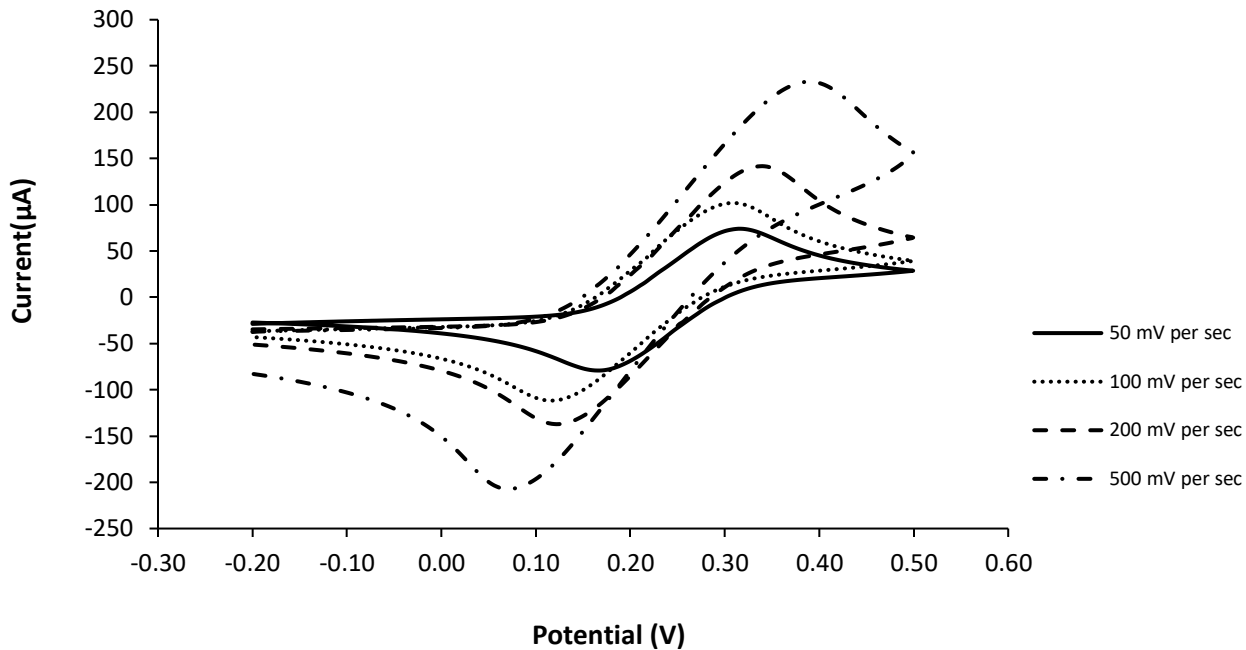
Figure 4.3. Biotinylation of O179 bacteriophage. The setups include incubating bacteriophages with increasing biotin concentrations before coupling it with streptavidin-coated Q-dots. Both (A)[in tabular] and (B)[in graphical], show the initial amount of biotin and the calculated biotin per mole protein or bacteriophage that was successfully incorporated onto bacteriophages, as well as the post-biotinylation % viability. (C) TEM images of biotinylated STEC O179 bacteriophage (i) = Control (untreated/unmodified), (ii) = 1 mM, (iii) = 5 mM, (iv) = 10 mM, (v) = 15 mM and (vi) = 20 mM biotin. Star indicates biotin bound Qdots nanocrystals. Scale bar: 100 nm.

4.3.2. Electrochemical Characterization of SPCEs

To evaluate the electrochemical properties of SPCEs (unmodified and modified), voltammograms of an electroactive redox model species, 0.5 mM $K_3[Fe(CN)_6]$, in aqueous solution were recorded (**Figure 4.4**). $K_3[Fe(CN)_6]$ contained in two supporting electrolytes, either 0.1 M H_2SO_4 (**Figure 4.4 A**) or 1X PBS (**Figure 4.4 B**) at varied scan conditions (50, 100, 200 and 500 mV/s) was prepared. In **Figure 4.5**, ΔE_p data were evaluated and compared according to the scan rates, supporting electrolytes and surface conditions of SPCEs.

The results of voltammograms showed that at 50 mV/s scan rate, $K_3[Fe(CN)_6]$ generated separation peaks ($\Delta E_p = E_p^c - E_p^a$, where E_p^c is the cathodic peak and E_p^a is anodic peak) with values of 182.4 mV and 74.3 mV for 0.1 M H_2SO_4 and 1X PBS, respectively. Other separation peaks (ΔE_p) values at 100 mV/s were 197.6 mV for 0.1 M H_2SO_4 and 150.3 mV for 1X PBS. As the scan rates increased, ΔE_p values also increased such as at 200 mV/s, $\Delta E_p = 243.2$ V, and 500 mV/s, $\Delta E_p = 324.3$ V for 0.1 M H_2SO_4 . Similar increasing trend was observed from 1X PBS supporting electrolyte at both scan rates, 200 mV/s ($\Delta E_p = 170.6$ mV) and 500 mV/s ($\Delta E_p = 216.2$ mV). Lower ΔE_p or peak separation values corresponds to excellent quality of electrodes surface as well as the optimum parameters used such as the scan rate which has been confirmed in this study. All succeeding electrochemical tests were conducted using 1X PBS at 100 mV/s scan rate unless otherwise indicated.

(A)



(B)

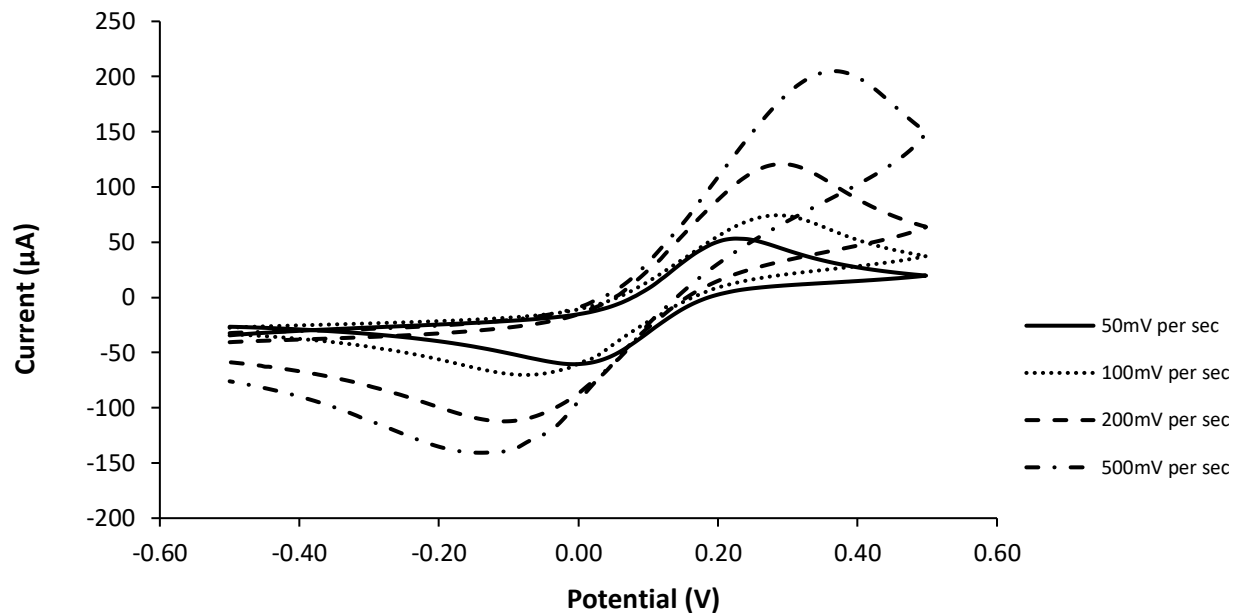


Figure 4.4. Cyclic voltammetry of 0.5 mM $K_3[Fe(CN)_6]$ in various supporting electrolytes conducted on unmodified SPCE. 0.5 mM $K_3[Fe(CN)_6]$ was used as a redox probe with (A) 0.1M sulfuric acid and (B) 1X PBS supporting electrolytes at increasing scan rates under the same potential step (-0.5 V to $+0.5$ V vs counter/reference electrode).

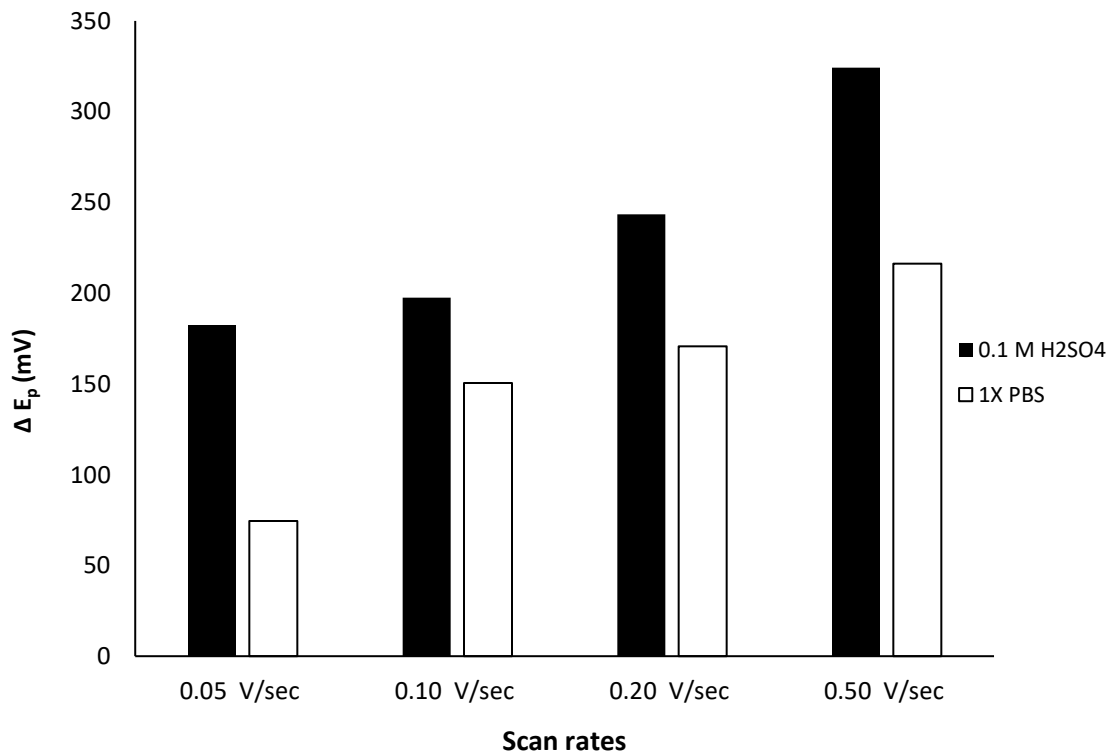


Figure 4.5. Bar graph representation of the electrochemical characterization of unmodified SPCEs. Voltammograms were recorded at increasing scan rates of 0.5 mM $K_3[Fe(CN)_6]$ in two different supporting electrolytes. The peak separation (ΔE_p , mV) between the oxidation and reduction potentials were recorded as a function of the surface of SPCEs.

4.3.3. Surface Modification and Biofunctionalization SPCEs

Subsequently, the surface of SPCEs was chemically modified and activated by applying individual components and reagents before air drying. Evaluation with CV test using $K_3[Fe(CN)_6]$ in 1X PBS at 100 mV/s scan rate was performed. Reagents partially formed self-assembled monolayer (SAM) on the surface of SPCEs upon modification. As shown in **Figure 4.6**, the voltammogram of unmodified SPCE (red line) had the highest cathodic peak (E_p^c) as compared to reagent-modified SPCEs. The blocking features of the chemicals may have affected the electron transfer kinetics of the redox probe, $K_3[Fe(CN)_6]$. Casein, a known excellent

blocking reagent, had the lowest E_p^c , and may have effectively blocked the surface of SPCEs, as can be seen from its voltammogram (light blue line) in comparison with other blocking reagents tested.

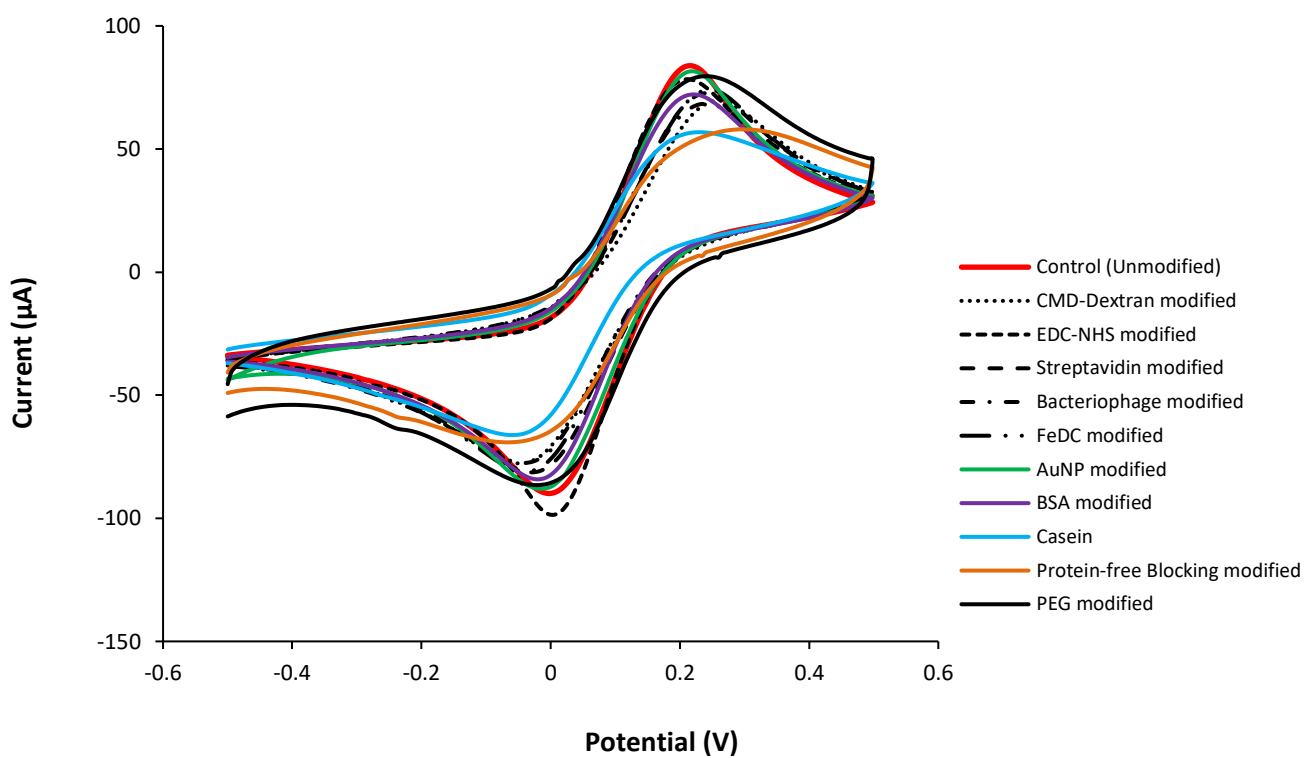


Figure 4.6. Cyclic voltammetry (CV) of chemically-modified SPCE. Individual reagents were applied to chemically modify and activated the surface of SPCE. 1X PBS was used as the supporting electrolyte and 0.5 mM $K_3[Fe(CN)_6]$ as a probe during the CV test at 100 mV/sec. Unmodified SPCE was used as control for comparison.

Figure 4.7 shows the comparison of two voltammograms generated from both unmodified and modified-biofunctionalized SPCE using 0.5 mM $K_3[Fe(CN)_6]$ in 1X PBS at 100 mV/s scan rate. The biofunctionalized SPCE was comprised of chemically immobilized and linked capture elements (biotinylated bacteriophages) via CMD-Dextran/EDC-NHS/streptavidin complex as well as blocking reagent (30% casein) and mediator (250 mM FeDC). Results showed the difference between ΔE_p of the unmodified and biofunctionalized SPCE which had 201.02 mV and 393.60 mV, respectively. This difference (ΔE_p), due to efficient electron transfer, indicated the successful modification of SPCE by chemical immobilization via SAM of various components onto the surface of the WE which at the end of the process, even after several incubation and washing steps, were still stable and active.

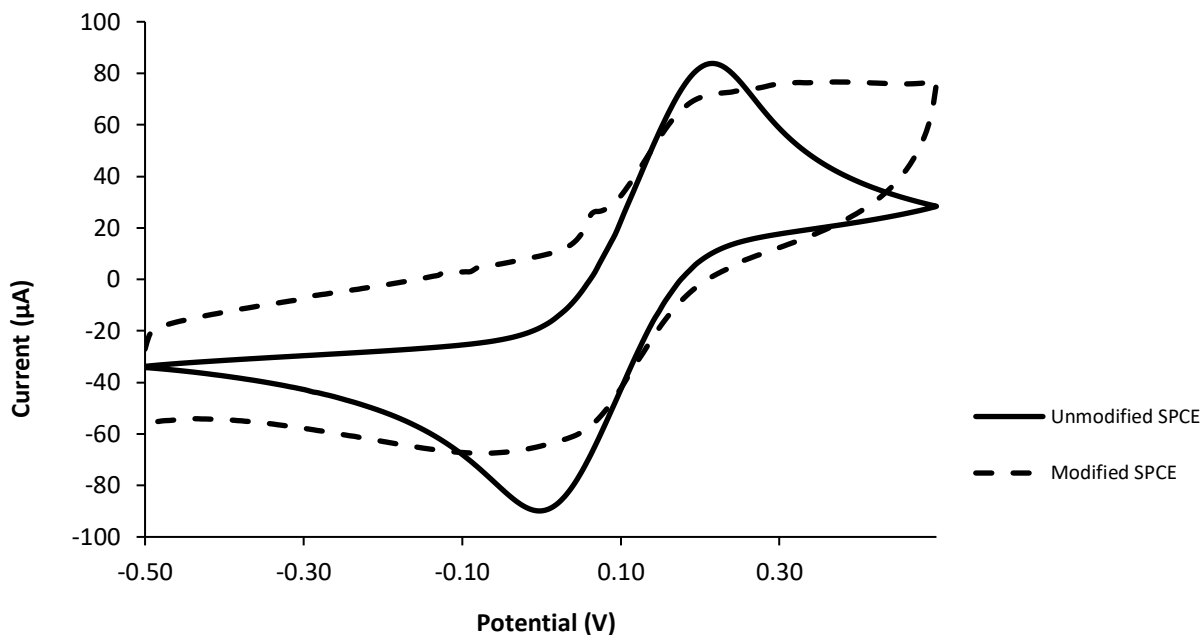
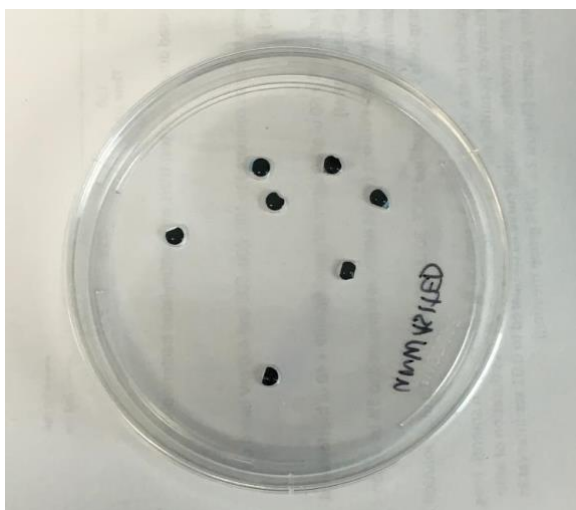


Figure 4.7. Cyclic voltammetry of 0.5 mM $K_3[Fe(CN)_6]$ in 1X PBS on both unmodified and modified SPCEs. The surface of unmodified SPCE was left untreated; however, the modified SPCE was initially activated with CMD-Dextran, EDC-NHS and streptavidin prior to the immobilization of STEC O179-specific biotinylated bacteriophage. Blocking reagent (30% casein) and mediator (FeDC) were also applied prior to the CV testing at 100 mV/sec

4.3.4. Viability and Stability of Capture and Detection Elements

After the modification and functionalization of the surface of SPCE, the stability and viability of immobilized biotinylated bacteriophages (STEC O179) on trimmed WE of SPCEs (**Figure 4.8 A**) were evaluated by conducting agar diffusion method (**Figure 4.8 B**). After a series of washing steps, the result of agar diffusion test of biofunctionalized WE carrying biotinylated STEC O179 on its surface, showed zone of clearing which was indicative of stable immobilization of the biorecognition elements process without negatively affecting its biofunctionality and biocompatibility. AuNPs were also incorporated onto the detection element to function as signal amplifiers. In **Figure 4.9**, it can be seen from the TEM image that AuNPs around 13 nm diameter were bound to the biotinylated bacteriophages (STEC O179) with the presence of other detection element component such as streptavidin-HRP (not visible). Most of AuNPs, seen as dark spots, were concentrated along the head and tail parts of bacteriophages but not directly on the tail fiber.

(A)



(B)

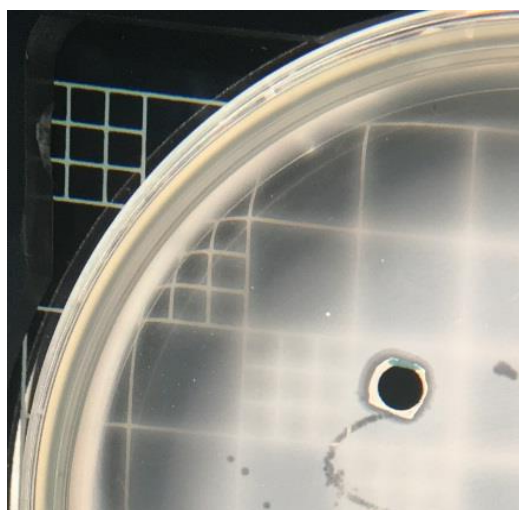


Figure 4.8. Agar diffusion test of bacteriophage-modified SPCE. (A) Biotinylated O179 bacteriophages were immobilized onto the surface of trimmed activated working electrode (WE) (B) After several washing and incubation steps prior to agar diffusion assay, WE showed zone of clearing.

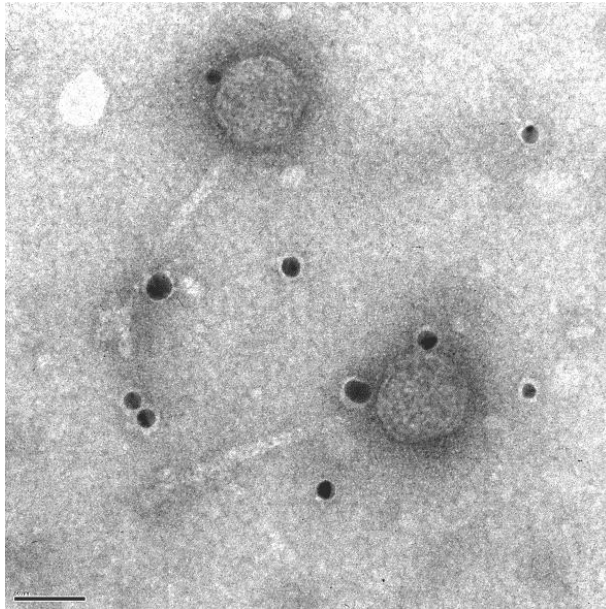


Figure 4.9. TEM image of detection element solution. The image shows AuNPs (signal amplifiers), as seen as dark spots, bound to the biotinylated STEC O179 bacteriophages. Biotinylated bacteriophages, streptavidin-HRP and AuNPs are the major components of the detection element. Scale bar: 20 nm

4.3.5. Determination of Background Noise

Sources of noise and indirect signals are presented in **Figure 4.10**. Reagents were classified into three major groups based on functionality. Current (μA) which was inert to the individual reagent that indirectly interfered the signal and ultimately contributed to the background noise of the system was measured. The results showed that the RC from the “reagents” and “detection elements” groups were almost negligible except for H_2O_2 ($230.66 \pm 6.32 \mu\text{A}$). Under the reagents group, 1X PBS, casein and live bacterial cells (STEC O179) had $3.33 \pm 0.072 \mu\text{A}$, $13.13 \pm 1.76 \mu\text{A}$, $64.86 \pm 4.02 \mu\text{A}$ RCs, respectively. Detection element solution (bacteriophage + AuNPs + S-HRP) under the detection element group generated $11.62 \pm$

1.26 μA while the strep-HRP + PBS solution had $10.15 \pm 0.821 \mu\text{A}$ RCs, respectively. The “modified SPCE” (CMD-Dextran + EDC-NHS + streptavidin) had the highest and most significant RC detected, $896.51 \pm 58.24 \mu\text{A}$. All these values were taken into consideration during RC data analysis. Based on these findings, the assigned baseline RC value was $900 \mu\text{A}$ and which was then subsequently used in all amperometric applications in this study.

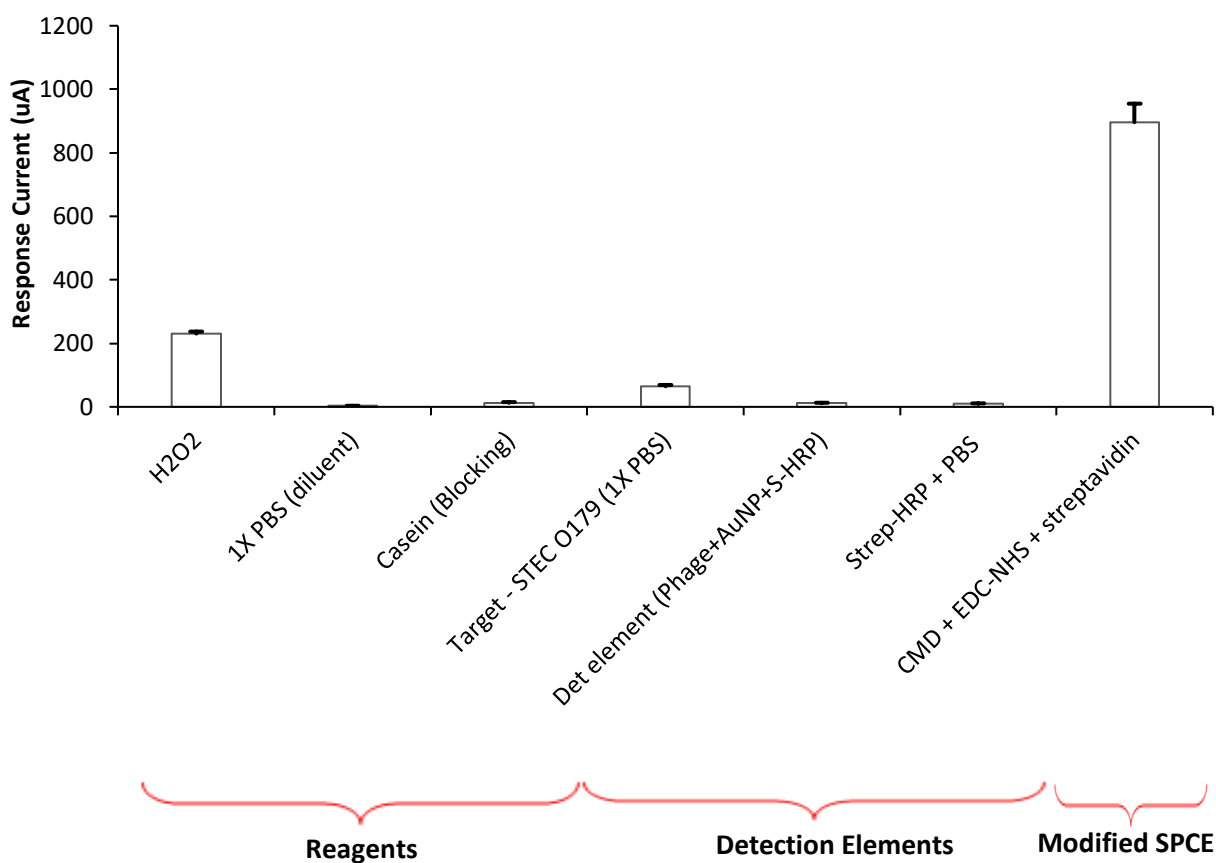


Figure 4.10. Determination of background noise. Different reagents and conditions were tested (Amp Test) to identify the potential sources of noise. It was determined that the background noise contribute to almost $900 \mu\text{A}$ ($896 \pm 58.24 \mu\text{A}$) even without bacterial samples. This identified value is considered as the baseline value when analyzing the data from amperometric reading.

4.3.6. Amperometric Tests

Three representative STEC strains in pure culture setup were prepared for amperometric tests. The inoculum level of target and various non-target strains ranged from 8 log CFU/mL and 3-1 log CFU/mL in 1X PBS. Results of plate count methods are presented in the Appendix Section. Specific modified SPCEs were used in this assay according to the target bacteria that were tested (ie STEC O26-specific bacteriophage modified SPCE for STEC O26 target).

The signal threshold for positive detection was defined by the signal-to-noise (S/N) characteristics as $S/N > 3$, where the target could provide a signal a least three times greater than the signal from non-targets. The limit of detection (LOD) was determined by the statistical significance of signals (Δ current) between non-target bacteria and the lowest inoculum of target bacteria which had a calculated Δ current above signal threshold for positive detection.

Amperometric curves for the response current (RC) of target STEC O26 and non-target strains are presented in **Figure 4.11 (A)** while **Figure 4.11 (B)** shows a bar graph of the corresponding average delta (Δ) current. Target STEC O26 had significantly higher delta (Δ) current value, $215.45 \pm 78 \mu\text{A}$ as compared to the other three non-target samples (*L. monocytogenes* = $-8.20 \pm 78 \mu\text{A}$, *S. Typhimurium* = $-5.52 \pm 98.6 \mu\text{A}$ and STEC O179 $-22.78 \pm 34.42 \mu\text{A}$). These results show the high specificity of the assay for target strain without observing cross-reactivity toward non-target samples. A linear relationship is shown as $R^2 = 0.95$ and a signal threshold for positive target detection of $66.9 \mu\text{A}$. The LOD was determined to be 1 log CFU/mL in 1X PBS.

Similar pattern was observed when STEC O179 (target) was tested with *S. Typhimurium* (non-target). **Figure 4.12 (A)** shows a bar graph of the average RC of STEC O179 ($172.90 \pm 28.01 \mu\text{A}$) which was significantly higher (3 times) than the RC of *S. Typhimurium* ($57.46 \pm$

31.6 μA) at 8 log CFU/mL inoculum level. The sensitivity was then challenged by testing lower inoculum levels (1-3 log CFU/mL) as shown in **Figure 4.12 (B)**. The low inoculum levels of STEC O179 and its Δ Current had linear correlation, $R^2 = 0.8749$. Linear relationship was described as Δ Current (μA) = 36.487(inoculum level in log CFU/mL of STEC O179) + 52.678, with a linear range of 1-3 log CFU/mL. The signal threshold for positive target detection was 101 μA while the LOD was determined to be 2 log CFU/mL in 1X PBS.

As shown in **Figure 4.13 (A)**, STEC O157 (target) had significantly higher (15 times) average RC ($126.90 \pm 5.55 \mu\text{A}$) as compared to *S. Typhimurium* (non-target) ($8.44 \pm 3.95 \mu\text{A}$) when both strains were tested at 8 log CFU/mL inoculum level in 1X PBS. Similar to the previous group, the sensitivity of the assay toward STEC O157 was also challenged by testing it at lower inoculum levels (1-3 log CFU/mL) as shown in **Figure 4.13 (B)**. The low inoculum levels of STEC O157 and its Δ Current had linear correlation, $R^2 = 0.9732$. Linear relationship was described as Δ Current (μA) = 26.998(inoculum level in log CFU/mL of STEC O157) + 65.67 with a linear range of 1-4 log CFU/mL. The signal threshold for positive target detection was 122.13 μA while the LOD was determined to be 2 log CFU/mL in 1X PBS.

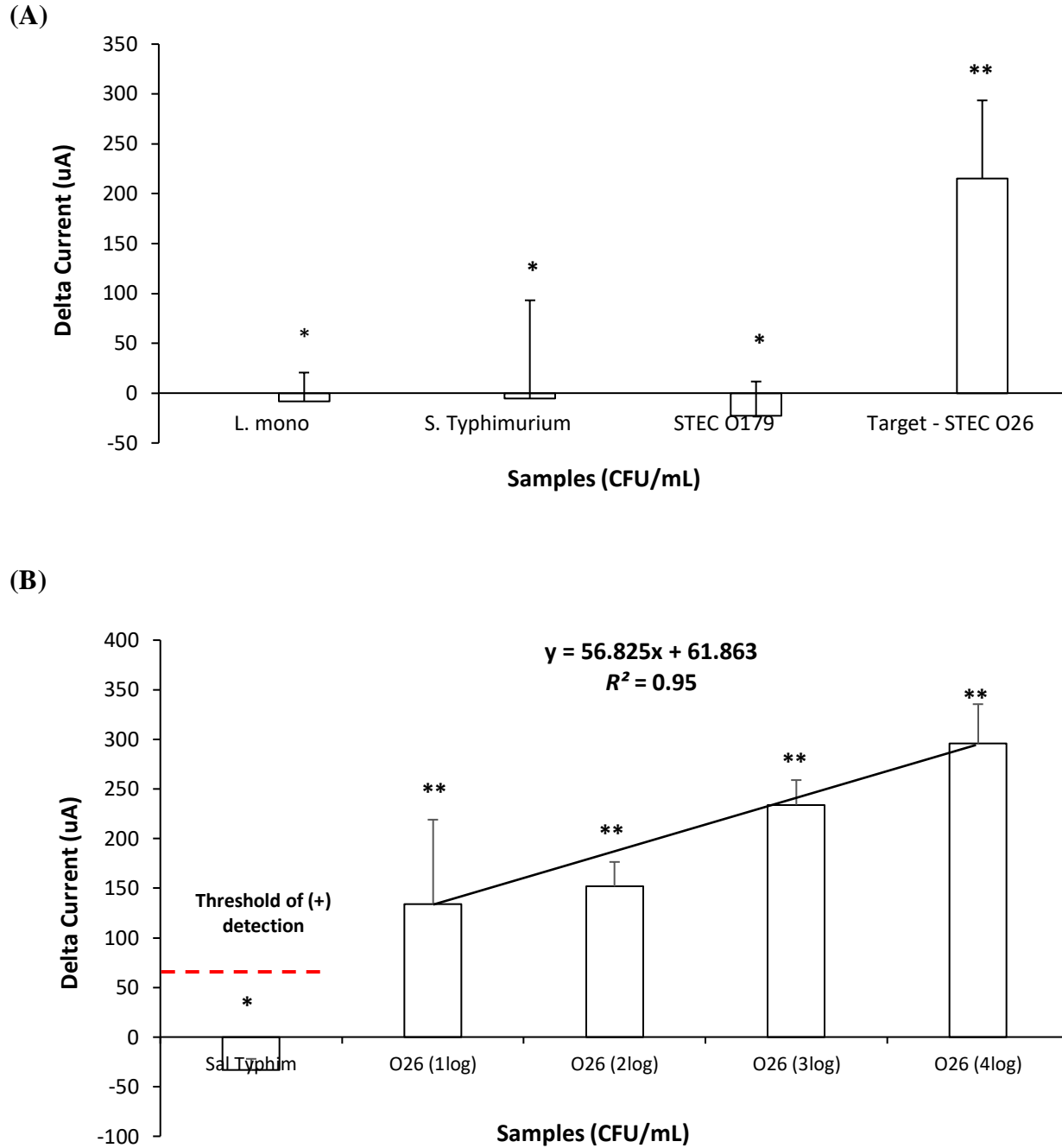
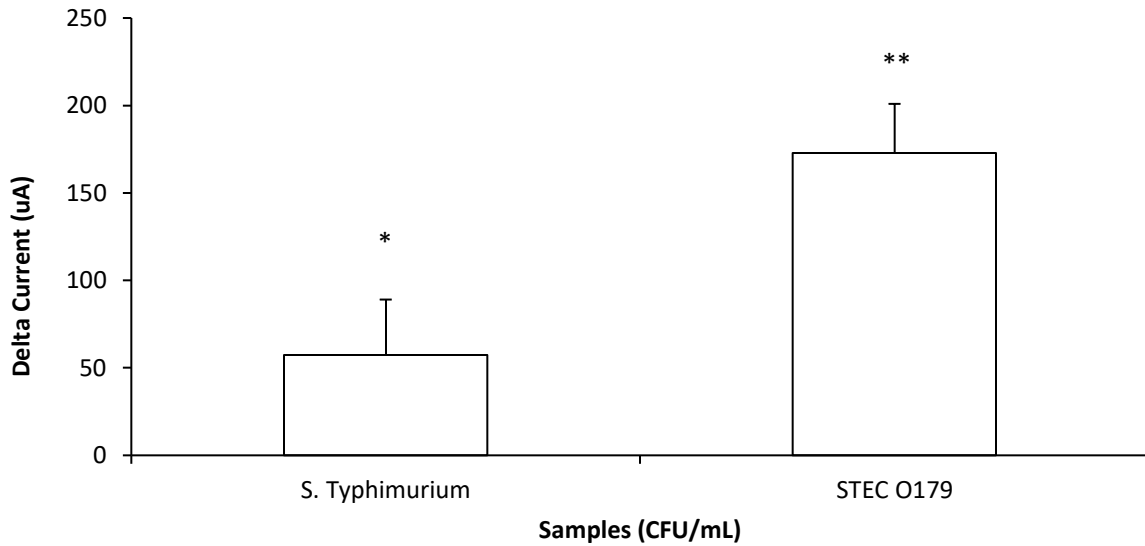


Figure 4.11. Amperometric test of STEC O26. (A) Amperometric tests between target (STEC O26) and non-target samples (*L. monocytogenes*, *S. Typhimurium* and STEC O179). Pure culture strains at 8 log CFU/mL inoculum level were used during the assay. (B) A linear calibration plot showing a positive linear regression of increasing STEC O26 inoculum levels, 1-4 log CFU/mL in 1X PBS. Dotted line (red) corresponds to the delta (Δ) current threshold (66.9 μ A) for positive target bacteria detection. The LOD is 1log CFU/mL. (*) indicates significant difference. $P < 0.05$

(A)



(B)

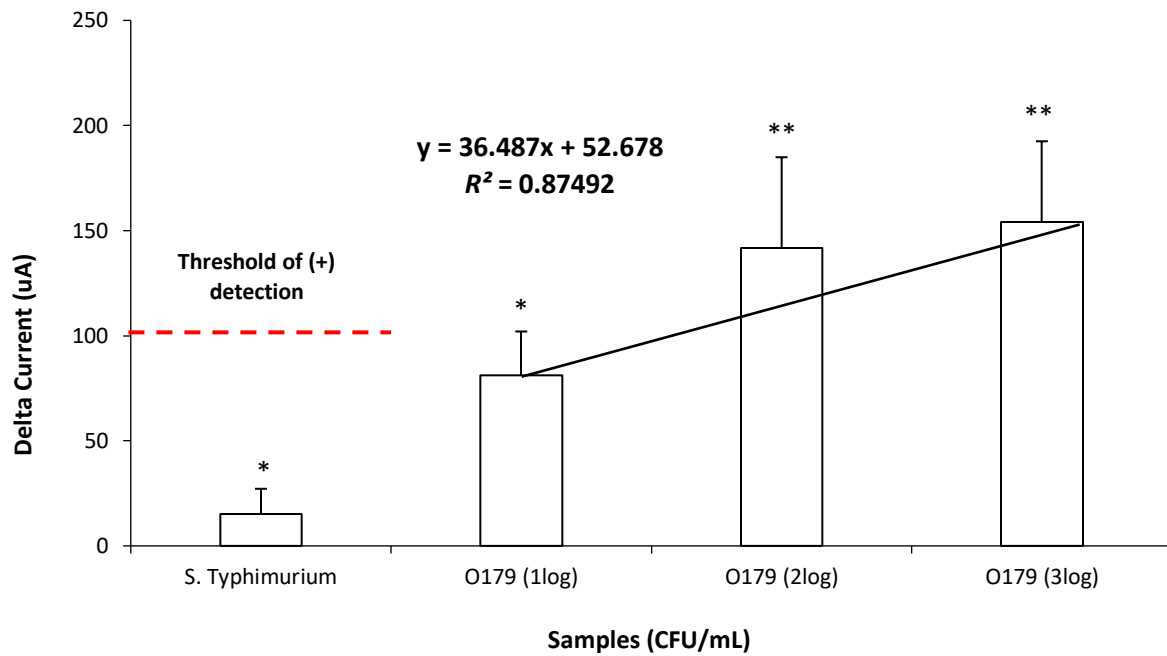
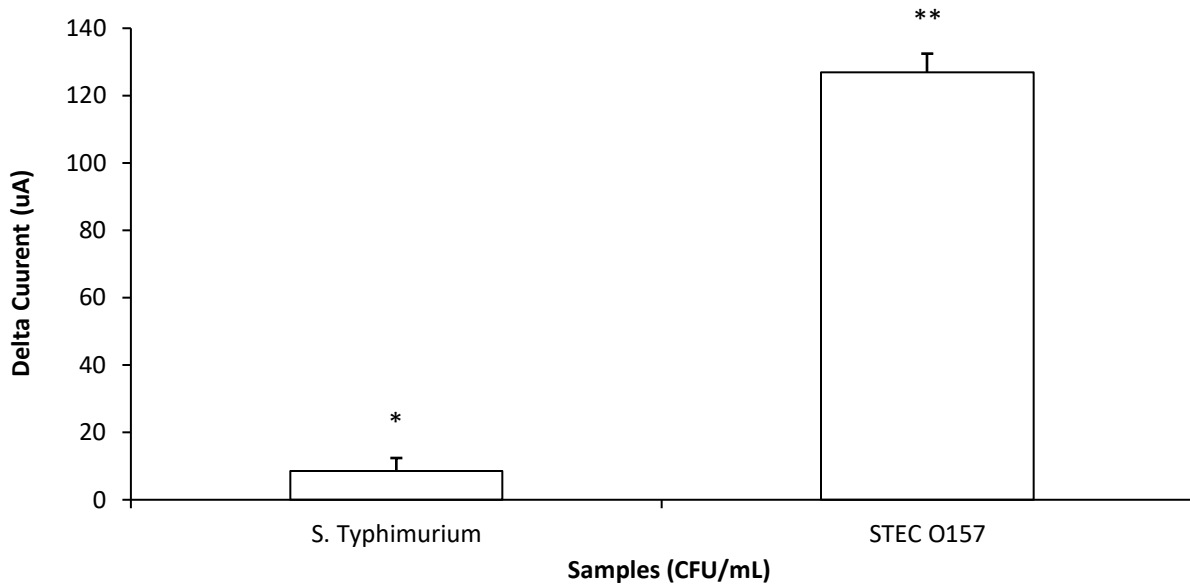


Figure 4.12. Amperometric test of STEC O179. (A) Amperometric tests between target (STEC O179) and non-target samples (*S. Typhimurium*) at 8 log CFU/mL inoculum levels. Delta current data (µA) shows the high specificity of the assay. (B) Challenging the sensitivity by testing lower inoculum levels (1-3 log CFU/mL). Dotted line (red) corresponds to the delta (Δ) current threshold (101 µA) for positive target bacteria detection. The LOD is 2log CFU/mL. (*) indicates significant difference. $P < 0.05$

(A)



(B)

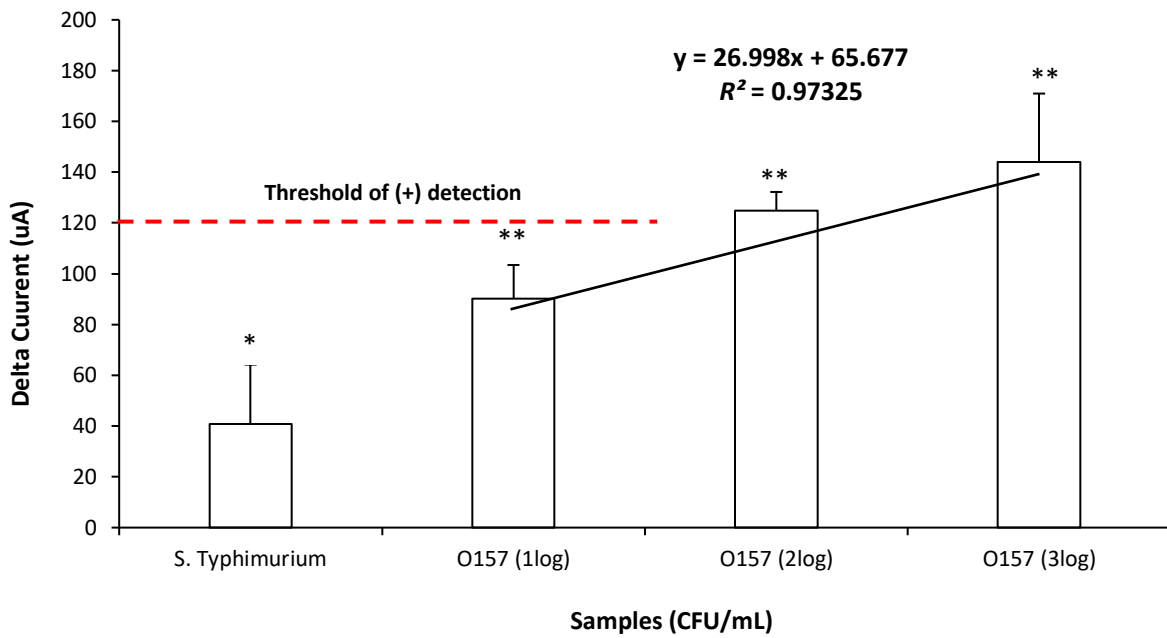


Figure 4.13. Amperometric test of STEC O157. (A) Amperometric tests between target (STEC O157) and non-target samples (*S. Typhimurium*) at 8 log CFU/mL inoculum levels. Delta current data (µA) shows the high specificity of the assay. (B) Challenging the sensitivity by testing lower inoculum levels (1-3 log CFU/mL). Dotted line (red) corresponds to the delta (Δ) current threshold (122.13 µA) for positive target bacteria detection. The LOD is 2log CFU/mL. (*) indicates significant difference. $P < 0.05$

4.4. Discussion

STEC-specific amperometric rapid biosensor integrated with novel bacteriophages as biorecognition and detection elements was developed. SPCE, one of the key elements of the detection system, was modified and utilized as a stable transducer for this new detection platform. SPCEs are highly advantageous mainly because of its single-use property and excellent reproducible signals (Tangkuaram, Ponchio et al. 2007).

Chemical modification of purified bacteriophages was conducted to enhance potential bacteriophage-based applications. Biotin is a soluble B-vitamin that is used for tagging biomolecules to detect proteins. In this study, biotinylated bacteriophages remained active and both its viability and infectivity remained superior as suggested by the viability assays (10 log PFU/ml). The relatively low amount of biotin (10 mM) does not negatively affect protein stability, three-dimensional structure and functions though modification of lysine residues may inactivate the binding sites (Kay, Thai et al. 2009). When higher concentration of biotin (20 mM) was used, changes in the ultrastructure of bacteriophages, specifically on its head, were observed. Although the infectivity of these biotinylated bacteriophages from higher dose of biotin did not suffer even some morphological changes (ie thickening of its capsid or head) have occurred, it is very significant to consider the optimum concentration (10 mM) and conditions (37°C) during *in vitro* modification especially for biosensing or biocontrol applications. Techniques in biocontrol or biosensor development that involve binding and immobilization of biotinylated bacteriophage structures may require maximum coverage or consistent and even distribution of bacteriophages, thus structural changes on its head may compromise its functions. Therefore, it is important to maintain structural stability of bacteriophages during its modification processes to ensure superior biological capabilities.

Electrochemical characterization of both the unmodified and modified state of SPCEs was conducted prior to amperometric testing which then allowed successful detection of representative STEC live strains. CV and other electrochemical techniques provide meaningful information about the properties of redox probes, formation of self-assembled monolayer (SAM) including its kinetics and mechanisms, as well as the properties of electrode materials (Campuzano, Pedrero et al. 2006, Daubinger, Kieninger et al. 2014). CV shows the patterns and changes of the electrode behavior after each modification and assembly steps that occur on its surface.

In this study, voltammograms of a redox probe, $K_3[Fe(CN)_6]$, in two supporting electrolytes (0.1 M sulfuric acid and 1X PBS) were compared. It was observed that the voltammogram had peaks (cathodic and anodic) which were dependent on the increasing scan rates. Supporting electrolytes do not participate in any electrode reactions, however it increases the conductivity of the solution (Newman and Thomas-Alyea 2012). Salt as a supporting electrolyte ensures high ionic strength (0.1M), thus maintaining a homogenous and near-zero electric field which shields the solution from the redox reactions of the target analytes as well as lowers the resistance of the electrodes to a negligible level (Dickinson, Limon-Petersen et al. 2009, Elgrishi, Rountree et al. 2017). Similarly, sulfuric acid reduces both the electric field in the solution as well as the transport of cupric ions (Newman and Thomas-Alyea 2012). Lower ΔE_p or peak separation values corresponds to excellent quality of electrodes surface and optimum condition of parameters (ie scan rate). Herewith, ΔE_p increased as the scan rate increased. Comparing the two electrolytes, 1X PBS generated lower ΔE_p than H_2SO_4 , therefore, the former was used in the subsequent characterization of SPCEs at 100 mV/sec scan rate.

Scan rates determine the speed the applied potential is scanned. A faster scan rate results in a decreased diffusion layer size and higher currents (Elgrishi, Rountree et al. 2017). The results of this study showed that 50 mV/s scan rate generated the lowest current among the other faster scan rates (100, 200 and 500 mV/s) irrespective of the supporting electrolytes. However, in this study, 100 mV/s final scan rate was used based on the consistent and stable current both during the CV and amperometric tests. Slower scan rates lead to reduced amount of protons which are either associated or dissociated at a specified time (Daubinger, Kieninger et al. 2014). In addition, the excitation signal of CV was the applied potential across the WE and RE which also varied linearly over time. The initial scan took the positive direction and scanned back in reverse to fully complete the cycle. Oxidation reaction occurs during the forward scan releasing the protons while reverse scan involves reduction reaction which absorbs the protons (Daubinger, Kieninger et al. 2014). CV plots the RC at the WE to the excitation potential that is applied. Majority of the electron transfer process primarily occurs at the interface between the solution and WE.

Voltammograms of the modified SPCEs generated lower current as compared to its unmodified version, primarily due to the blocking properties of SAM which formed on the surface of WEs. Properly ordered SAM of short molecules allows transfer of electrons from the solution to the electrode. If longer molecules are used, then an isolating layer forms which limits the electron transfer (Ölcer, Esen et al. 2015). When cyclic voltammograms peak is absent in monolayer-modified SPCEs, it translates to non-occurrence of redox reactions.

As compared to the unmodified SPCE, formation of SAM, attachment and the immobilization of capture elements on the surface were accompanied by a decrease of voltammogram response. Electron transfer barriers were built upon treating the surface with

various reagents, thereby hindering the redox species to penetrate and interact with the conductive electrode surface. Consequently, the reduced voltammogram response was directly observed in all modification steps, both after the addition of individual reagents or when the actual capture element linkages were assembled. CMD-dextran was added onto the surface to introduce carboxyl (-COOH) groups and then activated by the addition of EDC-NHS. This SAM was terminated by an active amine-carrying streptavidin via carboxyl-to-amine crosslinking which ultimately covalently bonded with biotinylated bacteriophages. These surface layers hindered the diffusion of redox probe toward the electrode surface which is an evidence of the efficient and successful immobilization and modification of the surface of SPCE (Tsai, Chen et al. 2016).

In terms of the functionalization of SPCE, chemical modification approach was chosen over other techniques due to ease and simplicity. Active chemical modification of SPCE allowed tethering of biotinylated bacteriophages via the strong streptavidin-biotin interaction. Previous bacteriophage immobilization techniques involved passive (Bennett, Davids et al. 1997), charge-directed oriented immobilization (Cademartiri, Anany et al. 2010, Zhou, Marar et al. 2017) and chemical immobilization via streptavidin on quantum dots (Edgar, McKinstry et al. 2006). Passive immobilization resulted in poor cell capture efficiency (Gervais, Gel et al. 2007) while chemical immobilization involved genetically-modified bacteriophages which is not always economical especially for comprehensive collection of environmental and genetically uncharacterized bacteriophages. The stability and viability of immobilized bacteriophages as capture elements specifically on trimmed WE was confirmed by the results of agar diffusion method. Zones of clearing were observed in the lawn of target bacterium which was an indicative of infectivity of the bacteriophages and bacterial cell lysis (Hosseinidoust, Van de Ven et al.

2011). These results also indicate that the biotinylated bacteriophages were strongly linked to the surface of WE via biotin-streptavidin bond rather than physical adsorption, otherwise most of the bacteriophages would be washed away during the washing steps and no clearing would be observed. The bacteriophages that were included in this study belong to families *Siphoviridae* and *Myoviridae*. Both families have been reported to be highly-resistant to long-term storage, dry conditions and large temperature fluctuations (Jończyk, Kłak et al. 2011).

Biofunctional nanomaterials such as AuNPs, have been utilized as signal amplifiers due to its biocompatibility, synergistic effects with various catalytic activity, conductivity by promoting electron transfer between mediators and electrodes, and large electrochemically active surface (Zhang, Yuan et al. 2007, Lin, Chen et al. 2008, Liu and Wong 2009). These properties allow amplification of numerous recognition events and accelerate signal transduction (Lei and Ju 2012). In this study, AuNPs were incorporated onto the detection element solution along with the biotinylated bacteriophages and streptavidin-HRP for signal enhancement in the event of capture and sandwich detection of target STEC live cells. This event was monitored and recorded by amperometric assay. TEM images showed that AuNPs were localized along the periphery of the biotinylated bacteriophages. None of the AuNPs were found directly bound on the tail fibers that might block the specific recognition and binding events of bacteriophage and target host cells. In addition, the infectivity of biotinylated bacteriophages in the detection element solution was not negatively affected by the binding of AuNPs as confirmed by the viability tests. Previous reports have demonstrated the biocompatibility of AuNPs with native or mutant bacteriophages as they assembled and bound to the bacteriophages' major capsid proteins via electrostatic interaction and charge-mediated forces (Souza, Yonel-Gumruk et al. 2008). However, it has also been reported that signal amplifiers can be a major noise source for

biosensors under certain conditions (Yao and Gillis 2012). Preliminary results in this study showed that incorporation of AuNPs in the capture element did not enhance the signal therefore, it was only added as a component of detection elements.

To determine the noise sources that were inherent in the system, all reagents involved in the development process were individually tested using amperometric assay. The data shows that most reagents contributed negligible current values (μA) except for H_2O_2 ($230.66 \pm 6.32 \mu\text{A}$) while the highest recorded current (μA) was from the activated SPCEs ($896.51 \pm 58.24 \mu\text{A}$). The dimension of WE strongly influences the noise and stability of the sensor. Specifically, the noise is directly proportional to the area of the electrode, where the smaller electrode area registers reduced noise level (Kuberský, Hamáček et al. 2013, Yao, Liu et al. 2015). Though microelectrodes with a diameter (WE) of 4 mm were used in this study, the transducer-induced noise highly likely originated from the thermal motion of ions in the electrolyte-electrode interface where electrode pores created a frictional environment (Yao and Gillis 2012). It is also possible for the system to experience line interference pickup which contributes to the overall background noise, therefore it is recommended to shield and insulate all the microelectrode connections (Yao and Gillis 2012). This assessment allowed the determination of baseline value ($900 \mu\text{A}$) that was used in analyzing amperometric data throughout this study.

The key novel feature of the current development was the bacteriophage-based capture and sandwich-type detection of target live cells. It is known that majority of the functional receptors of bacteriophages are found on its tail extremities. Sulfosuccinimido-biotin was used to modify bacteriophages heads. Specifically, sulfosuccinimido-biotin reacted with the primary amino groups of the phage coat proteins concentrated on the bacteriophage heads (Sun, Brovko et al. 2000). This modification process resulted in oriented immobilization of bacteriophages,

wherein the tails were directed upward, and allowed recognition and capture of target bacteria in a very efficient way (Gervais, Gel et al. 2007). Once the target STEC cells were captured by the SPCE-immobilized bacteriophages, a detection element which was composed of the same kind of bacteriophages but labeled with HRP to hasten catalytic reactions, and AuNPs to amplify signals, was added. The addition of detection element allowed the sandwich detection of target STEC cells to occur. The specific recognition and binding event of bacteriophage-host interaction was monitored by amperometric test via redox reactions. After the formation of the bacteriophage/target STEC/bacteriophage-HRP complex, a mixture of 40 mM H₂O₂ and FeDC was added onto the SPCE. H₂O₂ served as the substrate for HRP while FeDC acted as a mediator that shuttled electrons between the redox reaction center and working electrode (Lin, Chen et al. 2008). The high binding efficiency of bacteriophage to its target host cells enhanced the sensitivity of the biosensor due to the increased amount of HRP-labelled bacteriophage that was directly detected from the system.

Previous reports have utilized bacteriophages as biosensor recognition elements or reporters for the detection of pathogens such as *Salmonella* spp (Sun, Brovko et al. 2000, Fernandes, Martins et al. 2014), *Listeria* spp (Loessner, Rudolf et al. 1997), *Staphylococcus aureus* (Byeon, Vodyanoy et al. 2015) and others. Recently, modified bacteriophages were also immobilized on magnetic beads and utilized as capture and separation tools for *E. coli* (Wang, Wang et al. 2016). None of those reported bacteriophage-based studies utilized two sets of bacteriophages of the same kind for sandwich capture and detection of target live bacterial cells.

In the present study, three representative STEC strains in pure culture setup were detected with high specificity and superior sensitivity (LOD: STEC O26-1log CFU/mL, STEC O179-2 log CFU/mL and STEC O157-2log CFU/mL) using the newly developed bacteriophage-based

method. These results indicate that an antibodies-free portable detection system can be a viable option for rapid foodborne pathogen detection. Based on the available pure culture samples and serial dilutions that were tested in this study, the quantitative working range for STEC O26 was 1-4 log CFU/mL, STEC O179 was 2-3 log CFU/mL and 1-4 log CFU/mL for STEC O157. The turn-around time of the actual testing using the biofunctionalized SPCE (ie CV testing and data analysis) was < 1 hr.

An excellent biorecognition element is highly durable, easy to immobilize, cost efficient, and highly selective and sensitive (Byeon, Vodyanoy et al. 2015). These key attributes were fulfilled by bacteriophages, both as biorecognition or capture and detection elements. Bacteriophages possess high specificity and affinity for their specific host (Singh, Arutyunov et al. 2012). The specificity depends on the nature and physiological assembly, localization, spatial configuration and chemical composition of receptors on bacterial surface. Thus, specific bacteriophages can only infect a narrow bacterial host range (Rakhuba, Kolomiets et al. 2010). Excellent specificity is advantageous especially for samples with high-ratio of non-target to target bacteria. Preparation of a cocktail of bacteriophages to functionalize the transducer may be required to address the need for simultaneous detection of multiple targets.

Live pathogenic bacterial cells are the primary concerns in processed foods (Ray and Bhunia 2014) and bacteriophages can facilitate the monitoring and detection of live pathogens because it is capable of distinguishing between live and dead bacterial cells (Zourob and Ripp 2010). For future applications of the assay, real food or environmental samples may not need enrichment processes to recover injured bacterial cells for detection. Detection of viable targets and potential elimination of pre-treatment steps is a significant improvement from the traditional methods especially for on-site rapid testing of samples.

4.5. Conclusions

Bacteriophages could be utilized as highly effective analytical tools due to its specific interactions with its bacterial host cells. The incorporation of bacteriophages onto the detection system circumvents the drawbacks faced by using traditional biorecognition molecules such as antibodies. Monoclonal and polyclonal antibodies are both relatively expensive, possess instability issues and incapable of distinguishing live and dead cells. In this study, simple chemical modification of environmentally-isolated bacteriophages and activation of disposable and inexpensive transducer provided a rapid method of detecting live STEC cells in microvolume samples. The newly developed method that took advantage of a novel approach of sandwich type of capture and detection via electrochemistry of target cell resulted in a superior LOD of 1 log CFU/mL (STEC O126), 2 log CFU/mL (STEC O179) and 2 log CFU/mL (STEC O157) in less than 1 hour turn-around time. It is highly specific and no cross-reactivity was observed between target and non-target samples. Compared to other reported detection technologies, the proposed detection methods provided improvements in both sensitivity and flexibility. This new electrochemical method of rapid detection of significant foodborne pathogens allows future customization of its capture and detection components. By doing so, detection of various targets or analytes of interest can be designed, specifically; an alternative way is to utilize a different set of bacteriophages for different target bacterial hosts with optimized modification of SPCE.

CHAPTER 5

APPLICATION OF SHIGA TOXIN-PRODUCING *ESCHERICHIA COLI* (STEC) BACTERIOPHAGE-BASED BIOSENSOR ON FOOD AND ENVIRONMENTAL SAMPLES

5.1. Introduction

Shiga toxin-producing *Escherichia coli* (STEC) O157:H7 and non-O157:H7 serogroups (O26, O45, O103, O111, O12, and O145) are significant foodborne pathogens that are commonly associated with diarrhea, hemorrhagic colitis (HC), hemolytic uremic syndrome (HUS) and even fatalities (Smith, Fratamico et al. 2014). It is estimated that non-O157:H7 strains cause more illnesses than O157:H7 serogroup. In 2015, there were 4,831 cases of culture-confirmed STEC infections from the 49 states in the United States and 1,262 of these cases were caused by unknown STEC serogroups to the Laboratory-based Enteric Disease Surveillance (LEDS) system (CDC 2017).

Cattle are the global natural reservoir for both STEC O157 and non-O157 strains, and are important sources and vehicles of food and water contamination (Beutin and Fach 2015, Stromberg, Lewis et al. 2016). Shiga toxin-producing *Escherichia coli* (STEC) contamination can occur via livestock manure, animal waste on pastures, spread of wastewaters from abattoirs, treatment plant and wildlife (Balière, Rincé et al. 2015). Conventional foodborne pathogens laboratory-based detection methods for STEC and other foodborne pathogens such as *Salmonella* spp., *Campylobacter*, etc., employ time consuming procedures which can approximately take around 5-7 days before generating confirmed positive results. In addition, detection of non-O157:H7 strains in foods is not a straightforward process due to lack of distinguishable

phenotypic features with reference to a large number of non-STEC bacteria inhabiting in the same environment (Delannoy, Chaves et al. 2016). Traditional methods may be limited by their low sensitivity and failure to detect foodborne pathogens increases its transmission risks (Law, Ab Mutalib et al. 2015). Thus, rapid screening and detection methods designed with highly-selective platforms are needed to address these limitations. Specifically, on-site rapid screening approach, if applied, can circumvent the limitations of conventional laboratory-based culture methods which unfortunately incur high operating costs coupled with the need to hire highly-skilled staff to be operational.

Biosensor technology provides solutions to the limitations of traditional methods. Biosensors are on-site devices with rapid and highly-sensitive features due the nano and microfabrication techniques (Yamada, Choi et al. 2016). The latest development in the biosensor research and application are focused on optical, electrochemical and mass-based techniques. For immunological-based biosensing applications, the use of mono and polyclonal antibodies as recognition elements is very common due to its commercial availability and high affinity (Kumar, Aaron et al. 2008, Karoonuthaisiri, Charlermroj et al. 2009). However, cross-reactivity toward other strains or species and interference are innate to antibodies especially for polyclonal antibodies. In addition, immunosensors are not capable of discriminating live and dead bacterial cells because it can still recognize and bind to the antigen that is present in bacterial cellular membrane regardless of its physiological state (viable or not viable) (Tlili, Sokullu et al. 2013). Antibodies also require intermediate protein and rely on non-covalent protein-protein interaction that eventually reduces the lifespan of the biosensor. Monoclonal antibodies mainly require the use of live animals to stimulate immune response for its production; hence manufacturing is highly dependent on the environmental conditions and health of the host animals. More

importantly, the production cost of antibodies is generally expensive which has prompted the need to explore for other inexpensive alternatives for capture and recognition elements that can perfectly harmonized into the biosensing architecture.

Bacteriophages exist ubiquitously in nature and are inexpensive to propagate in the laboratory. Bacteriophages are highly-specific to its target bacterial host, safe to humans, can be easily and economically produced with relatively longer shelf-life and highly resistant to harsh environments (Zourob and Ripp 2010). Well-characterized bacteriophages are excellent substitutes to antibodies for recognition of target bacteria and analytes. Most of the current bacteriophage-based biosensors are coupled with screen-printed electrodes (SPEs) (ie gold and carbon electrodes) for electrochemical detection of target bacteria. Due to its low production cost, disposable SPEs are advantageous to use because it can be discarded after carrying out single analysis that prevents cross-contamination and erroneous read-outs during analysis. More importantly, SPEs offer great flexibility by allowing customization and modification of its surface depending on the composition and assembly required for the sensitive and specific electrochemical system

The primary aim of this study was to apply the newly developed and optimized Shiga toxin-producing *Escherichia coli* (STEC) bacteriophage-based biosensor on food and environmental samples. This STEC-specific amperometric rapid biosensor has been uniquely integrated with novel bacteriophages as its biorecognition and detection elements which contributed to its superior specificity and low limit of detection (LOD) in pure culture setups. Our objective was to challenge and evaluate these features on real complex matrices without pre-treatment prior to testing.

5.2. Materials and Methods

5.2.1. Reagents and Apparatus

Phosphate buffered saline 10X Solution (PBS), Pierce™ 20X TBS Tween™ 20 buffer (TBS-T20), biotin, sulfo-N-hydroxysulfosuccinimide (NHS), streptavidin, 30% hydrogen peroxide (H₂O₂) solution, dimethyl sulfoxide (DMSO) solvent, ethyl alcohol as well as blocking reagents - blocker-casein blocking buffer were all purchased from Thermofisher Scientific (Waltham, MA). N-(3-dimethylaminopropyl)-N'-ethylcarbodiimide hydrochloride (EDC), carboxymethyl dextran (CMD) sodium salt and horseradish peroxidase (HRP)-conjugated streptavidin (S-HRP) were from Sigma-Aldrich (St. Louis, MO) while the mediator, 1,1'-ferrocenedicarboxylic acid (FeDC) was purchased from Strem Chemicals (Newburyport, MA). Gold nanoparticles solution with an average diameter of 13 nm was synthesized following previous reports (Quintela, de los Reyes et al. 2015). All reagents used were of analytical-reagent grade and all solutions were prepared with deionized water from Millipore (Milli-Q, 18.2M Ω cm).

All cyclic voltammetry (CV) and amperometric tests were conducted using PalmSens3 Electrochemical Portable Apparatus - Potentiostat/Galvanostat/Impedance Analyser (PalmSens Instrument BV, Houten, The Netherlands) which was wirelessly connected via Bluetooth™ and controlled by an Android™ device. The PalmSens3 instrument which had a dynamic range that allowed microelectrodes applications such as SPCEs, was supported by its software-PSTrace5 (Palm Instrument BV) for data processing. All CV and amperometric data were exported to Microsoft Excel for analysis. Screen-printed carbon electrodes (SPCEs, reference # DRP-110, DRP-C110) with three electrodes in ceramic substrate support (3.4 length x 1.0 width x 0.05

height cm) and silver contacts ideal for microvolumes (50 μ L) were purchased from DropSens (Asturias, Spain).

5.2.2. Bacterial Strains and Biotinylated STEC-bacteriophages

All bacterial strains used in this study were obtained from University of Maine-Pathogenic Microbiology Laboratory, Orono, ME and USDA-Agricultural Research Services (ARS) Centers (Produce Safety and Microbiology Unit, Albany, CA and Wyndmoor, PA) strain collections. For target bacteria/analyte, representative strains of STEC serogroups (O26 O26:H11 HH8, O157:H7 ATCC 35150, and O179) were used while *Salmonella* Typhimurium ATCC 14028 was chosen as non-target bacterium. Frozen bacterial strains in cryogenic beads (CryoSavers; Hardy Diagnostics, Santa Maria, CA, USA) were initially activated and revived in Brain Heart Infusion (BHI) broth (Neogen, Lansing, MI, USA) at 37°C. Overnight cultures were washed with 10 mL 1X PBS by centrifugation at 5000 \times g for 10 mins. Pellets were resuspended in 1X PBS and serially diluted up to 10⁻⁷ for total plate count (TPC). STEC strains were confirmed using appropriate selective agar media, MacConkey Agar with Sorbitol (Neogen) for STEC strains and Xylose lysine deoxycholate (XLD) agar (Neogen) for *Salmonella* spp. strain.

In the previous chapters of this dissertation, STEC-specific bacteriophages were comprehensively characterized and chemically-modified with biotin. Among those STEC bacteriophages, three representative bacteriophages were utilized in this study as shown in **Table 5.1**. These three biotinylated bacteriophage groups were used to biologically activate the surface of SPCEs as the capture elements (CE) and detection elements (DE). Detection elements (DE) were labeled with horseradish peroxidase (HRP) (Sigma-Aldrich) cells and AuNPs for signal amplification, which were then used for sandwich recognition of target STEC live before directly detecting them using the amperometric biosensor.

Table 5.1. STEC-specific bacteriophages used in this study and their host bacteria.

Bacteriophage	Family	STEC Host	Abbreviation	Reference
Bacteriophage O26	<i>Myoviridae</i>	O26:H11 HH8	B-O26	<i>this study</i>
Bacteriophage O157	<i>Myoviridae</i>	O157:H7 35150	B-O157	<i>this study</i>
Bacteriophage O179	<i>Siphoviridae</i>	O179	B-O179	<i>this study</i>

5.2.3. Fabrication of the Bacteriophage-based Biosensor

The principles of the newly-developed STEC-specific bacteriophage-based biosensor are detailed in **Figure 4.2** while the complete system is shown in **Figure 4.3**. Both figures are presented in the previous chapter of this dissertation.

Carboxyl (-COOH) was introduced onto the clean working electrode (WE) surface by adding CMD (Sigma-Aldrich) (20 μ L, 50 mg/mL) and incubated for 3 hr with shaking (300 rpm) at room temperature. EDC (0.4M, Sigma-Aldrich) and NHS (0.1M, Thermofisher Scientific) in equal volumes (10 μ L) were added to activate -COOH. Streptavidin (20 μ L, 50 μ g/mL, Thermofisher Scientific) which carried the amine was then transferred onto the -COOH activated SPCE for carboxyl-to-amine crosslinking. Biotinylated bacteriophages (20 μ L, > 8 log PFU/mL) were then introduced and formed covalent bond via biotin-streptavidin interaction during its overnight incubation (4°C) on the surface of WE. Biofunctionalized SPCEs with immobilized biotinylated bacteriophages were blocked with 30% casein (20 μ L) overnight at 4°C before washing them twice (100 μ L) with TBS-T20 (Thermofisher Scientific) and once with 0.5 X PBS (100 μ L). All biofunctionalized SPCEs were stored at 4°C until further use. For the

purposes of this study, the term “capture elements” refers to biofunctionalized SPCEs and has been used thereafter.

To complete the detection system that would allow utilization of sandwich-type recognition of live STEC cells, the remaining integral component termed as “detection element” was constructed. In brief, streptavidin-horse radish peroxidase (100 µg/mL) (Sigma-Aldrich) and AuNP solution (ave 13 nm diameter, 20 µM, 100 µL) were both added onto biotinylated bacteriophages (700 µL, > 8 log PFU/mL) and incubated overnight at 4°C until further use. Detection element (DE) solution (20 µL) was added to the captured STEC live cells in the WE of biofunctionalized SPCE.

5.2.4. Food Samples

Direct detection of representative STEC strains spp. in complex matrices was conducted by using the newly developed and optimized Shiga toxin-producing *Escherichia coli* (STEC) bacteriophage-based biosensor. Unlike the common traditional methods, this technology did not require pre-enrichment of samples prior to its testing in micro volumes (50 µL).

In brief, fresh ground beef and pasteurized apple juice were purchased from a local retailer. Weighed fresh ground beef samples (25 g) were transferred into individual stomacher bags (Fisher Scientific). After which, washed overnight cultures of STEC O26:H11 HH8, O157:H7 ATCC 35150, O179 and *Salmonella* Typhimurium ATCC 14028 in 1X PBS were individually spiked onto the food samples before adding 225 mL of 1X PBS Buffered Peptone Water (BPW) (Thermofisher Scientific) to reach the final inoculum levels of 1-4 log CFU/mL and 8 log CFU/mL. Inoculated fresh ground beef samples were then homogenized (10 sec) using a Pulsifier (Microbiology International, MD, USA) before taking 50 µL of each sample for amperometric biosensing. For pasteurized apple juice, 1 mL of the inoculum was added onto 9

mL aliquoted samples and then diluted to reach the same inoculum levels as the fresh ground beef samples. For both food samples, 1X PBS was used to inoculate the control while *S. Typhimurium* ATCC 14028 for non-target samples. All artificially inoculated food samples were temporarily stored at 4°C until further use. Two sets of parallel tests were also conducted for verification: conventional PCR targeting *stx* genes and plate count method using the appropriate selective agar as mentioned in the previous section.

5.2.5. Environmental Water Samples

The prevalence of representative STEC serogroups in its natural environment was also determined. Natural environmental surface water samples were tested to demonstrate the reproducibility of the newly-developed biosensor on more complex and natural matrices. All environmental water samples were provided by the USDA-Agricultural Research Services (ARS) Center (Produce Safety and Microbiology Unit, Albany, CA) from its comprehensive environmental samples collection from different states in Northern California. **Figures 5.1-5.2** show the environmental water sampling sites in Pescadero, CA . Water samples were collected from ponds and sediments which were used to irrigate fields and farms with observed animal activities (ie coyote and deer tracks). From each sample, 50 µL volume was taken and directly tested for the presence of representative STEC serogroups. All samples were tested in duplicates and single repeat. For comparison, conventional PCR was also performed to determine the presence of STEC virulence genes, *stx1* and *stx2*. In brief, bacteriophage genomic DNA was extracted from purified bacteriophages using Phage DNA Isolation Kit (Norgen Biotek Corp, Ontario, Canada) following manufacturer's extraction. Extracted DNA was kept at -20°C until further use. Specific primers (**Table 5.2**) and amplification conditions as previously reported were used. The conventional PCR conditions were as follow, denaturation at 95°C for 2 min; 35

cycles of 30 sec denaturation at 95°C, annealing at 56°C for 30 sec, elongation at 72°C for 30 sec and final extension at 72°C for 5 min (Quintela, de los Reyes et al. 2015). **Table 5.3** shows the identification and description of each water and sediment water sample.

Table 5.2. Primers for *stx* genes (Quintela, de los Reyes et al. 2015).

Name	Sequence
<i>stx1</i> For(<i>stx1</i> -1-F)	5' - CATCGCGAGTTGCCAGAATG - 3'
<i>stx1</i> Rev(<i>stx1</i> -1-R)	5'- AATTGCCCCCAGAGTGGATG - 3'
<i>stx2</i> For(<i>stx2</i> -5-F)	5' - GTATAC GATGACGCCGGGAG - 3'
<i>stx2</i> For(<i>stx2</i> -5-R)	5'- TTCTCCCCACTCTGACACCA - 3'

Table 5.3. List of environmental water samples from Pescadero, CA. All samples were provided by USDA-WRRC-ARS (PSM Unit).

Sample/Site	Sample ID	Description	Sampling Sites
1	P1-D	Sediment water samples	Pescadero, CA
2	P8-W	Irrigation water samples	Pescadero, CA
3	P1-W	Irrigation water samples	Pescadero, CA
4	P7-W	Irrigation water samples	Pescadero, CA

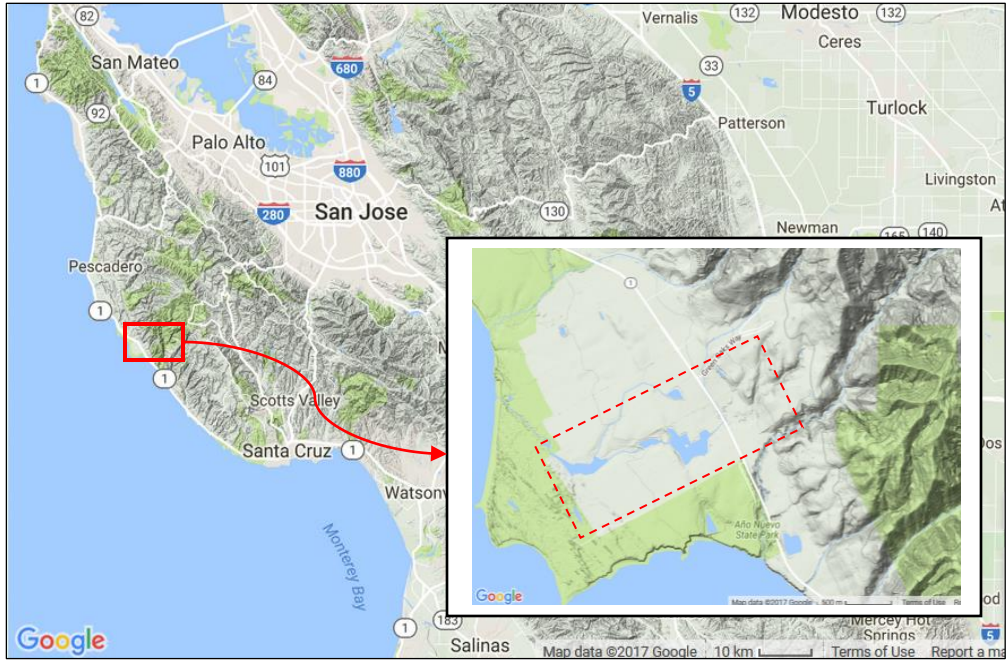


Figure 5.1. Location of the sampling sites where water samples were collected. Inserted is the enlarged image of the demarcated sampling site.

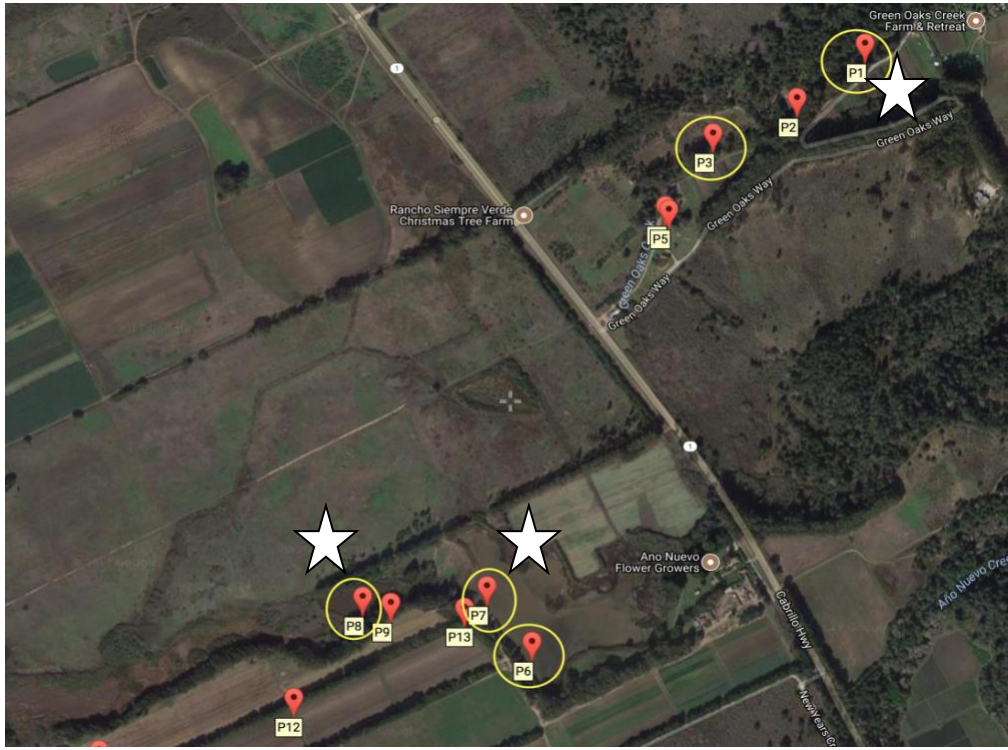


Figure 5.2. Map of the specific sampling sites (starred) where water and sediment samples were collected.

5.2.6. Amperometric Test

In brief, 50 μL of inoculated (target and non-target) samples (1-4 log CFU/mL and/or 8 log CFU/mL) and controls were individually dropped onto each working electrode (WE) of biofunctionalized SPCEs and incubated for 12 min at room temperature before washing with 0.5 X PBS (100 μL). Once the target STEC cells were captured by the immobilized bacteriophages, the detection element (20 μL) was then added for sandwich-type detection of another 10 min before washing twice with 100 μL volume of TBS-T20 and once with 0.5 X PBS. The mediator, 250 mM FeDC in DMSO was then added (5 μL) for 30 sec before transferring hydrogen peroxide (H_2O_2) (40 mM, 15 μL) for another 30 sec. After which amperometric tests were conducted using the PalmSens device. Amperometric detection was performed with a fixed potential of 0.5 V for 100 secs in all samples (triplicates) throughout the trials with an operating temperature around 25°C (room temp).

Amperometric test measured the response current (RC) that was generated by the substrate within a set of potentials over time and was used to calculate for the delta (Δ) current, [Δ current = response current of samples (target or non-target) – RC of control]. In this study, the signal threshold for positive detection was defined by the signal-to-noise (S/N) characteristics as $S/N > 3$, where the target could provide a signal a least three times greater than the signal from non-targets. The linear calibration curve ($y = mx + b$) assumed the response (y) is linearly related to the concentration (x)(Shrivastava and Gupta 2011, Tolba, Ahmed et al. 2012). The limit of detection (LOD) was determined by the statistical significance of signals (Δ current) between non-target bacteria and the lowest inoculum of target bacteria which had a calculated Δ current above the signal threshold for positive detection

5.2.7. Statistical Analysis

To evaluate the assay's reproducibility, triplicates of disposable and modified SPCE per each sample were setup and tested. For all food samples that were artificially spiked with bacteria, three trials were performed per each experiment. The mean of the data is shown in a bar graph and standard deviation (S.D) as error bars. Linear regression was calculated using Microsoft Excel. One-way ANOVA and Fisher's least significance difference (LSD) for post-hoc analysis to confirm the significant differences between groups were conducted using JMP software. $P < 0.05$ was considered statistically different.

5.3. Results

5.3.1. Food Matrices-Fresh Ground Beef

The capture and sandwich-type detection of target STEC live cells by the highly-specific bacteriophages are the key novel features of this newly-developed biosensor. Once the target STEC cells were captured from the complex matrices (ie food and environmental water samples) via the SPCE-immobilized bacteriophages, a detection element which was composed of the same kind of bacteriophages but labeled with HRP to hasten catalytic reactions and signal amplifier (AuNPs) was added. The procedures did not require pre-enrichment of food and environmental water samples but only needed a quick homogenization (ie for solid samples) steps before directly testing them using 50 μL micro volumes. The amperometric results are shown in the succeeding figures that include the response current (RC, μA) of each experiment in the form of amperometric curves as well as the mean delta (Δ) current in bar graphs with standard deviation as error bars.

Figures 5.3-5.5 present the results of artificially-inoculated fresh ground beef with three representative STEC serogroups at various low inoculum levels (1-4 log CFU/g). **Figure 5.3** shows the detection of STEC O26:H11 HH8 as the target bacterium with bacteriophage B-O26. **Figure 5.3 (A)** is the amperometric curve showing the response current (RC) of samples at fixed potential (0.5 V) for 100 secs. **Figure 5.3 (B)** is a bar graph showing delta Δ current with a linear correlation, $R^2 = 0.98$. Linear relationship was described as Δ Current (μA) = 42.986 x (inoculum level in log CFU/mL of STEC O26) + 47.509, with a linear range of 1-4 log CFU/mL. The signal threshold for positive target detection was 48.511 μA . Non-target (*S. Typhimurium*) was significantly different. The LOD was determined to be 1 log CFU/g.

In **Figure 5.4**, it presents the detection of STEC O157 in artificially inoculated fresh ground beef using B-O157 bacteriophage. **Figure 5.4 (A)** shows the amperometric curves of the RC generated from various inoculums. **Figure 5.4 (B)** provides a bar graph of the delta Δ current with a linear correlation, $R^2 = 0.96$. Linear relationship was described as Δ Current (μA) = 41.552 x (inoculum level in log CFU/mL of STEC O157) + 39.833, with a linear range of 2-4 log CFU/mL. Non-target (*S. Typhimurium*) was significantly different from STEC (2 log CFU/b) and the LOD was determined to be 2 log CFU/g.

The last STEC strain that was artificially spiked on fresh ground beef was STEC O179 and detected using its specific bacteriophage, B-O179 (**Figure 5.5**). **Figure 5.5 (A)** shows the amperometric curves of the RC generated from various inoculums. **Figure 5.5 (B)** provides a bar graph of the delta Δ current with a linear correlation, $R^2 = 0.97$. Linear relationship was described as Δ Current (μA) = 19.932 x (inoculum level in log CFU/mL of STEC O179) + 77.186, with a linear range of 1-4 log CFU/mL. The signal threshold for positive target detection was 126.23 μA while the LOD was determined to be 3 log CFU/g as the result of statistical analysis.

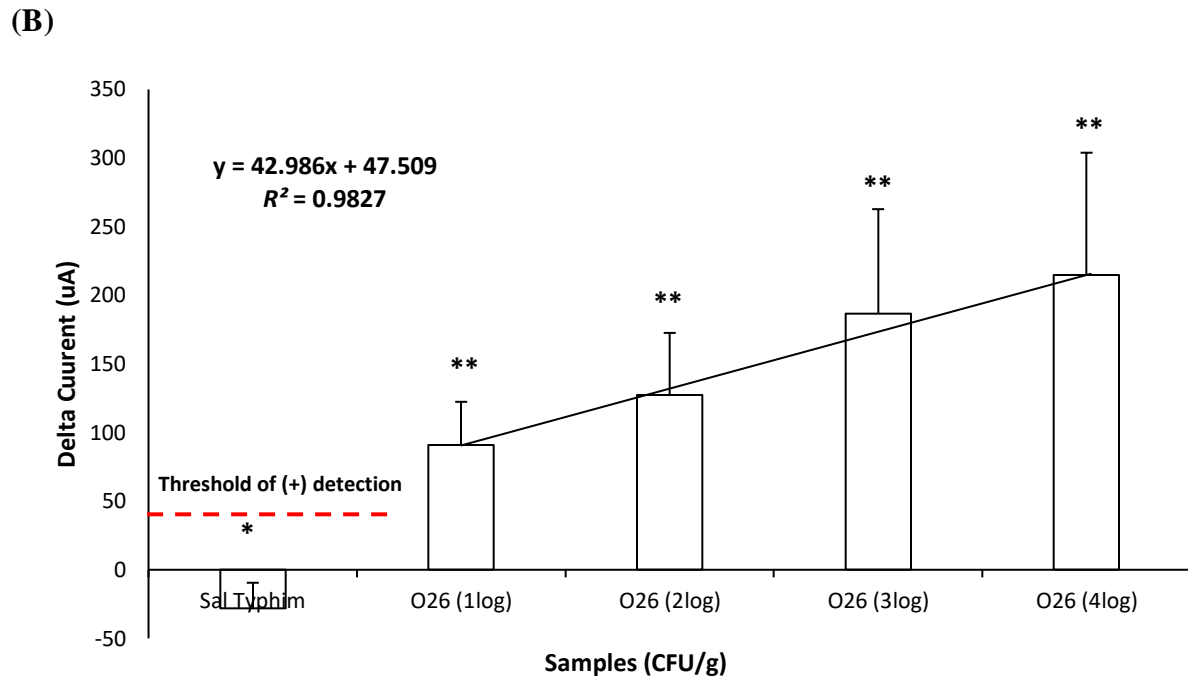
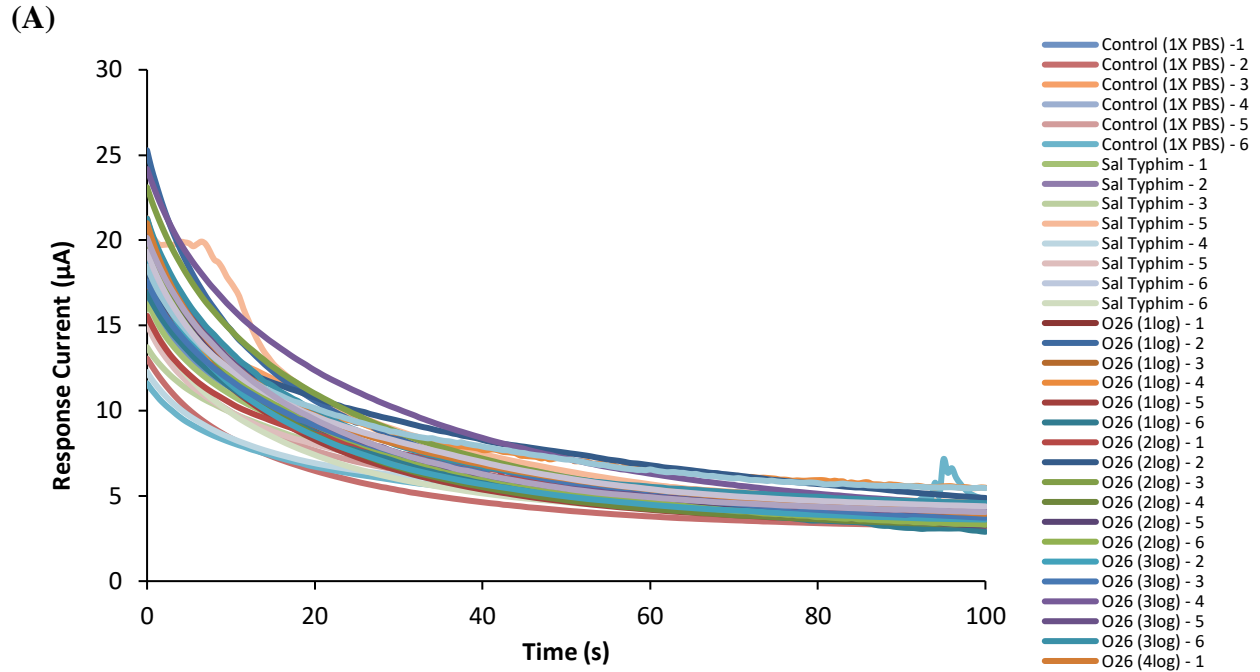


Figure 5.3. Amperometric test of artificially-inoculated fresh ground beef (STEC O26). (A) Amperometric curves showing the response current (RC) of samples at fixed potential (0.5 V) for 100 secs (B) The delta (Δ) Current (μA) of low-level STEC O26 inoculums showing a positive linear regression, $R^2 = 0.95$. Dotted red line is the calculated delta (Δ) current threshold (48.511 μA) for positive detection. Non-target (*S. Typhimurium*) was significantly different. LOD was 1 log CFU/g. (*) indicates significant difference. $P < 0.05$

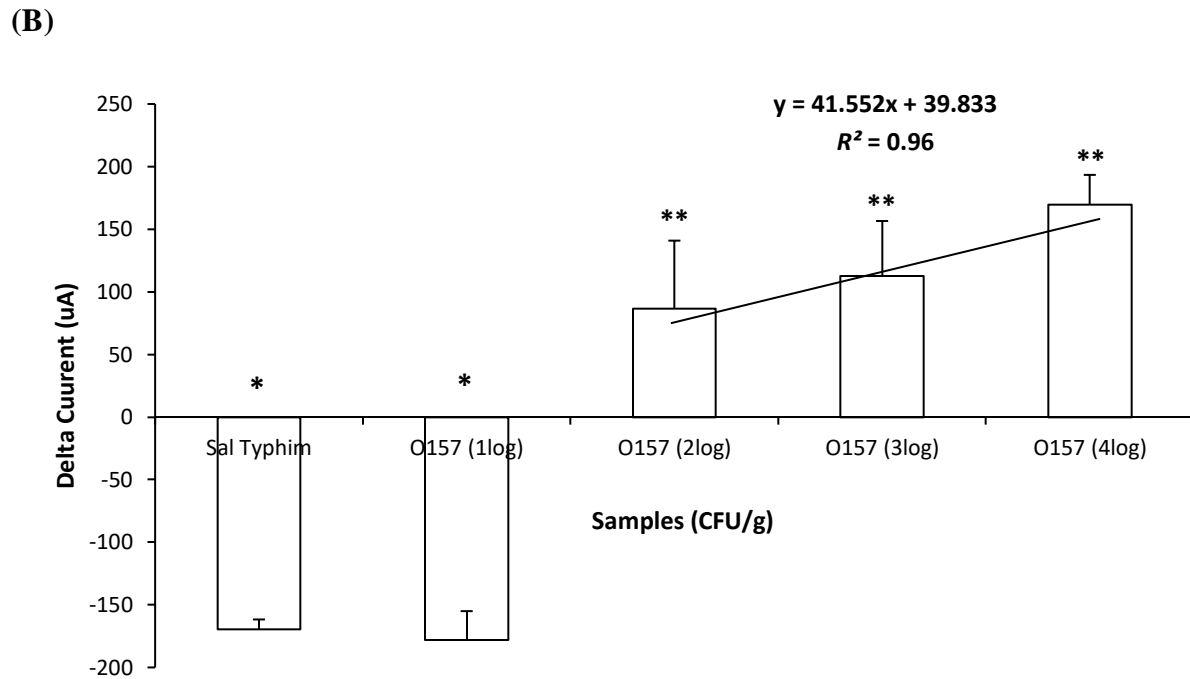
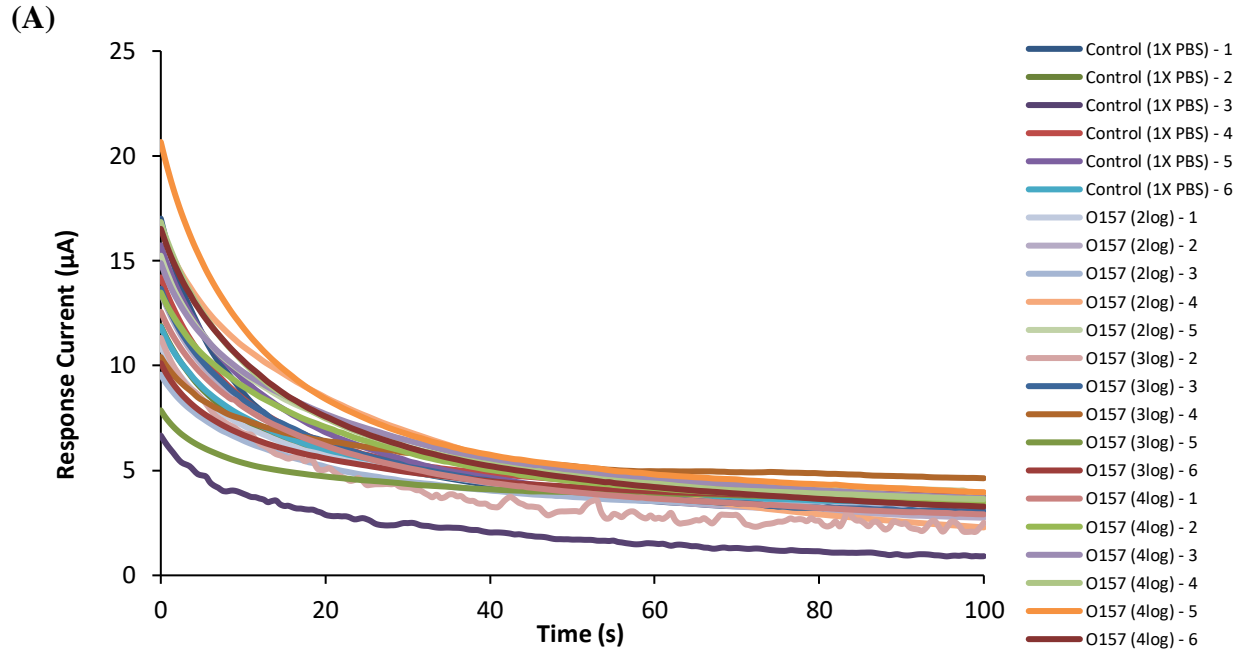


Figure 5.4. Amperometric test of artificially-inoculated fresh ground beef (STEC O157). (A) Amperometric curves showing the response current (RC) of samples at fixed potential (0.5 V) for 100 secs (B) The delta (Δ) Current (μA) of low-level STEC O157 inoculums showing a positive linear regression, $R^2 = 0.96$. Non-target (*S. Typhimurium*) was significantly different from STEC (2 log CFU/g). The LOD for this assay was 2 log CFU/g. (*) indicates significant difference. $P < 0.05$

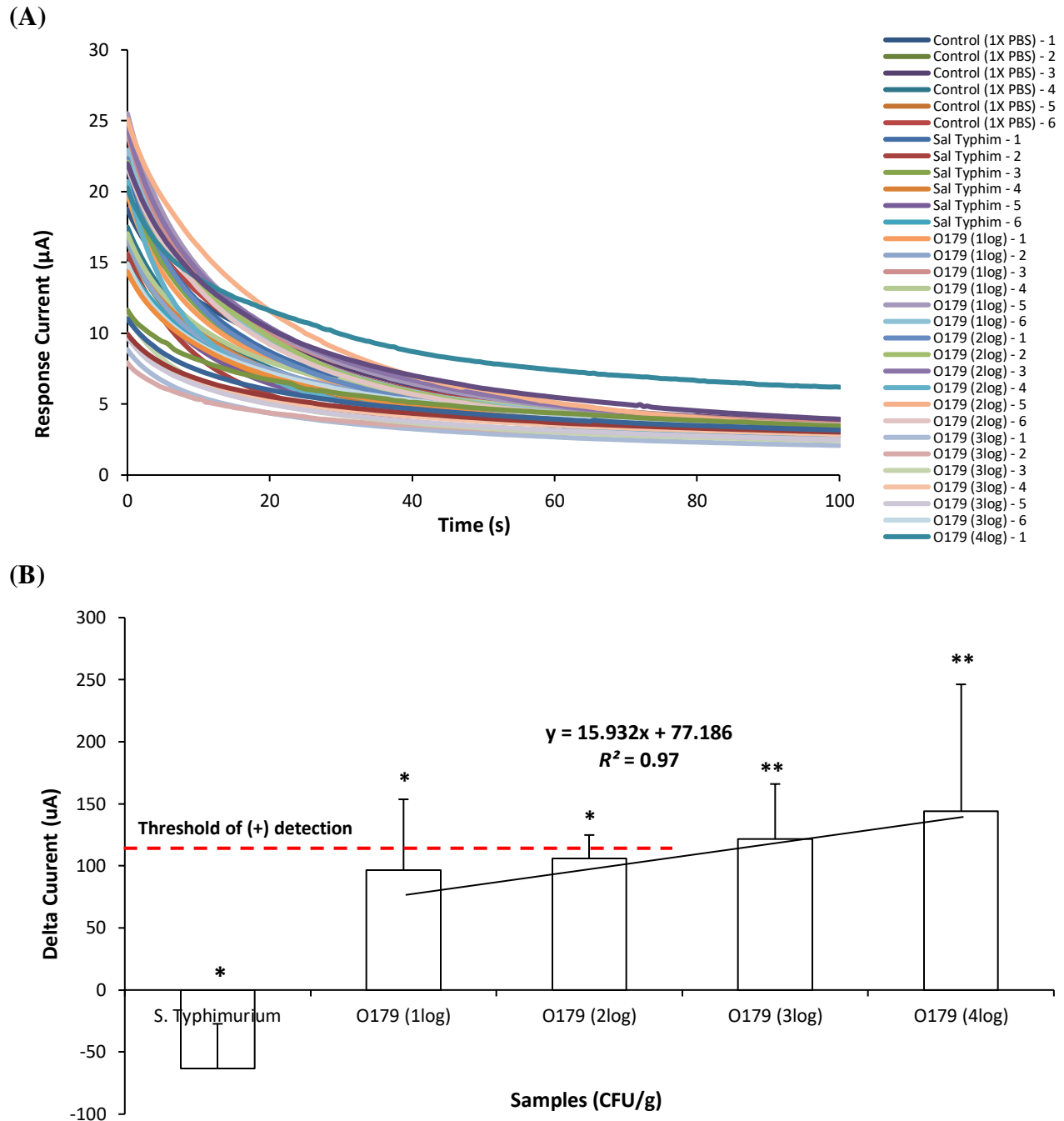


Figure 5.5. Amperometric test of artificially-inoculated fresh ground beef (STEC O179). (A) Amperometric curves showing the response current (RC) of samples at fixed potential (0.5 V) for 100 secs (B) The delta (Δ) Current (μA) of low-level STEC O179 inoculums showing a positive linear regression, $R^2 = 0.97$. Dotted red line is the calculated delta (Δ) current threshold (126.23 μA) for positive detection. Non-target, *S. Typhimurium* was significantly different from STEC O179 (3 log CFU/g). The LOD for this assay was 3 log CFU/g. (*) indicates significant difference. $P < 0.05$

5.3.2. Food Matrices-Pasteurized Apple Juice

The second food sample that was tested was pasteurized apple juice. **Figures 5.6-5.8** present the results of artificially-inoculated pasteurized apple juice with three representative STEC serogroups at various low inoculum levels (1-4 log CFU/mL). These inoculum levels of the representative STEC serogroups were similar to that of fresh ground beef presented in the previous section with *S. Typhimurium* as non-target (8 log CFU/mL).

Figure 5.6 shows the detection of STEC O26:H11 HH8 as the target bacterium with bacteriophage B-O26 biosensor. **Figure 5.6 (A)** presents the amperometric curve showing the response current (RC) of samples at fixed potential (0.5 V) for 100 secs. SPCEs were functionalized using B-O26 bacteriophage. The bar graph in **Figure 5.6 (B)** shows the delta Δ current with a linear correlation, $R^2 = 0.8112$. Linear relationship was described as delta Δ current (μA) = 35.328 x (inoculum level in log CFU/mL of STEC O26) + 24.278. Both 1 log CFU/mL of STEC O26 and non-target sample, *S. Typhimurium* generated a negative delta Δ current (μA) value and relatively wide standard deviation. Interestingly, the delta Δ current (μA) values of non-target sample *S. Typhimurium*, 1 log CFU/mL and 2 log CFU/mL of STEC O26 were not significantly different from each other. Therefore, the LOD was determined to be 3 log CFU/mL of STEC O26.

Figure 5.7 (A) presents the RC of STEC O157 in amperometric curve format. The delta Δ current with a linear correlation, $R^2 = 0.8934$. Linear relationship was described as delta Δ current (μA) = 38.2 (inoculum level in log CFU/mL of STEC O157) + 24.278. The threshold for positive detection was 178 μA . The delta Δ current (μA) of non-target sample *S. Typhimurium* was not statistically significant from 1-2 log CFU/mL of STEC O157. Therefore, the LOD was determined to be 3 log CFU/mL of STEC O157.

Figure 5.8 (A) presents the RC of STEC O179 in amperometric curve format. The delta Δ current with a linear correlation, $R^2 = 0.8834$. Linear relationship was described as delta Δ current (μA) = 716.77 (inoculum level in log CFU/mL of STEC O179) – 897.07. Similar to the results of the two STEC serogroups (O26 and O157), the delta Δ current (μA) of non-target sample *S. Typhimurium* was not statistically significant from 1-2 log CFU/mL of STEC O179. The limit of detection (LOD) was determined by the significant difference of signals (Δ current) between non-target bacteria and the lowest inoculum of target bacteria (3 log CFU/mL) which had a calculated Δ current above signal threshold (10.69 μA) for positive detection. The LOD was 3 log CFU/mL since non-target sample *S. Typhimurium*, 1 log CFU/mL and 2 log CFU/mL of STEC O179 were not significantly different from each other.

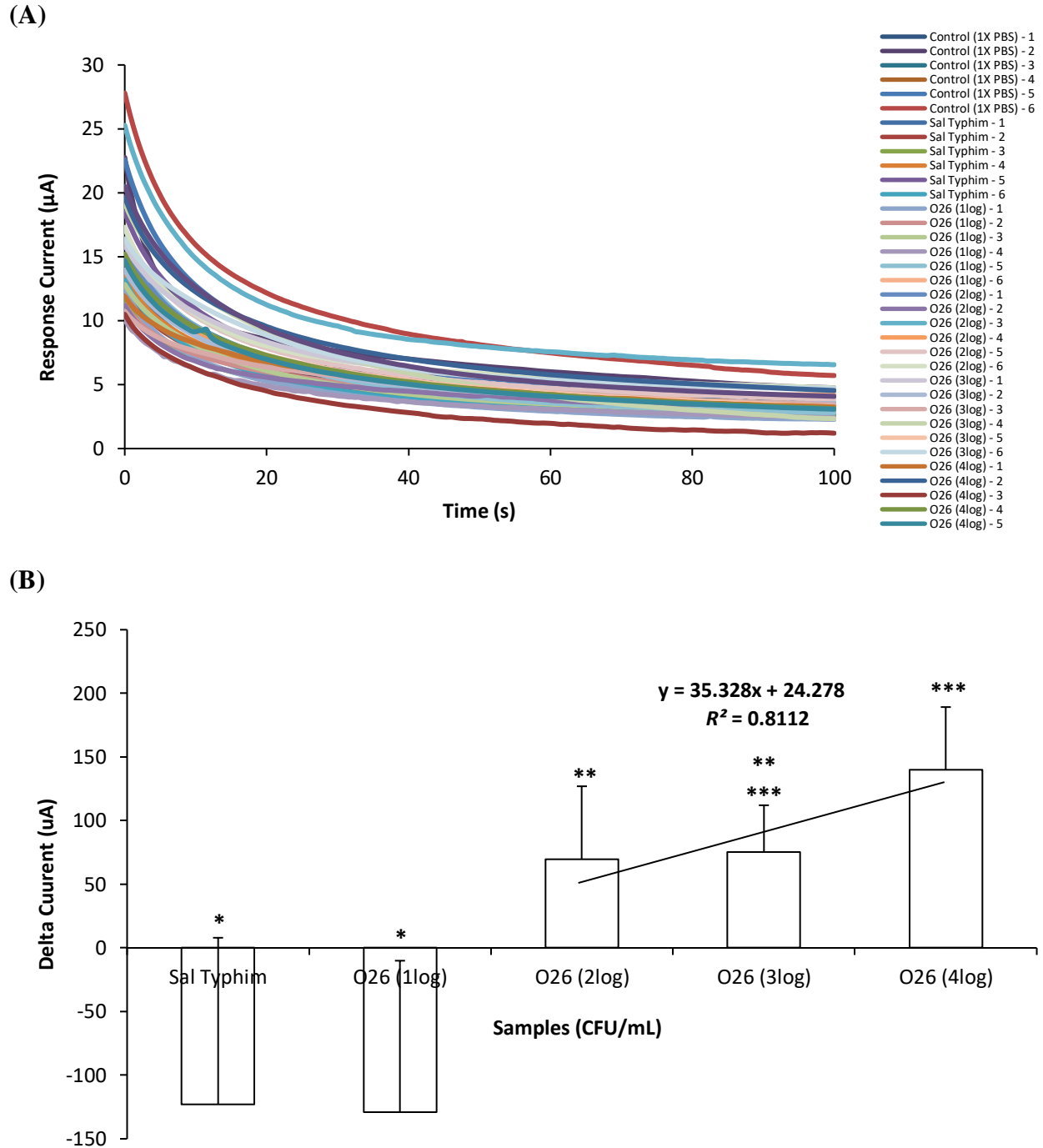


Figure 5.6. Amperometric test of artificially-inoculated pasteurized apple juice (STEC O26). (A) Amperometric curves showing the response current (RC) of samples at fixed potential (0.5 V) for 100 secs (B) The delta (Δ)Current (μA) of low-level STEC O157 inoculums showing a positive linear regression, $R^2 = 0.81$. Non-target, *S. Typhimurium* was significantly different from STEC O26 (2 log CFU/mL). The LOD for this assay was 2 log CFU/mL. (*) indicates significant difference. $P < 0.05$

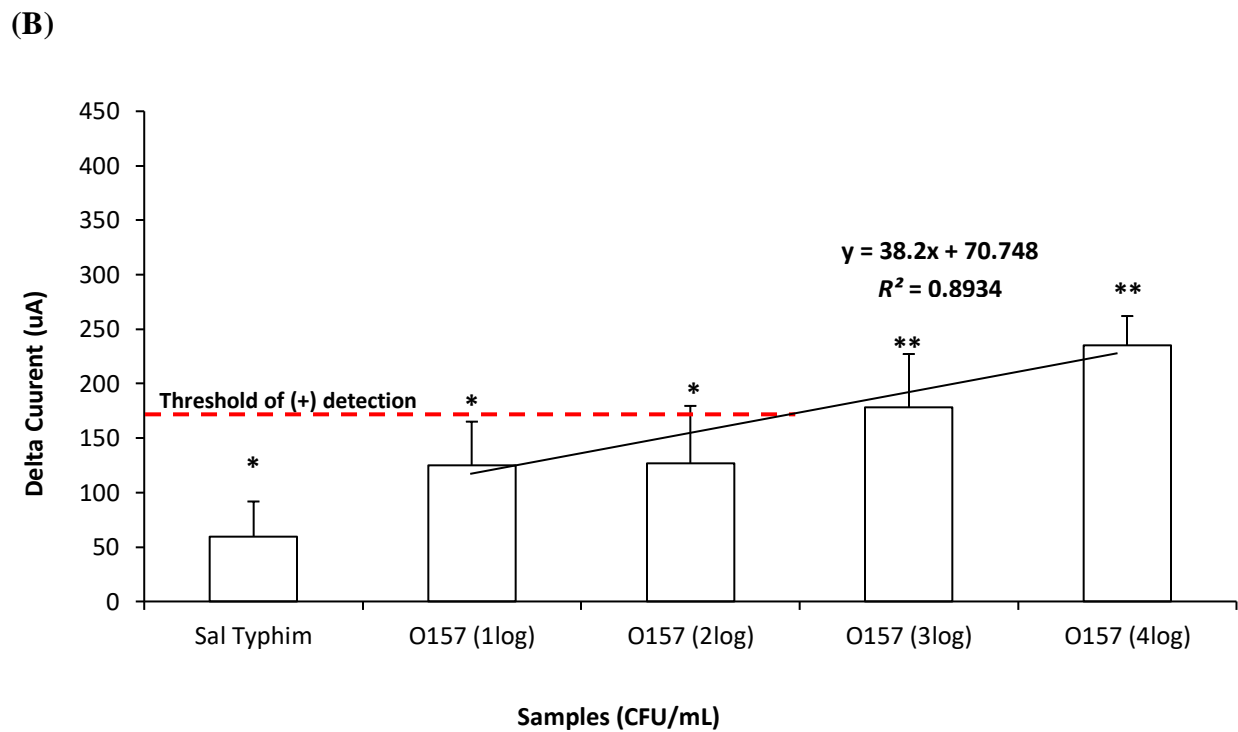
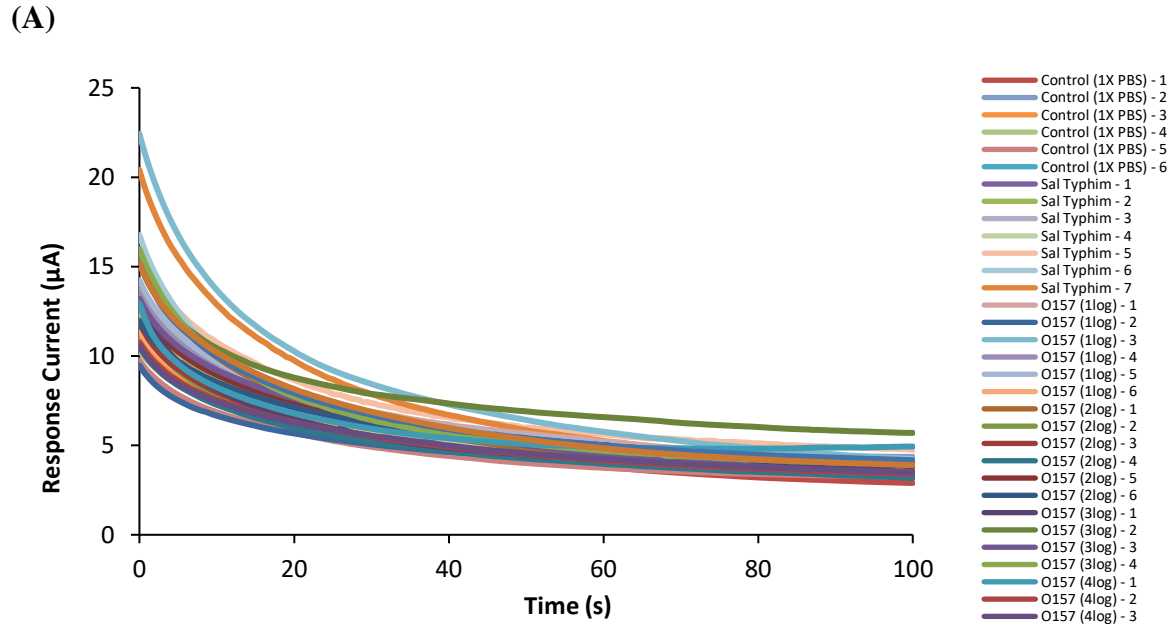


Figure 5.7 Amperometric test of artificially-inoculated pasteurized apple juice (STEC O157). (A) Amperometric curves showing the response current (RC) of samples at fixed potential (0.5 V) for 100 secs (B) The delta (Δ)Current (μA) of low-level STEC O157 inoculums showing a positive linear regression, $R^2 = 0.89$. Dotted red line is the calculated delta (Δ) current threshold (178 μA). Non-target, *S. Typhimurium* was significantly different from STEC O157 (3 log CFU/mL). The LOD for this assay was 3 log CFU/mL. (*) indicates significant difference. $P < 0.05$

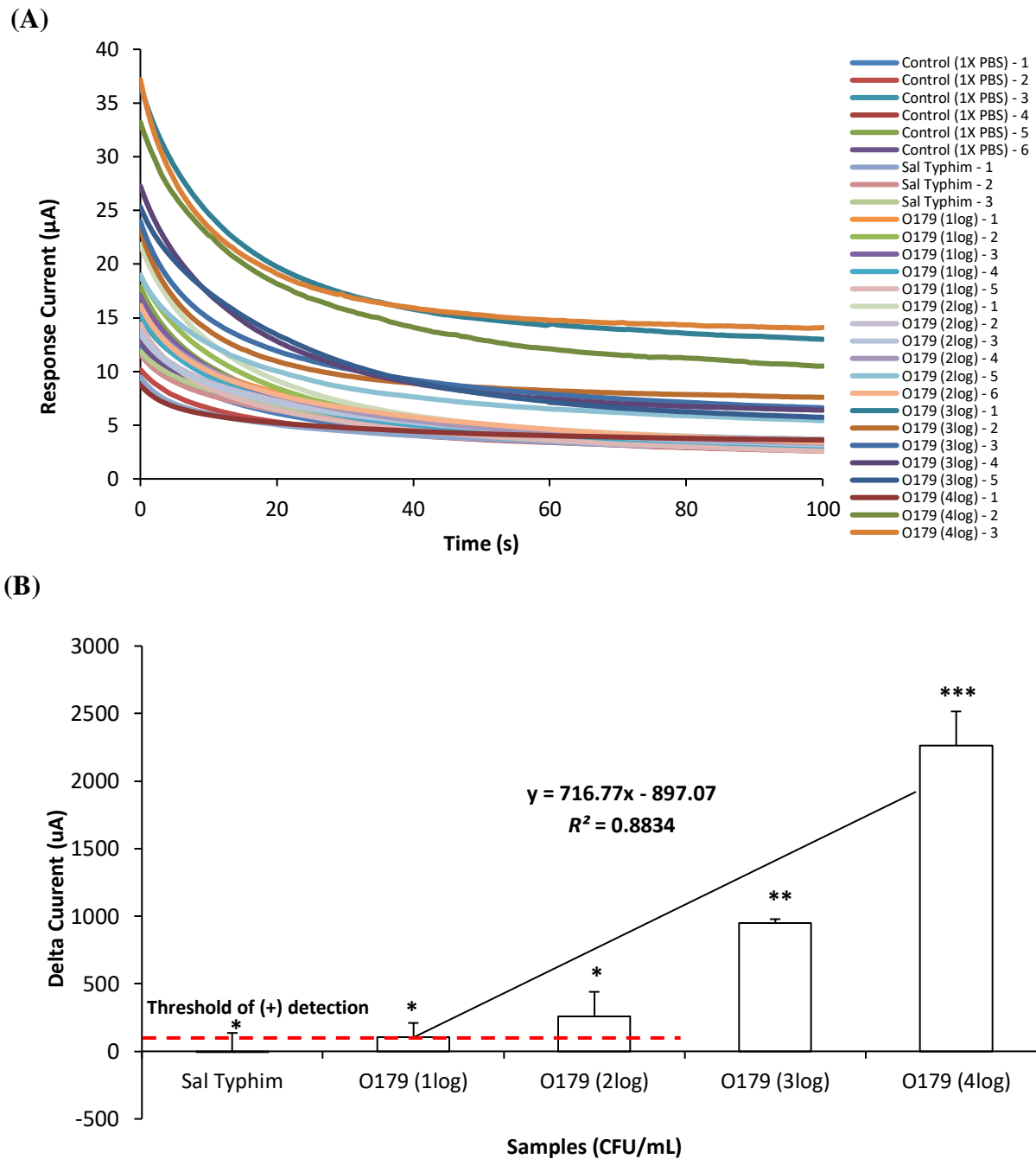


Figure 5.8. Amperometric test of artificially-inoculated pasteurized apple juice (STEC O179). (A) Amperometric curves showing the response current (RC) of samples at fixed potential (0.5 V) for 100 secs (B) The delta (Δ)Current (μA) of low-level STEC O179 inoculums showing a positive linear regression, $R^2 = 0.88$. Dotted red line is the calculated delta (Δ) current threshold (10.69 μA). Non-target, *S. Typhimurium* was significantly different from STEC O179 (3 log CFU/mL). The LOD for this assay was 3 log CFU/mL. (*) indicates significant difference. $P < 0.05$

5.3.3. Environmental Water Samples

Figures 5.9-5.11 present the amperometric data from testing environmental water samples. These environmental samples were uninoculated and untreated and each was directly tested using different bacteriophage-based SPCEs. These modified SPCEs were specific to STEC serogroup. Parallel tests such as selective plating and conventional PCR were also conducted to evaluate the presence of STEC bacteria and confirm the biosensor results. The delta Δ current (μA) of each sample/site was presented and compared with the signal threshold that was previously generated and optimized from the pure culture study presented in Chapter 4 of this dissertation. These thresholds are shown in **Table 5.4** as a reference.

Table 5.4. Reference signal threshold [Delta Δ current (μA)] optimized from pure culture study. These reference signals were used to interpret the results [delta Δ current (μA)] from testing various environmental water samples using the newly-developed STEC specific bacteriophage-based biosensor.

Target STEC	Signal Threshold [Delta Δ current (μA)]	LOD/Inoculum Level (CFU/mL)	Reference
STEC O26	66.9 μA	1 log CFU/mL	<i>This study</i>
STEC O157	122.13 μA	2 log CFU/mL	<i>This study</i>
STEC O179	101 μA	2 log CFU/mL	<i>This study</i>

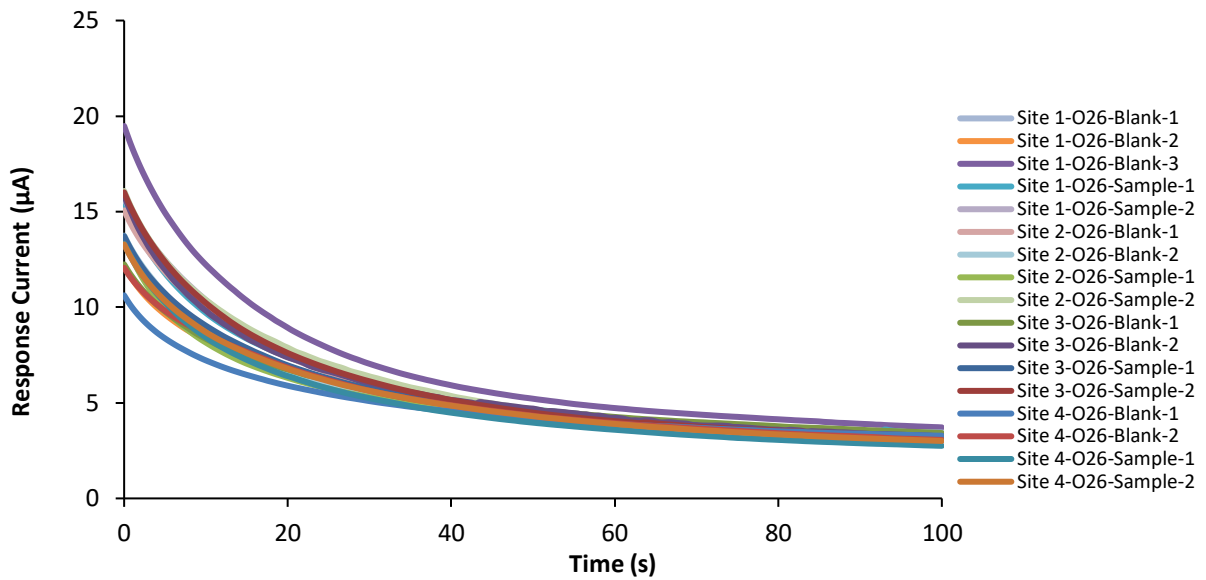
Figures 5.9. (A) and (B) show the response current (RC) and delta Δ current (μA) of four environmental water samples from different sampling sites, respectively. None of the water samples generated a delta Δ current (μA) that was higher than the signal threshold (66.9 μA) for positive detection of STEC O26.

Figures 5.10. (A) and (B) present the response current (RC) and delta Δ current (μA), respectively, of the four environmental water samples after testing them for the presence of

STEC O157. Similarly, all sampling sites had lower delta Δ current (μA) as compared to the signal threshold ($122.13 \mu\text{A}$) for positive detection of STEC O157.

Finally, the data for the detection of STEC O179 from the environmental water samples are shown in **Figures 5.11. (A)** and **(B)**. With reference to the signal threshold ($101\mu\text{A}$) for positive detection of STEC O179, all sampling sites had lower delta Δ current (μA) as compared to the signal threshold for positive detection of STEC O179.

(A)



(B)

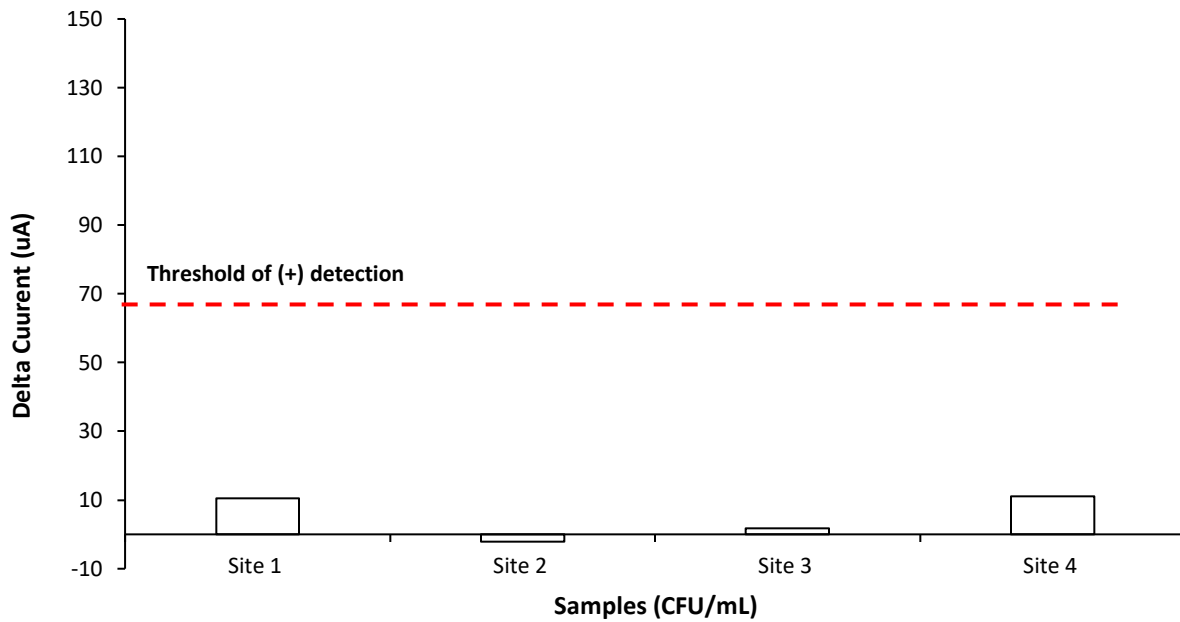
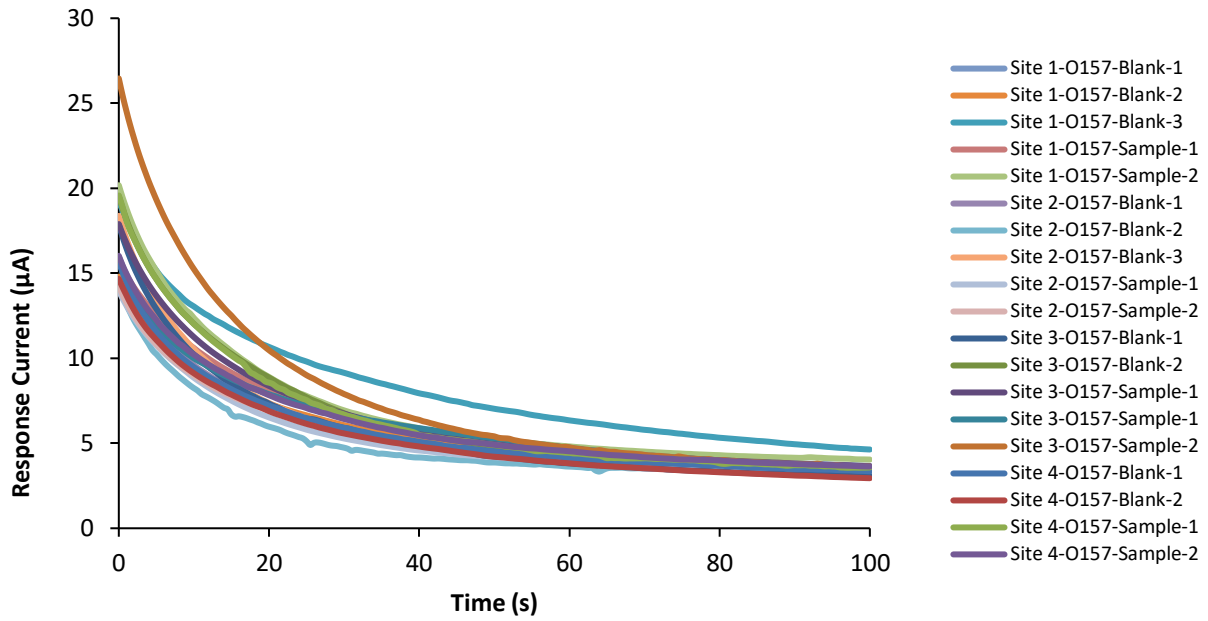


Figure 5.9. Amperometric test of environmental samples using STEC O26-specific bacteriophage biosensor. (A) Amperometric curves showing the response current (RC) of samples from four different sites at fixed potential (0.5 V) for 100 secs **(B)** The delta (Δ) Current (μA) of each sampling site is shown. Dotted red line is the reference delta (Δ) current threshold (66.9 μA) for positive detection from pure culture study targeting STEC O26.

(A)



(B)

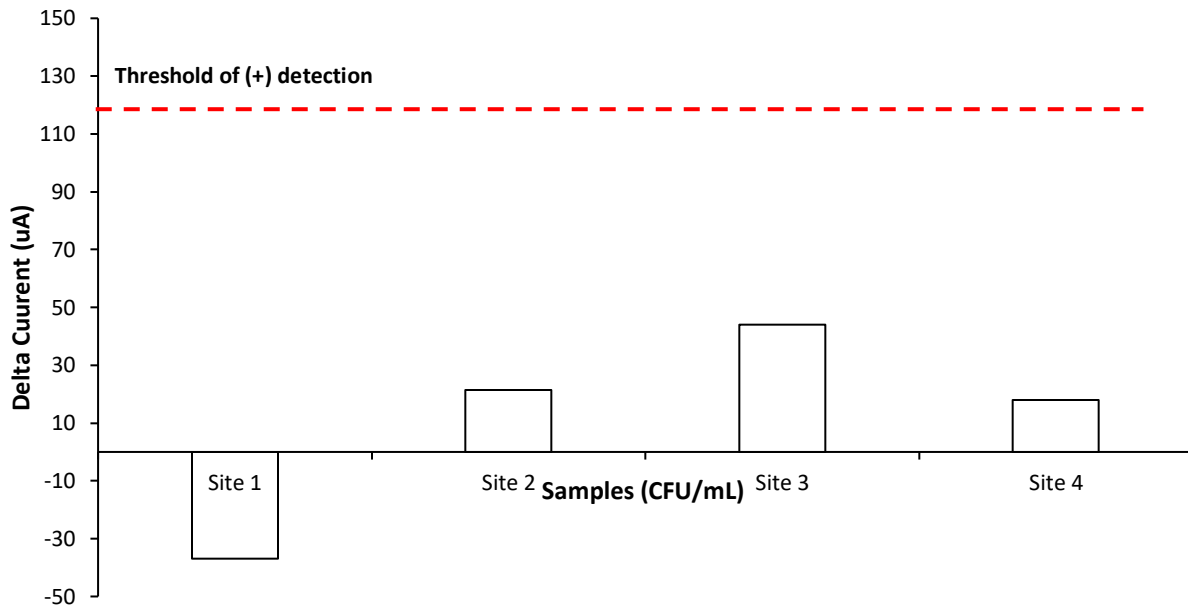


Figure 5.10. Amperometric test of environmental samples using STEC O157-specific bacteriophage biosensor. (A) Amperometric curves showing the response current (RC) of samples from four different sites at fixed potential (0.5 V) for 100 secs (B) The delta (Δ) Current (μA) of each sampling site is shown. Dotted red line is the reference delta (Δ) current threshold (122.13 μA) for positive detection from pure culture study targeting STEC O157.

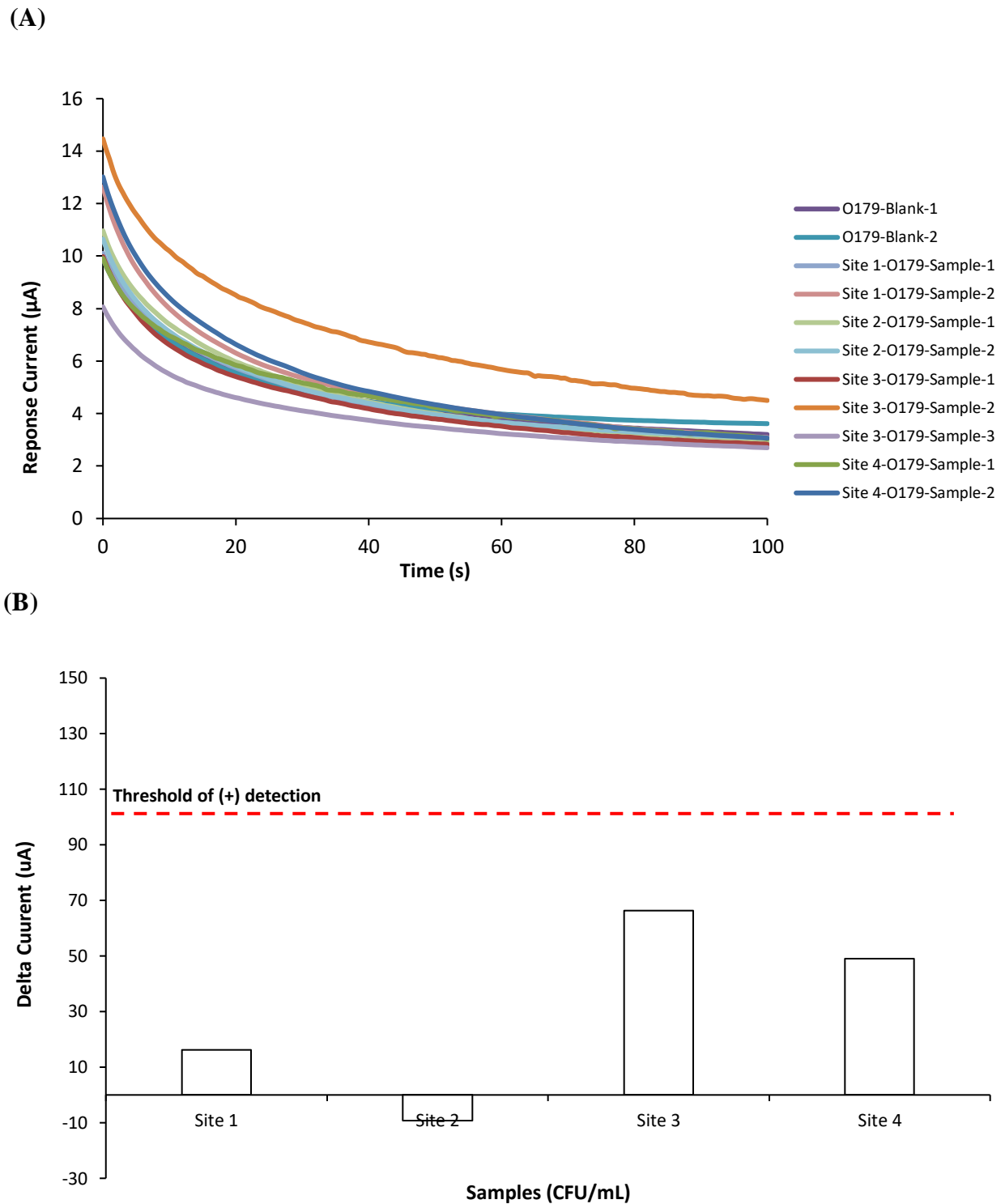


Figure 5.11. Amperometric test of environmental samples using STEC O179-specific bacteriophage biosensor. (A) Amperometric curves showing the response current (RC) of samples from four different sites at fixed potential (0.5 V) for 100 secs (B) The delta (Δ) Current (μA) of each sampling site is shown. Dotted red line is the reference delta (Δ) current threshold (101 μA) for positive detection from pure culture study targeting STEC O179.

All four environmental water samples (Site 1, Site 2, Site 3, and Site 4) were enriched and plated on selective medium. Presumptive colonies for STEC strains were grown overnight in enrichment broth for DNA extraction and conventional PCR. Results presented in **Figures 5. 10-5. 11** show that all conventional PCR products from environmental water samples did not generate both of the virulence genes specific for STEC serogroups. **Figure 5.10** shows a gel loaded with PCR products which were amplified using primers specific for *stx1*(119-bp) while **Figure 5.11** was for *stx2* (104-bp) gene.

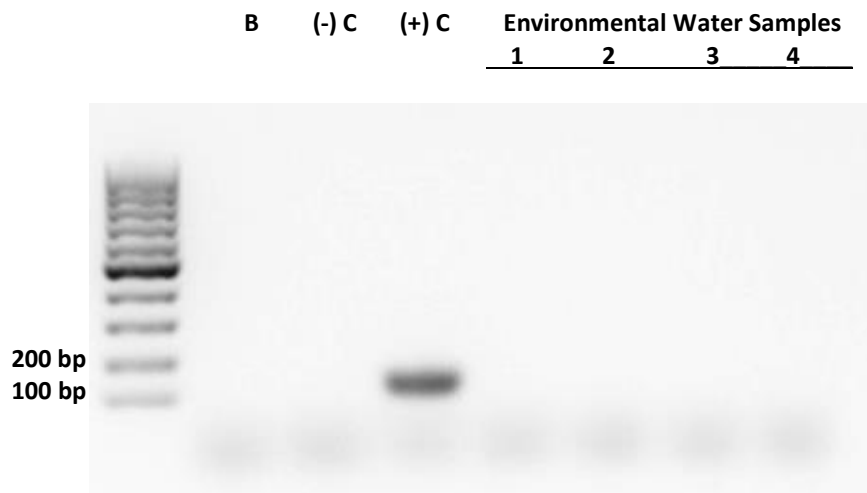


Figure 5.12. Gel image showing four environmental samples after conventional PCR targeting *stx1* gene. None of the samples showed bands for *stx1*(119-bp) gene. B-Blank, (-) C- Negative Control (*S. Typhimurium*), (+)C-Positive Control (O157:H7), 1-Site 1(P1-D), 2-Site 2(P8-W), 3-Site 3(P1-W) and 4-Site 4(P7-W)

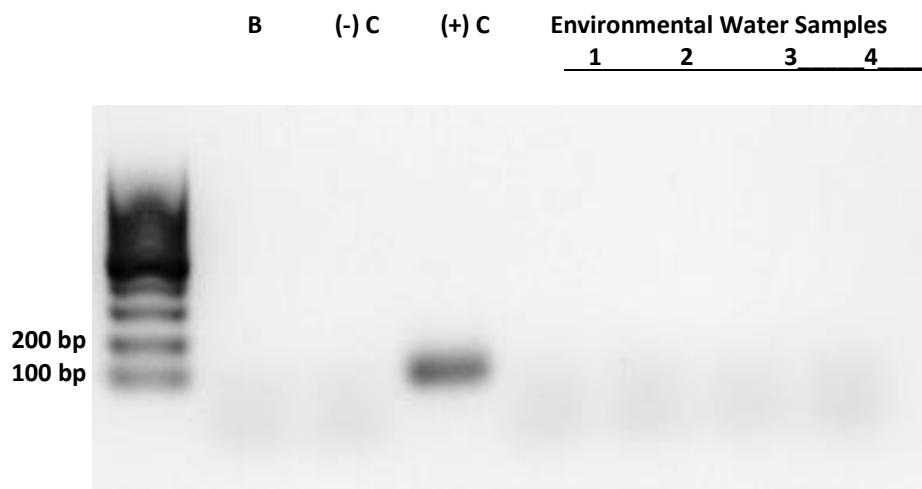


Figure 5.13. Gel image showing four environmental samples after conventional PCR targeting *stx2* gene. None of the samples showed bands for *stx2* (104-bp) gene. B-Blank, (-) C-Negative Control (*S. Typhimurium*), (+) C-Positive Control (O157:H7), 1-Site 1(P1-D), 2-Site 2(P8-W), 3-Site 3(P1-W) and 4-Site 4(P7-W)

5.4. Discussion

Bacteriophages survive in very complex environments and still are capable of sensing, recognizing and infecting its host bacterium despite of the abundance of competing background microflora as well as the presence of biologically active materials in elevated amounts (Anany, Brovko et al. 2018). Bacteriophages are relatively easy and inexpensive to propagate, stable in a wide range of temperature, and resistant to proteases and organic solvents (Richter, Matuła et al. 2016). These features of bacteriophages provide opportunities for monitoring and detecting bacteria as major contaminants in food and environmental samples (Schmelcher and Loessner 2014, Anany, Brovko et al. 2018). This study has shown the portability of the biosensor for

screening STEC strains in various complex matrices which would allow onsite testing of samples without the need of processing and testing of samples in the laboratory.

In this study, bacteriophages were incorporated onto the biosensor to screen for the presence of STEC strains in complex food and environmental matrices. Two groups of food samples were included; solid food sample in which fresh ground beef was artificially spiked with representative target STEC serogroups (1-4 log CFU/ g), while the second group included pasteurized apple juice samples which were inoculated with exactly the same STEC strains and concentration levels (1-4log CFU/mL) as with the fresh ground beef. For environmental water samples, the bacteriophage-based biosensor was directly applied without artificial inoculation.

For fresh ground beef samples, the three representative STEC strains were positively detected based on the amperometric results.. For STEC O26, the LOD was 1 log CFU/g and 2 log CFU/g and 3 log CFU/g for STEC O179. For pasteurized apple juice tests, the three strains that were artificially spiked on pasteurized apple juice. The LOD for the three target strains (O26, O157 and O179) was 3 log CFU/mL.

For apple juice, the LOD was relative higher than fresh ground beef probably due to the interaction and behavior of bacteriophages in an acidic environment. It was likely that the long contractile tail of the members of the families *Myoviridae* and *Siphoviridae* which is consisted of proteins (approx 20) denatured at some level upon exposure to low acid food matrix such as apple juice. Bacteriophage tails are often comprised of the receptor-binding proteins (RBPs) that specifically recognize and anchor to the unique proteins and polysaccharide sequences present on the bacteriophage host cell membrane (Anany, Chou et al. 2017). When these RBPs are compromised, the bacteriophage capture efficiency toward its target host cell decreases, which can be the plausible reason for a relatively higher LOD on pasteurized apple juice matrix versus

the LOD on fresh ground beef. However, this limit of detection is still comparable to the published rapid methods such as nucleic acid-based (ie fluorescent in situ hybridization or FISH) and direct epifluorescent filter technique (DEFT) which generally have LOD $>3 \log$ CFU/mL or gram (López-Campos, Martínez-Suárez et al. 2012). In addition, considering that the procedures in this study did not include pre-enrichment steps, this technology still holds the premise for on-site testing and field applications.

In this study, the delta Δ current (μA) was the basis for detection of STEC strains on both complex matrices. This normalized data was obtained from the difference of response current (RC) of samples (target or non-target) and response current (RC) of control/blank (Lin, Chen et al. 2008). It can be observed that a few complex matrix samples generated negative delta Δ current (μA) values. This can be attributed, more than to any other factors, to the matrix effects. Biological matrices largely influence the outcome of analysis, the sensitivity of the assay (ligand-binding assay) and its reproducibility (Chiu, Lawi et al. 2010). Non-specific binding (NSB) of matrix components onto the surface of chip is the most commonly discussed matrix effect (Johansson and Hellenas 2004). Since homogenization was the only pre-treatment step performed in this study, sample filtration would most likely improve the sensitivity of the biosensor and eliminate the negative delta Δ current (μA) value. In addition, by neutralizing acidic samples such as beverages and fruit juices can bring its pH up to the neutral level that can maintain the stability of bacteriophages as well as reduce the effects of other inhibitors that are present in the samples.

Finally, four environmental water samples from different sampling sites were tested for the presence of three representative STEC strains. The results of the newly-developed biosensor showed that none of the environmental water samples were positive for STEC O26, O157 and

O179 which was also confirmed and verified by plating and conventional PCR that targeted STEC virulence genes (*stx1* and *stx2*).

5.5. Conclusions

The detection of STEC strains has been generally based on traditional microbiological culture and immunological methods that take several days to complete. The development of this novel rapid, portable and highly-sensitive bacteriophage-based amperometric biosensor which is specific to major STEC serogroups can address the limitations of the conventional approach. The screen-printed carbon electrode (SPCE) platforms which were biofunctionalized with biotinylated bacteriophages offered tremendous flexibility, both in terms of performance and cost. The electrochemical analysis using a portable amperometric device that was wirelessly conducted to an Android tablet has proven the concept of “laboratory-free” screening and testing of food and environmental samples at a fraction of a cost of traditional methods. Requiring only simple steps prior to sample testing in microvolumes, this newly-developed biosensor had a comparable LOD when applied on fresh ground beef (1-2 log CFU/mL) and pasteurized apple juice (3 log CFU/mL) without enrichment. The robustness and sensitivity of biosensor was also successfully confirmed and verified on natural environmental water samples as its results were similar to both plating and conventional PCR methods. This enrichment and antibodies-free detection technology offers great opportunities and applications not only for routine on-site STEC strains detection but also advantageous in areas where resources are limited.

CHAPTER 6

COST ANALYSIS OF THE NEWLY-DEVELOPED BACTERIOPHAGE- BASED STEC BIOSENSOR

6.1. Introduction

The global market of food analysis requires low-cost and reliable tools in order to evaluate quality and safety of food (Scognamiglio, Arduini et al. 2014). Biosensors can meet these demands due to its automated, easy-to-operate, inexpensive, highly-sensitive and specific features that make them ideal candidates for improving the screening and monitoring processes of food contaminants such as toxins and pathogens. A report of Global Industry Analysts Inc suggested that the global market of biosensors increased from \$6.1 billion (2004) to \$8.2 billion (2009) and projected to continue to grow annually at 6.3% (Scognamiglio, Pezzotti et al. 2010). Specifically, the market size of global food safety testing is estimated to increase to \$ 17.16 billion by 2021 at a staggering 7.4% compound annual growth rate (CAGR) from 2016 (Philpott 2009). The main driving force for this market is the increase in outbreak cases directly related to foodborne illnesses, strict implementation of food safety regulations and ease of food supply trading.

In 2008 estimates, food processors around the world performed 138 million tests for various foodborne pathogens which accounted for a market value of over \$ 1 billion. Eighty percent of these tests were routine microbiology assays. Specifically, *Salmonella* spp., *Listeria* spp., STEC O157 and *Campylobacter* spp. were the target pathogens detected (Philpott 2009). It is very obvious that the global market for biosensors will maintain its steady growth in the years to come. However, it is also likely that majority of the new biosensors will face hurdles as

it enters the market, or worse will not be able to penetrate the thriving and fiercely competitive market at all. The success of commercializing biosensor technology relies on extensive research and development, and marketing of companies that can financially support it. (Scognamiglio, Pezzotti et al. 2010). Therefore it is important that companies who are developing new technologies create a sound cost estimating solution for their new products, otherwise, underestimation can result in losses while overestimation will prevent the company from maintaining its competitiveness (H'mida, Martin et al. 2006).

Individual project or product has to be estimated based on its merits due to the nature of its cost drivers (Roy, Colmer et al. 2005). The connection between the technical features and economic variables can be delivered by a cost model that provides a reasoning procedure and knowledge related to cost estimation and analysis. Product cost structures may include cost for materials, manufacturing process, assembly, packaging and transport and other related costs. To be more effective, cost modeling tools need to include all cost elements that have a great impact on the overall product cost.

Product cost estimation is an important procedure in every stage of developing a new product (Chwastyk and Kołosowski 2014). It provides opportunities to evaluate cost-effectiveness during the development and adjust the parameters at the latter part if needed that can ultimately add value to the product. Accurate data costing is a major factor to successfully implement cost estimation system (Shehab and Abdalla 2001).

In this study, a product cost structure was defined to be able to determine the total cost of the newly-developed bacteriophage-based electrochemical biosensor and compared with other currently existing rapid detection methods. This cost analysis was a generic approach which can be modified to estimate costs of other new products. In addition, this analysis is significant for

future decision-making in relation to the commercialization potential and market value of the newly-developed bacteriophage-based biosensor.

6.2. Methodology

The initial step in constructing a new product cost to establish a product cost structure by gathering all the possible accurate costs of the materials. Secondary to the materials cost was labor and the manufacturing and process costs. The product cost structure was defined per each breakdown to facilitate a reasonable estimation of the fixed and variable costs incurred during the development of the biosensor.

6.2.1. Material Cost

Direct material cost included the costs of consumables and materials that were used to develop the product and those that have become part of the product. Material cost was estimated based on the equation (**Equation 6.1**):

$$C_{mt} = V\alpha C_w \text{ (Equation 6.1)}$$

where V is the raw material component volume, α is the material density or concentration and C_w is unit price (\$) (Shehab and Abdalla 2001).

6.2.2. Basic Process Cost

Basic process cost mainly included the equipment cost, operating cost and processing times. The basis for computing for fixed cost is shown in **Table 6.1**.(Anderson 2009). The process cost (P_c) was the the minimum cost for the specific process:

$$P_c = \beta T + \gamma/N \text{ (Equation 6.2)}$$

where β was the operating and setting up process cost including overhead, labor and monitoring the process, and manufacturing site, T was the time consumed for processing, γ was the tooling

cost for producing the part and N pertained to the number of products produced. In this study, β was allocated to labor cost (Lc) and additional overhead cost.

Labor cost (Lc) with or without overhead can be estimated using the following equation **(Equation 6.3)**:

$$Lc = E_R \times H \text{ (Equation 6.3)}$$

where E_R was the employee rate (hourly) and H was the hours worked per year.

Table 6.1. General rules for computing fixed costs (Anderson 2009).

Fixed Cost	Factors for computing fixed costs
Operating labor	= 2 to 6 person per shift x 4 shifts x \$/yr
Non-operating labor eg. Tech support	= 0.60 x Cost of Operating Labor (\$/yr)
Supplies (eg protective equipment, office supplies)	= 0.30 x Cost of Operating Labor (\$/yr)
Administration	= 0.90 x Cost of Operating Labor (\$/yr)
Maintenance	= 0.02 x Capital Investment (\$)
Miscellaneous (eg. taxes, insurance	= 0.01 x 0.02 x Capital Investment (\$)

6.2.3. Manufacturing Cost

The base factors for the estimation of the total manufacturing costs of a product were the volume of the product used and the process cost (Swift, Booker et al. 2003). The total manufacturing cost (M_c) is the total material cost (C_{mt}) and the process cost (P_c) **(Equation 6.3)**:

$$M_c = C_{mt} + P_c \text{ (Equation 6.3)}$$

6.3. Results

In this study, the cost of the product was the sum of all elemental units and processes that represented various resources used throughout the entire development cycle. Empirical data results were based on the theoretical methods and formula. **Table 6.2** shows the estimated material cost (C_{mt}) that was incurred during the development cycle which amounted to \$15,690.891.

Table 6.2. Estimated material cost incurred during the development cycle.

Items	Source	Quantity	Material density	Unit price (\$)	C_{mt}
Devices and Chips					
SPCE	Metro-Ohm	1875 pcs	1	2.8	5250
Palmsens device	PalmSens	1 pc	1	5000	5000
Android Phone	Amazon	1 pc	1	150	150
Reagents					
CMD-Dextran	Sigma Aldrich	25 g	1	5.05	126.25
EDC-NHS	Thermo- Fisher	75 g	1	13.04	978
Streptavidin	Thermo- Fisher	50 mg	1	3.68	1840
Biotin	Thermo- Fisher	30 mg	1	30	1600
Streptavidin-HRP	Thermo- Fisher	4 mL	1	398	1592
Hydrogen peroxide (30%)	Thermo- Fisher	50 mL	1	0.35472	17.736
Others					
Miscellaneous	Lab supplies				1500
Total					15690.891

For the actual processing and developing a functional biosensor, the bulk of the basic process costs came from the two major steps of the development stage (1) biotinylation of bacteriophages and (2) biofunctionalization of SPCEs. Combining the two processes, the process cost was calculated to be $P_c = \$ 25,350.06$ for the entire development cycle. This included the labor cost (\$19,200) for the two processes and the tooling cost divided by the number of products produced or the functionalized SPCEs produced (\$6,150.00). The manufacturing cost of the entire development which was the sum of material and process costs for the entire cycle was estimated to be around \$ 41,040.95. An approximation value of \$ 3.28 for each functionalized SPCE has been determined.

6.4. Discussion

This study presents the indication costs of developing the bacteriophage-based biosensor specific to STEC strains. These costs should not be treated as absolute values due to other contributing factors that were not captured and included during the analysis but rather a close estimate to the actual costing of the biosensor development. A rough estimate of the overhead cost was also provided to cover the cost of laboratory activities and processes such as sampling and collection of bacteriophages and its characterization (ie Transmission Electron Microscopy) which were difficult to evaluate in terms of material and labor costs. The major procedures such as biotinylation of bacteriophages and modification of SPCEs which required almost one year to conduct before generating reliable results were included as process costs. However, once the biosensing system has been fully-developed for commercialization, these process steps will be reduced since the optimized conditions are determined for batch and mass production. Biotinylation of bacteriophages and modification of SPCEs are the key-critical steps in the construction of the architecture of the biosensor system.

A typical microbiology test costs \$ 3.52, while *Salmonella* spp. test and PCR both cost around \$11.75 (Philpott 2009). The main components of immunoassay-based methods are antibodies. Monoclonal antibodies usually incur high production costs and take 10-14 days to manufacture which also involves 10 distinct processes (Shaughnessy 2012). The minimum cost of 15 commercially-available monoclonal antibodies in the US is approximately \$ 2000/g and the median cost is around \$ 8000/g (Kelley 2009). These relatively high material costs are also reflected on various immunoassay-based methods. Specifically, rapid immunoassay-based screening and detection methods for STEC strains such as O157:H7 in food samples can range from \$7 to \$23 per test, depending on the platforms (**Table 6.3**).

Table 6.3. Immunoassay-based commercial products for STEC serogroup (O157) detection.
All values are in USD₂₀₁₈.

Commercial Product (Immunoassay-based)	Target STEC serogroups	Manufacturer/Supplier	Cost/test	Reference
3M Tecra <i>E. coli</i> O157 Visual Immunoassay, 48 well kit	STEC O157:H7	3M Company	\$10/test	(3M 2018)
VIP® Gold-EHEC	STEC O157:H7	Sigma-Aldrich	\$17/test	(Sigma-Aldrich 2018)
DrySpot™ <i>E. coli</i> O157 Latex Agglutination Test	STEC O157:H7	Fisher-Scientific	\$22.34/test	(Fisher 2018)
Singlepath® <i>E.coli</i> O157	STEC O157:H7	Sigma-Aldrich	\$7.96/test	(Sigma-Aldrich 2018)

An approximation value of \$ 3.28 for each functionalized SPCE has been determined. All calculations are shown in **Appendix-Tables 7.1-7.4**. The value of individual functionalized SPCE that was determined in this study was lower than molecular-based (75% cheaper) and immunoassay based (77% cheaper), showing that this bacteriophage-based detection method is an excellent alternative especially to the antibodies-based methods for STEC detection.

The most accurate estimation for product costing is the generative approach (Shehab and Abdalla 2001). The cost estimation system that was used here is the generic approach and can be modified in the future depending on the features of the products. Costing systems provide allocation methods which are important for decision-makers in the development process (Maruszewska 2015). Product costing is only one of two steps before a new product can be successfully commercialized while the other one is market analysis. A thorough market analysis is needed to make it possible to generate a clearer picture of the commercialization potential, risks and benefits of the newly-developed bacteriophage-based biosensor.

6.5. Conclusion

The goal of this research was to construct a product cost structure to be able to determine the total cost of the newly-developed bacteriophage-based STEC biosensor. Using a generative approach, it was estimated that cost of the functionalized SPCE was lower than the typical microbiological, immunoassay-based as well as with molecular-based approach for testing pathogens. The functionalized SPCE and the detection approach (ie sandwich-type recognition) for STEC strains are the novel features of the newly-developed system. With the costing system, the commercial viability of this technology can be further enhanced by conducting cost distribution and adjustments to achieve a competitive price once it enters the biosensor market.

CONCLUSIONS

A novel STEC-bacteriophage based electrochemical biosensor was developed in the present study. The bacteriophage-based biosensor was successfully developed by satisfying four main objectives (1) isolating and characterizing STEC-specific bacteriophages from the natural environment (2) optimizing the bacteriophage-based biosensor and (3) apply the developed biosensor in food and environmental samples matrices to screen for the presence of STEC strains, and finally by (4) conducting cost analysis and evaluating its commercial potential. The goal of this project was to improve the current screening and detection of viable foodborne pathogen such as STEC by using a rapid and portable antibodies-free handheld device without pre-enrichment steps.

The isolation and characterization of STEC-specific bacteriophages from various environmental samples such as cow manures, irrigation and farm waters has successfully obtained novel bacteriophage isolates. The bacteriophages belonged to at least two families, *Myoviridae* and *Siphoviridae* based on their morphological features. These STEC-specific bacteriophages were found to be effective for the development of STEC- bacteriophage based electrochemical biosensor due to its high-specificity.

The incorporation of the fully-characterized bacteriophages onto the detection system can circumvent the drawbacks encountered by rapid techniques coupled with traditional biorecognition molecules (ie antibodies). The bacteriophages were found to be highly-compatible with the transducer, the disposable screen-printed carbon electrodes (SPCE) for electrochemical biosensor applications. In optimized conditions, chemically-modified (ie biotin) bacteriophages were successfully immobilized on the surface of SPCE, without losing its

viability, and utilized as biorecognition elements for capture and detection of target live STEC strains. This approach has provided an alternative biorecognition element that is more affordable, stable and sensitive than antibodies. In addition, this newly-developed assay was highly-specific to the representative strains of STEC serogroups (O26, O179 and O57) and highly-sensitive based on the results at the pure-culture setup. The following limits of detection (LOD) were achieved: STEC O26-1 log CFU/mL, STEC O157-2 log CFU/mL and STEC O179-2log CFU/mL.

The electrochemical analysis using a portable electrochemical/amperometric device that was wirelessly conducted to an Android tablet has proven the concept of “laboratory-free” screening and testing of food and environmental samples. Requiring only simple steps prior to sample testing in microvolumes, this newly-developed biosensor had LOD of 1-3 log CFU/g when applied to fresh ground beef and 3 log CFU/mL on and pasteurized apple juice. The robustness and sensitivity of biosensor was also successfully confirmed and verified on natural environmental water samples. This enrichment and antibodies-free detection technology offers great opportunities and application for routine on-site STEC strains screening and detection.

Using a generative approach, it was estimated that the cost of the functionalized SPCE was lower than the typical microbiological test as well as with the immunoassay-based approach for testing pathogens. With the costing system, the commercial viability of this technology can be further enhanced by conducting cost distribution and adjustments to achieve a competitive price once it enters the biosensor market.

The key novel features of this technology: (1) sandwich-detection of target bacterial cells with highly-specific bacteriophages (2) detection of live cells (3) utilization of naturally-isolated bacteriophages with simple chemical labelling to act as capture elements on the surface of the

biosensing platform (4) antibodies-free platform (5) no pre-enrichment steps required (6) designed for on-site testing/portable (7) uses inexpensive and (8) disposable chips that can meet the demands of the food industry as well as food regulatory authorities in maintaining safe and healthy foods.

For future plans, this technology like any biosensing device will be continuously improved and optimized for patent and commercialization purposes. Its key novel features offer great potentials that would allow it to move from the laboratory version to its upscale and commercial form. With this, it is expected to improve the current detection and screening methods of STEC strains and meet the demands of the food industry as well as food regulatory authorities in maintaining safe and healthy foods.

REFERENCES

"MCP-3310:Biosensors - Global Strategic Business Report."

3M (2018). "3M Pathogen Testing." Retrieved March, 2018, from https://www.3m.com/3M/en_US/company-us/.

Ackermann, H.-W. (1998). "Tailed bacteriophages: the order Caudovirales." Advances in virus research **51**: 135-201.

Ackermann, H.-W. (2012). Chapter 1 - Bacteriophage Electron Microscopy. Advances in virus research. M. Łobocka and W. T. Szybalski, Academic Press. **82**: 1-32.

Ackermann, H.-W. and G. Węgrzyn (2014). "General characteristics of bacteriophages." Phage Therapy: 1.

Afonso, A. S., et al. (2012). "Electrochemical Detection of Salmonella using Gold Nanoparticles." Biosensors and Bioelectronics.

Afonso, A. S., et al. (2013). "Electrochemical detection of Salmonella using gold nanoparticles." Biosensors and Bioelectronics **40**(1): 121-126.

Alonso-Lomillo, M., et al. (2010). "Screen-printed biosensors in microbiology; a review." Talanta **82**(5): 1629-1636.

Anany, H., et al. (2018). "Print to detect: a rapid and ultrasensitive phage-based dipstick assay for foodborne pathogens." Analytical and Bioanalytical Chemistry **410**(4): 1217-1230.

Anany, H., et al. (2017). From Bits and Pieces to Whole Phage to Nanomachines: Pathogen Detection Using Bacteriophages. Annual Review of Food Science and Technology, Vol 8. M. P. Doyle and T. R. Klaenhammer. **8**: 305-329.

Anderson, J. (2009). "Determining manufacturing costs." CEP: 27-31.

Bach, S. J., et al. (2003). "Effect of bacteriophage DC22 on Escherichia coli O157: H7 in an artificial rumen system (Rusitec) and inoculated sheep." Animal Research **52**(2): 89-101.

Balamurugan, S., et al. (2008). "Surface immobilization methods for aptamer diagnostic applications." Analytical and Bioanalytical Chemistry **390**(4): 1009-1021.

Balasubramanian, S., et al. (2007). "Lytic phage as a specific and selective probe for detection of *Staphylococcus aureus*—a surface plasmon resonance spectroscopic study." Biosensors and Bioelectronics **22**(6): 948-955.

Balière, C., et al. (2015). "Prevalence and Characterization of Shiga Toxin-Producing and Enteropathogenic *Escherichia coli* in Shellfish-Harvesting Areas and Their Watersheds." Frontiers in Microbiology **6**(1356).

Banerjee, P., et al. (2007). "A novel and simple cell-based detection system with a collagen-encapsulated B-lymphocyte cell line as a biosensor for rapid detection of pathogens and toxins." Laboratory Investigation **88**(2): 196-206.

Ben Aissa, A., et al. (2017). "Comparing nucleic acid lateral flow and electrochemical genosensing for the simultaneous detection of foodborne pathogens." Biosensors and Bioelectronics **88**: 265-272.

Bennett, A. R., et al. (1997). "The use of bacteriophage-based systems for the separation and concentration of *Salmonella*." Journal of Applied Microbiology **83**(2): 259-265.

Beutin, L. and P. Fach (2014). "Detection of Shiga Toxin-Producing *Escherichia coli* from Nonhuman Sources and Strain Typing." Microbiology Spectrum **2**(3).

Beutin, L. and P. Fach (2015). Detection of Shiga toxin-producing *Escherichia coli* from nonhuman sources and strain typing. Enterohemorrhagic *Escherichia coli* and Other Shiga Toxin-Producing *E. coli*, American Society of Microbiology: 299-319.

Bhardwaj, N., et al. (2017). "Fluorescent nanobiosensors for the targeted detection of foodborne bacteria." TrAC Trends in Analytical Chemistry **97**: 120-135.

Bhunia, A. K., et al. (2014). High throughput screening for food safety assessment: Biosensor technologies, hyperspectral imaging and practical applications, Elsevier.

Bian, X., et al. (2015). "A microfluidic droplet digital PCR for simultaneous detection of pathogenic *Escherichia coli* O157 and *Listeria monocytogenes*." Biosensors and Bioelectronics **74**: 770-777.

Birnbaumer, G. M., et al. (2009). "Detection of viruses with molecularly imprinted polymers integrated on a microfluidic biochip using contact-less dielectric microsensors." Lab on a Chip **9**(24): 3549-3556.

Bole, A. L. and P. Manesiotis (2016). "Advanced Materials for the Recognition and Capture of Whole Cells and Microorganisms." Advanced Materials **28**(27): 5349-5366.

Bonanno, L., et al. (2016). "Heterogeneity in induction level, infection ability, and morphology of Shiga toxin-encoding phages (Stx phages) from dairy and human Shiga toxin-producing *Escherichia coli* O26: H11 isolates." Applied and Environmental Microbiology **82**(7): 2177-2186.

Bouguelia, S., et al. (2013). "On-chip microbial culture for the specific detection of very low levels of bacteria." Lab on a Chip **13**(20): 4024-4032.

Brooks, J. T., et al. (2005). "Non-O157 Shiga Toxin–Producing *Escherichia coli* Infections in the United States, 1983–2002." Journal of Infectious Diseases **192**(8): 1422-1429.

Byeon, H. M., et al. (2015). "Lytic Phage-Based Magnetoelastic Biosensors for On-site Detection of Methicillin-Resistant *Staphylococcus aureus* on Spinach Leaves." Journal of The Electrochemical Society **162**(8): B230-B235.

Byrne, L., et al. (2014). "Epidemiology and microbiology of Shiga toxin-producing *Escherichia coli* other than serogroup O157 in England, 2009–2013." Journal of Medical Microbiology **63**(9): 1181-1188.

Cademartiri, R., et al. (2010). "Immobilization of bacteriophages on modified silica particles." Biomaterials **31**(7): 1904-1910.

Callaway, T. R., et al. (2008). "Bacteriophage isolated from feedlot cattle can reduce *Escherichia coli* O157: H7 populations in ruminant gastrointestinal tracts." Foodborne Pathogens and Disease **5**(2): 183-191.

Campuzano, S., et al. (2006). "Characterization of alkanethiol-self-assembled monolayers-modified gold electrodes by electrochemical impedance spectroscopy." Journal of Electroanalytical Chemistry **586**(1): 112-121.

CDC, C. f. D. C. a. P. (2017). "National Shiga toxin-producing Escherichia coli (STEC) Surveillance Annual Report, 2015." Atlanta, Georgia: US Department of Health and Human Services, CDC, 2017.

Chiu, M. L., et al. (2010). "Matrix effects—a challenge toward automation of molecular analysis." JALA: Journal of the Association for Laboratory Automation **15**(3): 233-242.

Church, D., et al. (2007). "Evaluation of BBL CHROMagar O157 versus sorbitol-MacConkey medium for routine detection of Escherichia coli O157 in a centralized regional clinical microbiology laboratory." Journal of Clinical Microbiology **45**(9): 3098-3100.

Chwastyk, P. and M. Kołosowski (2014). "Estimating the Cost of the New Product in Development Process." Procedia Engineering **69**: 351-360.

Clokie, M. R. J., et al. (2011). "Phages in nature." Bacteriophage **1**(1): 31-45.

Cooley, M. B., et al. (2013). "Development of a Robust Method for Isolation of Shiga Toxin-Positive Escherichia coli (STEC) from Fecal, Plant, Soil and Water Samples from a Leafy Greens Production Region in California." PLoS ONE **8**(6): e65716.

Daubinger, P., et al. (2014). "Electrochemical characteristics of nanostructured platinum electrodes—a cyclic voltammetry study." Physical Chemistry Chemical Physics **16**(18): 8392-8399.

Delannoy, S., et al. (2016). "Revisiting the STEC Testing Approach: Using espK and espV to Make Enterohemorrhagic Escherichia coli (EHEC) Detection More Reliable in Beef." Frontiers in Microbiology **7**(1).

Deng, H., et al. (2012). "Gold nanoparticles with asymmetric polymerase chain reaction for colorimetric detection of DNA sequence." Analytical Chemistry **84**(3): 1253-1258.

Dewsbury, D. M., et al. (2015). "Summer and winter prevalence of Shiga toxin-producing Escherichia coli (STEC) O26, O45, O103, O111, O121, O145, and O157 in feces of feedlot cattle." Foodborne Pathogens and Disease **12**(8): 726-732.

Dickinson, E. J. F., et al. (2009). "How Much Supporting Electrolyte Is Required to Make a Cyclic Voltammetry Experiment Quantitatively "Diffusional"? A Theoretical and Experimental Investigation." Journal of Physical Chemistry C **113**(25): 11157-11171.

Dini, C. and P. De Urza (2010). "Isolation and selection of coliphages as potential biocontrol agents of enterohemorrhagic and Shiga toxin - producing E. coli (EHEC and STEC) in cattle." Journal of Applied Microbiology **109**(3): 873-887.

Durso, L. and J. Keen (2007). "Shiga - toxigenic Escherichia coli O157 and non - Shiga - toxigenic E. coli O157 respond differently to culture and isolation from naturally contaminated bovine faeces." Journal of Applied Microbiology **103**(6): 2457-2464.

Edgar, R., et al. (2006). "High-sensitivity bacterial detection using biotin-tagged phage and quantum-dot nanocomplexes." Proceedings of the National Academy of Sciences of the United States of America **103**(13): 4841-4845.

Eersels, K., et al. (2016). "A Review on Synthetic Receptors for Bioparticle Detection Created by Surface-Imprinting Techniques—From Principles to Applications." ACS Sensors **1**(10): 1171-1187.

Elgrishi, N. m., et al. (2017). "A Practical Beginner's Guide to Cyclic Voltammetry." Journal of Chemical Education.

Ertürk, G. and R. Lood (2018). "Bacteriophages as biorecognition elements in capacitive biosensors: Phage and host bacteria detection." Sensors and Actuators B: Chemical **258**: 535-543.

Ertürk, G. and B. Mattiasson (2017). "Molecular imprinting techniques used for the preparation of biosensors." Sensors **17**(2): 288.

Esseili, M. A., et al. (2012). "Internalization of Sapovirus, a surrogate for Norovirus, in romaine lettuce and the effect of lettuce latex on virus infectivity." Applied and Environmental Microbiology **78**(17): 6271-6279.

Etcheverría, A. I., et al. (2010). "Occurrence of Shiga toxin-producing E. coli (STEC) on carcasses and retail beef cuts in the marketing chain of beef in Argentina." Meat Science **86**(2): 418-421.

Fernandes, E., et al. (2014). "A bacteriophage detection tool for viability assessment of Salmonella cells." Biosensors and Bioelectronics **52**: 239-246.

Fisher (2018). "Thermo Scientific™ DrySpot™ E. coli O157 Latex Agglutination Test." Retrieved March, 2018, from <https://www.fishersci.com/shop/products/oxid-dryspot-e-coli-o157-latex-test-kit/oxdr0120m#?keyword=DrySpot%26trade%3B+E.+coli+O157+Latex+Agglutination+Test>.

Fratamico, P. M., et al. (2011). "Detection by Multiplex Real-Time Polymerase Chain Reaction Assays and Isolation of Shiga Toxin–Producing Escherichia coli Serogroups O26, O45, O103, O111, O121, and O145 in Ground Beef." Foodborne Pathogens and Disease **8**(5): 601-607.

Fremaux, B., et al. (2008). "Long-term survival of Shiga toxin-producing Escherichia coli in cattle effluents and environment: An updated review." Veterinary Microbiology **132**(1): 1-18.

Fuller, C. A., et al. (2011). "Shiga toxin subtypes display dramatic differences in potency." Infection and immunity **79**(3): 1329-1337.

Galikowska, E., et al. (2011). "Specific detection of Salmonella enterica and Escherichia coli strains by using ELISA with bacteriophages as recognition agents." European journal of clinical microbiology & infectious diseases **30**(9): 1067-1073.

Gerritzen, A., et al. (2011). "Rapid and Sensitive Detection of Shiga Toxin-Producing Escherichia Coli Directly From Stool Samples by Real-Time PCR in Comparison to Culture, Enzyme Immunoassay, and Vero Cell Cytotoxicity Assay." Clinical laboratory **57**(11): 993.

Gervais, L., et al. (2007). "Immobilization of biotinylated bacteriophages on biosensor surfaces." Sensors and Actuators B: Chemical **125**(2): 615-621.

Gracias, K. S. and J. L. McKillip (2004). "A review of conventional detection and enumeration methods for pathogenic bacteria in food." Canadian Journal of Microbiology **50**(11): 883-890.

Guo, X., et al. (2012). "A piezoelectric immunosensor for specific capture and enrichment of viable pathogens by quartz crystal microbalance sensor, followed by detection with antibody-functionalized gold nanoparticles." Biosensors and Bioelectronics **38**(1): 177-183.

Gyles, C. L. (2007). "Shiga toxin-producing Escherichia coli: An overview." Journal of Animal Science **85**(13 suppl): E45-E62.

H'mida, F., et al. (2006). "Cost estimation in mechanical production: The Cost Entity approach applied to integrated product engineering." International Journal of Production Economics **103**(1): 17-35.

Hagens, S. and M. J. Loessner (2007). "Application of bacteriophages for detection and control of foodborne pathogens." Applied Microbiology and Biotechnology **76**(3): 513-519.

Hancock, D. D., et al. (1997). "A longitudinal study of Escherichia coli O157 in fourteen cattle herds." Epidemiology and Infection **118**(2): 193-195.

Hegde, N. V., et al. (2012). "Detection of the Top Six Non-O157 Shiga Toxin-Producing Escherichia coli O Groups by ELISA." Foodborne Pathogens and Disease **9**(11): 1044-1048.

Heselpoth, R. D., et al. (2015). "Increasing the stability of the bacteriophage endolysin PlyC using rationale-based FoldX computational modeling." Protein Engineering, Design and Selection **28**(4): 85-92.

Hiramatsu, R., et al. (2002). "Characterization of Shiga toxin-producing Escherichia coli O26 strains and establishment of selective isolation media for these strains." Journal of Clinical Microbiology **40**(3): 922-925.

Hosseinioust, Z., et al. (2011). "Bacterial Capture Efficiency and Antimicrobial Activity of Phage-Functionalized Model Surfaces." Langmuir **27**(9): 5472-5480.

Hussain, M., et al. (2013). "Biomimetic strategies for sensing biological species." Biosensors **3**(1): 89-107.

Idil, N., et al. (2017). "Whole cell based microcontact imprinted capacitive biosensor for the detection of Escherichia coli." Biosensors & Bioelectronics **87**: 807-815.

Imamovic, L. and M. Muniesa (2011). "Quantification and evaluation of infectivity of Shiga toxin-encoding bacteriophages in beef and salad." Applied and Environmental Microbiology **77**(10): 3536-3540.

Jasson, V., et al. (2010). "Alternative microbial methods: an overview and selection criteria." Food Microbiology **27**(6): 710-730.

Johansson, M. A. and K. E. Hellenas (2004). "Matrix effects in immunobiosensor determination of clenbuterol in urine and serum." Analyst **129**(5): 438-442.

Jończyk, E., et al. (2011). "The influence of external factors on bacteriophages—review." Folia Microbiologica **56**(3): 191-200.

Jung, Y. L., et al. (2010). "Direct colorimetric diagnosis of pathogen infections by utilizing thiol-labeled PCR primers and unmodified gold nanoparticles." Biosensors and Bioelectronics **25**(8): 1941-1946.

Junillon, T., et al. (2012). "Simplified detection of food-borne pathogens: An in situ high affinity capture and staining concept." Journal of Microbiological Methods **91**(3): 501-505.

Jurczak-Kurek, A., et al. (2016). "Biodiversity of bacteriophages: morphological and biological properties of a large group of phages isolated from urban sewage." Scientific reports **6**.

Kanchi, S., et al. (2017). "Smartphone based bioanalytical and diagnosis applications: A review." Biosensors and Bioelectronics.

Karoonuthaisiri, N., et al. (2009). "Development of antibody array for simultaneous detection of foodborne pathogens." Biosensors and Bioelectronics **24**(6): 1641-1648.

Kay, B. K., et al. (2009). "High-throughput Biotinylation of Proteins." Methods in molecular biology (Clifton, N.J.) **498**: 185-196.

Kelley, B. (2009). Industrialization of mAb production technology: the bioprocessing industry at a crossroads. MAbs, Taylor & Francis.

Kimmel, D. W., et al. (2011). "Electrochemical Sensors and Biosensors." Analytical Chemistry **84**(2): 685-707.

Koskella, B. and M. A. Brockhurst (2014). "Bacteria–phage coevolution as a driver of ecological and evolutionary processes in microbial communities." FEMS Microbiology Reviews **38**(5): 916-931.

Kropinski, A. M., et al. (2009). Enumeration of Bacteriophages by Double Agar Overlay Plaque Assay. Bacteriophages: Methods and Protocols, Volume 1: Isolation, Characterization, and Interactions. M. R. J. Clokie and A. M. Kropinski. Totowa, NJ, Humana Press: 69-76.

Krüger, A. and P. M. A. Lucchesi (2014). "Shiga toxins and stx-phages: highly diverse entities." Microbiology: mic. 0.000003.

Kuberský, P., et al. (2013). "Effect of the geometry of a working electrode on the behavior of a planar amperometric NO₂ sensor based on solid polymer electrolyte." Sensors and Actuators B: Chemical **187**(Supplement C): 546-552.

Kumar, S., et al. (2008). "Directional conjugation of antibodies to nanoparticles for synthesis of multiplexed optical contrast agents with both delivery and targeting moieties." Nature Protocols **3**(2): 314-320.

Lakhin, A., et al. (2013). "Aptamers: problems, solutions and prospects." Acta Naturae (англоязычная версия) **5**(4 (19)).

Lakshmanan, R. S., et al. (2007). "Detection of Salmonella typhimurium in fat free milk using a phage immobilized magnetoelastic sensor." Sensors and Actuators B: Chemical **126**(2): 544-550.

Länge, K., et al. (2008). "Surface acoustic wave biosensors: a review." Analytical and Bioanalytical Chemistry **391**(5): 1509-1519.

Law, J. W.-F., et al. (2015). "Rapid methods for the detection of foodborne bacterial pathogens: principles, applications, advantages and limitations." Frontiers in Microbiology **5**(770).

Lazcka, O., et al. (2007). "Pathogen detection: A perspective of traditional methods and biosensors." Biosensors and Bioelectronics **22**(7): 1205-1217.

Leach, K. M., et al. (2010). "Same-day detection of Escherichia coli O157: H7 from spinach by using electrochemiluminescent and cytometric bead array biosensors." Applied and Environmental Microbiology **76**(24): 8044-8052.

Lei, J. and H. Ju (2012). "Signal amplification using functional nanomaterials for biosensing." Chemical Society Reviews **41**(6): 2122-2134.

Lin, Y.-H., et al. (2008). "Disposable amperometric immunosensing strips fabricated by Au nanoparticles-modified screen-printed carbon electrodes for the detection of foodborne pathogen Escherichia coli O157: H7." Biosensors and Bioelectronics **23**(12): 1832-1837.

Liu, H., et al. (2015). "Control of Escherichia coli O157 on beef at 37, 22 and 4 C by T5-, T1-, T4- and O1-like bacteriophages." Food Microbiology **51**: 69-73.

Liu, Q. and P. Wang (2009). Cell-based biosensors: principles and applications, Artech House.

Liu, Q. J., et al. (2014). "Cell-Based Biosensors and Their Application in Biomedicine." Chemical reviews **114**(12): 6423-6461.

Liu, X. and D. K. Y. Wong (2009). "Picogram-detection of estradiol at an electrochemical immunosensor with a gold nanoparticle|Protein G-(LC-SPDP)-scaffold." Talanta **77**(4): 1437-1443.

Loessner, M. J., et al. (1997). "Evaluation of luciferase reporter bacteriophage A511:: luxAB for detection of *Listeria monocytogenes* in contaminated foods." Applied and Environmental Microbiology **63**(8): 2961-2965.

López-Campos, G., et al. (2012). Detection, identification, and analysis of foodborne pathogens. Microarray Detection and Characterization of Bacterial Foodborne Pathogens, Springer: 13-32.

Luo, C., et al. (2012). "A Rapid and Sensitive Aptamer - Based Electrochemical Biosensor for Direct Detection of *Escherichia Coli* O111." Electroanalysis **24**(5): 1186-1191.

Manafi, M. and B. Kremsmaier (2001). "Comparative evaluation of different chromogenic/fluorogenic media for detecting *Escherichia coli* O157: H7 in food." International Journal of Food Microbiology **71**(2-3): 257-262.

Mao, S., et al. (2015). "Characterising the bacterial microbiota across the gastrointestinal tracts of dairy cattle: membership and potential function." Scientific reports **5**.

March, S. B. and S. Ratnam (1986). "Sorbitol-MacConkey medium for detection of *Escherichia coli* O157: H7 associated with hemorrhagic colitis." Journal of Clinical Microbiology **23**(5): 869-872.

Maruszewska, E. W. (2015). "Applicability of activity based costing in new product development processes." Management Systems in Production Engineering(1 (17)): 35--39.

Mayer, C. L., et al. (2012). "Shiga toxins and the pathophysiology of hemolytic uremic syndrome in humans and animals." Toxins **4**(11): 1261-1287.

Mejri, M., et al. (2010). "Impedance biosensing using phages for bacteria detection: Generation of dual signals as the clue for in-chip assay confirmation." Biosensors and Bioelectronics **26**(4): 1261-1267.

Moll, N., et al. (2007). "A Love wave immunosensor for whole E. coli bacteria detection using an innovative two-step immobilisation approach." Biosensors and Bioelectronics **22**(9): 2145-2150.

Mustafa, F., et al. (2017). "Multifunctional Nanotechnology-Enabled Sensors for Rapid Capture and Detection of Pathogens." Sensors **17**(9): 2121.

Nanduri, V., et al. (2007). "SPR biosensor for the detection of *L. monocytogenes* using phage-displayed antibody." Biosensors and Bioelectronics **23**(2): 248-252.

Narsaiah, K., et al. (2012). "Optical biosensors for food quality and safety assurance—a review." Journal of food science and technology **49**(4): 383-406.

Newell, D. G., et al. (2010). "Food-borne diseases — The challenges of 20 years ago still persist while new ones continue to emerge." International Journal of Food Microbiology **139**, **Supplement**(0): S3-S15.

Newman, J. and K. E. Thomas-Alyea (2012). Electrochemical systems, John Wiley & Sons.

Niu, Y., et al. (2009). "Prevalence and impact of bacteriophages on the presence of Escherichia coli O157: H7 in feedlot cattle and their environment." Applied and Environmental Microbiology **75**(5): 1271-1278.

Niu, Y. D., et al. (2014). "Four Escherichia coli O157: H7 phages: a new bacteriophage genus and taxonomic classification of T1-like phages." PLoS ONE **9**(6): e100426.

Niu, Y. D., et al. (2012). "Characterization of 4 T1-like lytic bacteriophages that lyse Shiga-toxin Escherichia coli O157: H7." Canadian Journal of Microbiology **58**(7): 923-927.

Niu, Y. D., et al. (2012). "Genomic, proteomic and physiological characterization of a T5-like bacteriophage for control of Shiga toxin-producing Escherichia coli O157: H7." PLoS ONE **7**(4): e34585.

Nyambe, S., et al. (2016). "Survival studies of a temperate and lytic bacteriophage in bovine faeces and slurry." Journal of Applied Microbiology **121**(4): 1144-1151.

O'lynn, G., et al. (2004). "Evaluation of a cocktail of three bacteriophages for biocontrol of *Escherichia coli* O157: H7." Applied and Environmental Microbiology **70**(6): 3417-3424.

Oh, J.-W., et al. (2014). "Biomimetic virus-based colourimetric sensors." Nature communications **5**.

Ölcer, Z., et al. (2015). "Microfluidics and nanoparticles based amperometric biosensor for the detection of cyanobacteria (*Planktothrix agardhii* NIVA-CYA 116) DNA." Biosensors and Bioelectronics **70**(Supplement C): 426-432.

Parsons, B. D., et al. (2016). "Detection, characterization, and typing of Shiga toxin-producing *Escherichia coli*." Frontiers in Microbiology **7**: 478.

Pérez-López, B. and A. Merkoçi (2011). "Nanomaterials based biosensors for food analysis applications." Trends in Food Science & Technology **22**(11): 625-639.

Philpott, A. C. (2009). "A Summary Profile of Pathogen Detection Technologies." Foodsafety magazine.

Quintela, I. A., et al. (2015). "Simultaneous direct detection of Shiga-toxin producing *Escherichia coli* (STEC) strains by optical biosensing with oligonucleotide-functionalized gold nanoparticles." Nanoscale **7**(6): 2417-2426.

Rakhuba, D. V., et al. (2010). "Bacteriophage receptors, mechanisms of phage adsorption and penetration into host cell." Pol J Microbiol **59**(3): 145-155.

Ratani, G., et al. (2017). "Smartphone-based food diagnostic technologies: a review." Sensors **17**(6): 1453.

Ray, B. and A. Bhunia (2014). *Fundamental Food*, Taylor and Francis Group: 548.

Richter, Ł., et al. (2016). "Ordering of bacteriophages in the electric field: Application for bacteria detection." Sensors and Actuators B: Chemical **224**: 233-240.

Rocha-Gaso, M.-I., et al. (2009). "Surface generated acoustic wave biosensors for the detection of pathogens: A review." Sensors **9**(7): 5740-5769.

Roy, R., et al. (2005). "Estimating the cost of a new technology intensive automotive product: A case study approach." International Journal of Production Economics **97**(2): 210-226.

Samson, J. E., et al. (2013). "Revenge of the phages: defeating bacterial defences." Nature Reviews Microbiology **11**(10): 675-687.

Sankaran, S., et al. (2011). "Odorant binding protein based biomimetic sensors for detection of alcohols associated with Salmonella contamination in packaged beef." Biosensors and Bioelectronics **26**(7): 3103-3109.

Sayad, A. A., et al. (2016). "A microfluidic lab-on-a-disc integrated loop mediated isothermal amplification for foodborne pathogen detection." Sensors and Actuators B: Chemical **227**: 600-609.

Schmelcher, M. and M. J. Loessner (2014). "Application of bacteriophages for detection of foodborne pathogens." Bacteriophage **4**(1).

Scognamiglio, V., et al. (2014). "Biosensing technology for sustainable food safety." TrAC Trends in Analytical Chemistry **62**: 1-10.

Scognamiglio, V., et al. (2010). "Biosensors for effective environmental and agrifood protection and commercialization: from research to market." Microchimica Acta **170**(3-4): 215-225.

Sefah, K., et al. (2010). "Development of DNA aptamers using Cell-SELEX." Nature Protocols **5**(6): 1169-1185.

Shabani, A., et al. (2008). "Bacteriophage-Modified Microarrays for the Direct Impedimetric Detection of Bacteria." Analytical Chemistry **80**(24): 9475-9482.

Shahrbabak, S. S., et al. (2013). "Isolation, characterization and complete genome sequence of PhaxI: a phage of Escherichia coli O157: H7." Microbiology **159**(8): 1629-1638.

Shapiro, O. H., et al. (2009). "Bacteriophage predation regulates microbial abundance and diversity in a full-scale bioreactor treating industrial wastewater." The ISME journal **4**: 327.

Shaughnessy, A. F. (2012). "Monoclonal antibodies: magic bullets with a hefty price tag." BMJ: British Medical Journal (Online) **345**.

Shehab, E. M. and H. S. Abdalla (2001). "Manufacturing cost modelling for concurrent product development." Robotics and Computer-Integrated Manufacturing **17**(4): 341-353.

Shen, Z.-Q., et al. (2011). "QCM immunosensor detection of Escherichia coli O157: H7 based on beacon immunomagnetic nanoparticles and catalytic growth of colloidal gold." Biosensors and Bioelectronics **26**(7): 3376-3381.

Shrivastava, A. and V. Gupta (2011). "Methods for the determination of limit of detection and limit of quantitation of the analytical methods." Chronicles of Young Scientists **2**(1): 21-21.

Shrivastava, S., et al. (2018). "Culture-free, highly sensitive, quantitative detection of bacteria from minimally processed samples using fluorescence imaging by smartphone." Biosensors and Bioelectronics **109**: 90-97.

Sigma-Aldrich (2018). "Singlepath® E.coli O157." from <https://www.sigmaaldrich.com/catalog/product/mm/104141?lang=en®ion=US>

Sigma-Aldrich (2018). "VIP Gold EHEC." Retrieved March, 2018, from <https://www.sigmaaldrich.com/catalog/search?term=VIP%C2%AE+Gold-EHEC&interface=All&N=0&mode=match%20partialmax&lang=en®ion=US&focus=product>.

Singh, A., et al. (2012). "Bacteriophage based probes for pathogen detection." Analyst **137**(15): 3405-3421.

Singh, A., et al. (2009). "Immobilization of bacteriophages on gold surfaces for the specific capture of pathogens." Biosensors and Bioelectronics **24**(12): 3645-3651.

Singh, A., et al. (2013). "Recent advances in bacteriophage based biosensors for food-borne pathogen detection." Sensors **13**(2): 1763-1786.

Smartt, A. and S. Ripp (2011). "Bacteriophage reporter technology for sensing and detecting microbial targets." Analytical and Bioanalytical Chemistry **400**(4): 991-1007.

- Smith, J. L., et al. (2014). Shiga toxin-producing Escherichia coli. Advances in applied microbiology, Elsevier. **86**: 145-197.
- Souza, G. R., et al. (2008). "Bottom-Up Assembly of Hydrogels from Bacteriophage and Au Nanoparticles: The Effect of Cis- and Trans-Acting Factors." PLoS ONE **3**(5): e2242.
- Stromberg, Z. R., et al. (2016). "Prevalence and Level of Enterohemorrhagic Escherichia coli in Culled Dairy Cows at Harvest." Journal of Food Protection **79**(3): 421-431.
- Stroot, J. M., et al. (2012). "Capture antibody targeted fluorescence in situ hybridization (CAT-FISH): Dual labeling allows for increased specificity in complex samples." Journal of Microbiological Methods **88**(2): 275-284.
- Su, L., et al. (2011). "Microbial biosensors: a review." Biosensors and Bioelectronics **26**(5): 1788-1799.
- Sun, W., et al. (2000). "Use of bioluminescent Salmonella for assessing the efficiency of constructed phage-based biosorbent." Journal of Industrial Microbiology and Biotechnology **25**(5): 273-275.
- Swift, K. G., et al. (2003). Process Selection : from design to manufacture. Oxford, UNITED KINGDOM, Elsevier Science.
- Tangkuaram, T., et al. (2007). "Design and development of a highly stable hydrogen peroxide biosensor on screen printed carbon electrode based on horseradish peroxidase bound with gold nanoparticles in the matrix of chitosan." Biosensors & Bioelectronics **22**(9-10): 2071-2078.
- Tanji, Y., et al. (2004). "Toward rational control of Escherichia coli O157: H7 by a phage cocktail." Applied Microbiology and Biotechnology **64**(2): 270-274.
- Tillman, G. E., et al. (2012). "Isolation of Shiga Toxin-Producing Escherichia coli Serogroups O26, O45, O103, O111, O121, and O145 from Ground Beef Using Modified Rainbow Agar and Post-Immunomagnetic Separation Acid Treatment[dagger]." Journal of Food Protection **75**(9): 1548-1554.
- Tlili, C., et al. (2013). "Bacteria screening, viability, and confirmation assays using bacteriophage-impedimetric/loop-mediated isothermal amplification dual-response biosensors." Analytical Chemistry **85**(10): 4893-4901.

Tolba, M., et al. (2012). "A bacteriophage endolysin-based electrochemical impedance biosensor for the rapid detection of *Listeria* cells." *Analyst* **137**(24): 5749-5756.

Trachtman, H., et al. (2012). "Renal and neurological involvement in typical Shiga toxin-associated HUS." *Nature Reviews Nephrology* **8**(11): 658-669.

Trilling, A. K., et al. (2014). "Orientation of llama antibodies strongly increases sensitivity of biosensors." *Biosensors and Bioelectronics* **60**(0): 130-136.

Tsai, J.-Z., et al. (2016). "Screen-printed carbon electrode-based electrochemical immunosensor for rapid detection of microalbuminuria." *Biosensors and Bioelectronics* **77**(Supplement C): 1175-1182.

Valadez, A. M., et al. (2009). "Evanescent wave fiber optic biosensor for *Salmonella* detection in food." *Sensors* **9**(7): 5810-5824.

Vallières, E., et al. (2013). "Comparison of Three Different Methods for Detection of Shiga Toxin-Producing *Escherichia coli* in a Tertiary Pediatric Care Center." *Journal of Clinical Microbiology* **51**(2): 481-486.

Vanegas, D. C., et al. (2017). "Emerging Biorecognition and Transduction Schemes for Rapid Detection of Pathogenic Bacteria in Food." *Comprehensive Reviews in Food Science and Food Safety* **16**(6): 1188-1205.

Velusamy, V., et al. (2010). "An overview of foodborne pathogen detection: In the perspective of biosensors." *Biotechnology Advances* **28**(2): 232-254.

Wang, D., et al. (2017). "Efficient separation and quantitative detection of *Listeria monocytogenes* based on screen-printed interdigitated electrode, urease and magnetic nanoparticles." *Food Control* **73**: 555-561.

Wang, J., et al. (2015). "Feces of feedlot cattle contain a diversity of bacteriophages that lyse non-O157 Shiga toxin-producing *Escherichia coli*." *Canadian Journal of Microbiology* **61**(7): 467-475.

Wang, P., et al. (2005). "Cell-based biosensors and its application in biomedicine." *Sensors and Actuators B: Chemical* **108**(1): 576-584.

Wang, Z., et al. (2016). "Development of a novel bacteriophage based biomagnetic separation method as an aid for sensitive detection of viable Escherichia coli." Analyst **141**(3): 1009-1016.

Wiedmann, M., et al. (2014). "Assessment criteria and approaches for rapid detection methods to be used in the food industry." Journal of Food Protection **77**(4): 670-690.

Wring, S. A. and J. P. Hart (1992). "Chemically modified, screen-printed carbon electrodes." Analyst **117**(8): 1281-1286.

Yakes, B. J., et al. (2013). "Surface plasmon resonance biosensor for detection of feline calicivirus, a surrogate for norovirus." International Journal of Food Microbiology **162**(2): 152-158.

Yamada, K., et al. (2016). "Rapid detection of multiple foodborne pathogens using a nanoparticle-functionalized multi-junction biosensor." Biosensors & Bioelectronics **77**: 137-143.

Yan, Z., et al. (2006). "Rapid quantitative detection of Yersinia pestis by lateral-flow immunoassay and up-converting phosphor technology-based biosensor." Sensors and Actuators B: Chemical **119**(2): 656-663.

Yang, M., et al. (2013). "Highly specific and cost-efficient detection of Salmonella Paratyphi A combining aptamers with single-walled carbon nanotubes." Sensors **13**(5): 6865-6881.

Yao, J. and K. D. Gillis (2012). "Quantification of noise sources for amperometric measurement of quantal exocytosis using microelectrodes." The Analyst **137**(11): 2674-2681.

Yao, J., et al. (2015). "Two approaches for addressing electrochemical electrode arrays with reduced external connections." Analytical Methods **7**(14): 5760-5766.

Yilmaz, E., et al. (2015). "Whole cell imprinting based Escherichia coli sensors: A study for SPR and QCM." Sensors and Actuators B: Chemical **209**: 714-721.

Yoo, J. H., et al. (2014). "Microfluidic based biosensing for Escherichia coli detection by embedding antimicrobial peptide-labeled beads." Sensors and Actuators B-Chemical **191**: 211-218.

Yoon, J.-Y. and B. Kim (2012). "Lab-on-a-chip pathogen sensors for food safety." Sensors **12**(8): 10713-10741.

Yu, X., et al. (2018). "Whole-bacterium SELEX of DNA aptamers for rapid detection of E.coli O157:H7 using a QCM sensor." Journal of Biotechnology **266**: 39-49.

Zeinhom, M. M. A., et al. (2018). "A portable smart-phone device for rapid and sensitive detection of E. coli O157:H7 in Yoghurt and Egg." Biosensors and Bioelectronics **99**: 479-485.

Zhang, L. Y., et al. (2007). "Investigation of the electrochemical and electrocatalytic behavior of positively charged gold nanoparticle and L-cysteine film on an Au electrode." analytica chimica acta **596**(1): 99-105.

Zhao, L., et al. (2012). "Tuning the size of gold nanoparticles in the citrate reduction by chloride ions." Nanoscale **4**(16): 5071-5076.

Zhao, Y., et al. (2016). "Rapid multiplex detection of 10 foodborne pathogens with an up-converting phosphor technology-based 10-channel lateral flow assay." Scientific reports **6**: 21342.

Zhou, Y., et al. (2017). "Charge-Directed Immobilization of Bacteriophage on Nanostructured Electrode for Whole-Cell Electrochemical Biosensors." Analytical Chemistry **89**(11): 5735-5742.

Zourob, M. and S. Ripp (2010). Bacteriophage-based biosensors. Recognition receptors in biosensors, Springer: 415-448.

**APPENDIX: OPTIMIZATION, COST CALCULATION AND ANALYSIS OF
THE BACTERIOPHAGE-BASED BIOSENSOR**

Figure 6. Multiplicity of infection (MOI) of STEC representative strains determined by spectrophotometric data.
Bacteriophage A = O26:H2 TB285, Bacteriophage B = O45:H2 SJ7-1, Bacteriophage C = O45:H2 SJ7-2, Bacteriophage D = O45:H2 05-6545.

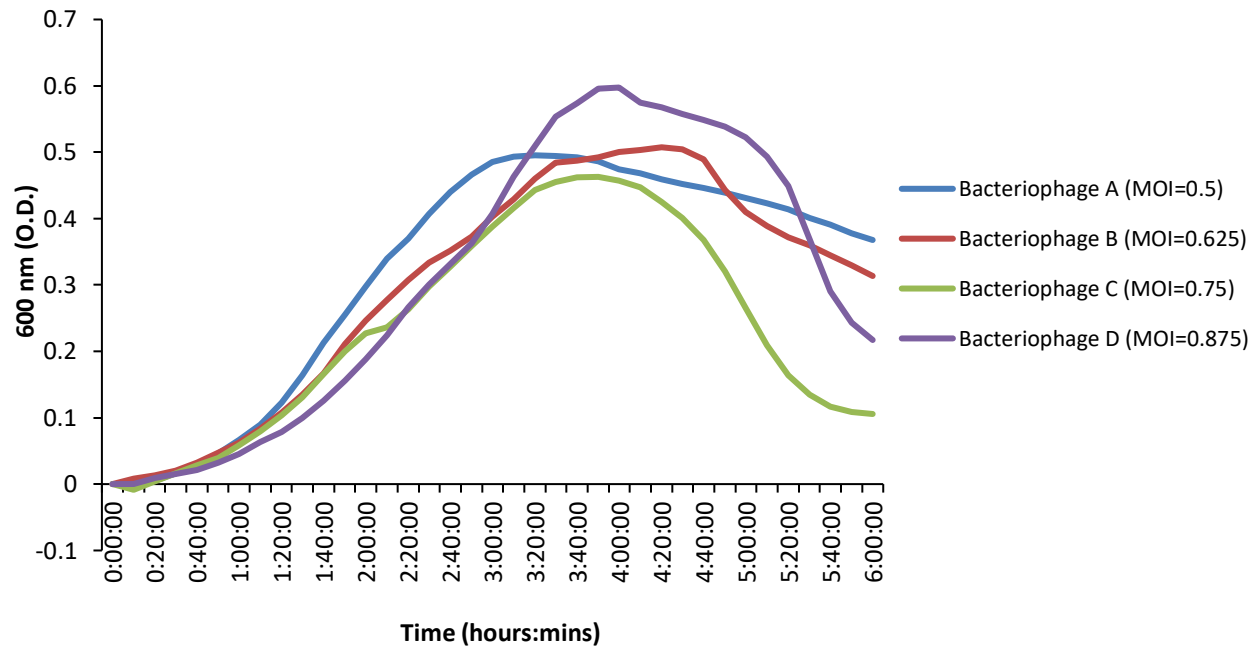


Figure 7. Gel electrophoresis from conventional PCR of STEC bacteriophage DNA targeting *stx1* and *stx2*. One bacteriophage isolate specific to STEC O26 (#11) was positive for *stx1*. The rest of representative isolates were *stx* genes negative. Individual samples were labeled 1,2,3..., L=ladder, N=*S.Typhimurium* (negative control), P=STEC O157:H7 (positive control)

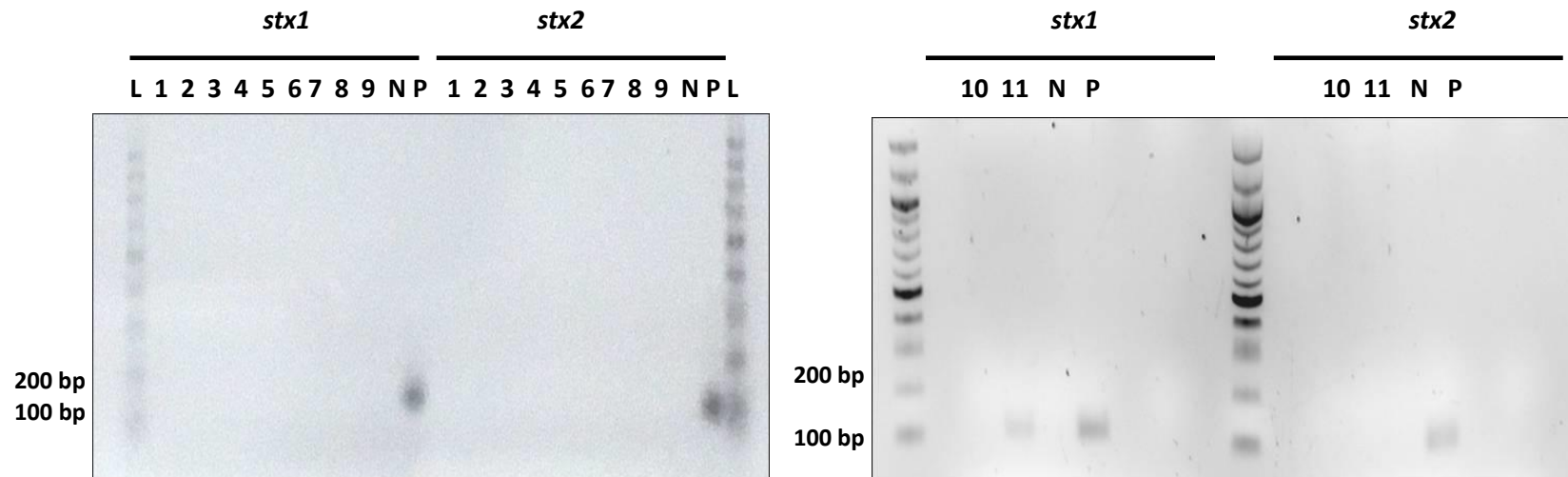


Figure 8.1. Amperometric test of STEC O26 and blocking reagent optimization using Protein-free Blocking Reagent and TBS-T20 washing buffer.

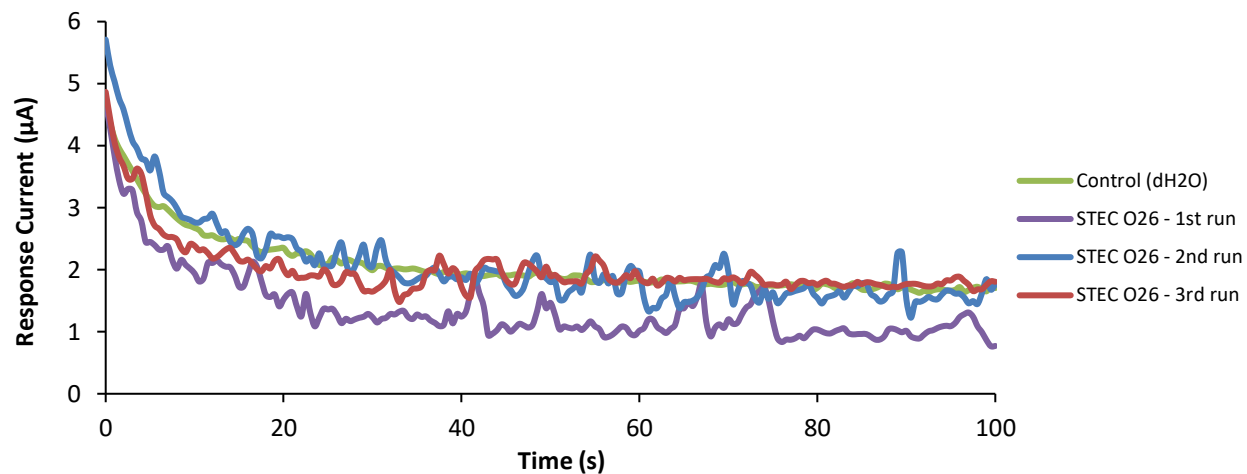


Figure 8.2. Response current (RC) of STEC O26 with Protein-free Blocking Reagent and TBS-T20 washing buffer.

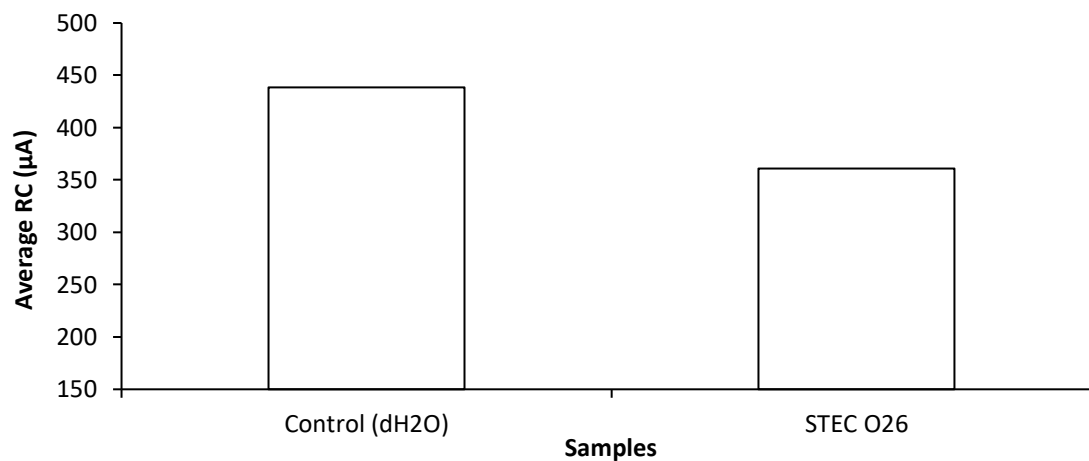


Figure 9.1. Amperometric test of STEC O26 and blocking reagent optimization using 10% BSA and TBS-T20 washing buffer.

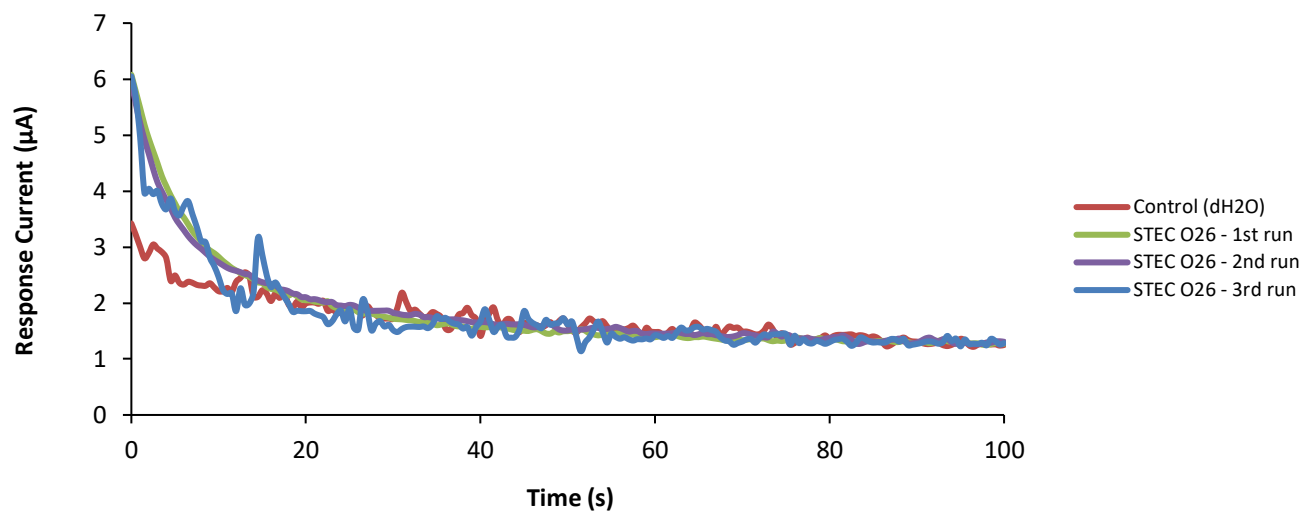


Figure 9.2. Response current of STEC O26 with 10% BSA and TBS-T20 washing buffer.

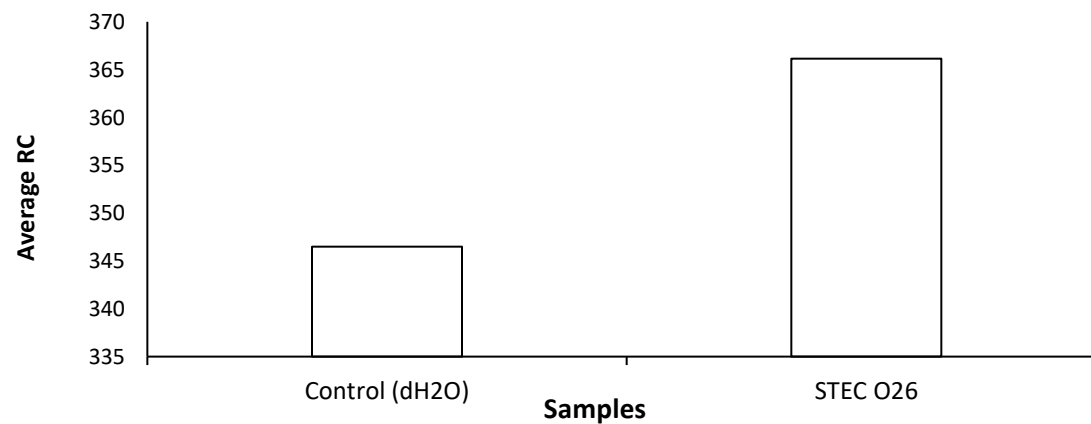


Figure 10.1. Amperometric test of STEC O26 and blocking reagent optimization using PEG (Polyethylene glycol) and TBS-T20 washing buffer.

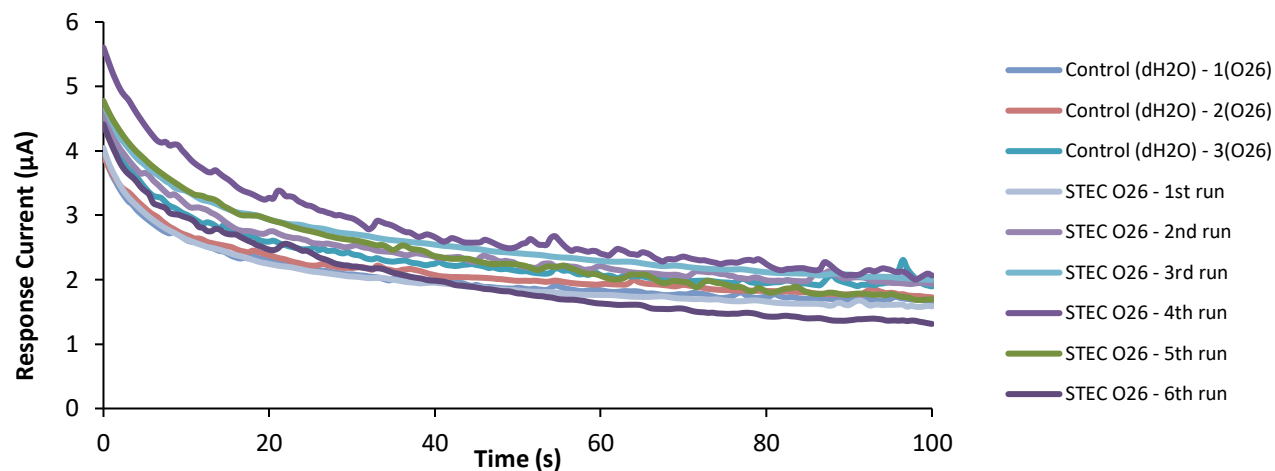


Figure 10.2. Response current of STEC O26 with PEG (Polyethylene glycol) and TBS-T20 washing buffer.

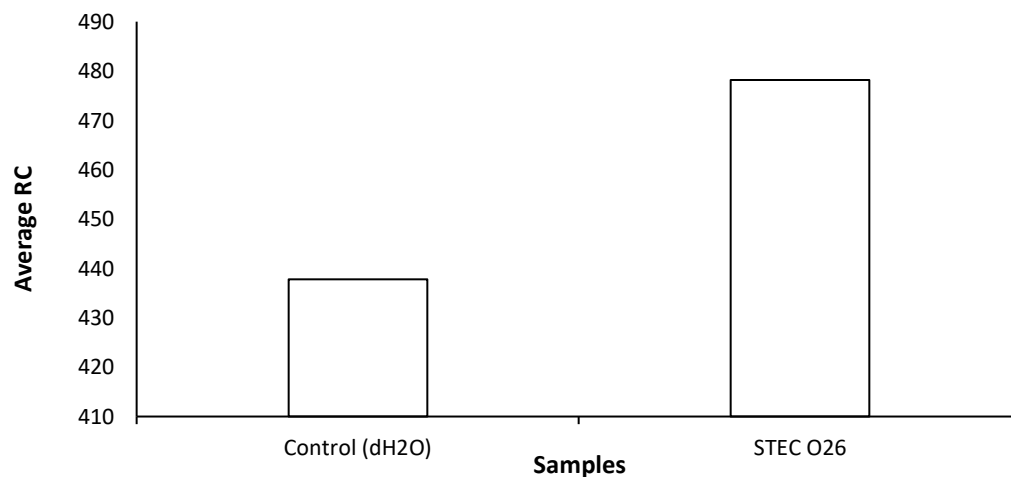


Figure 11.1. Amperometric test of STEC O26 and blocking reagent optimization using 30% Casein and TBS-T20 washing buffer.

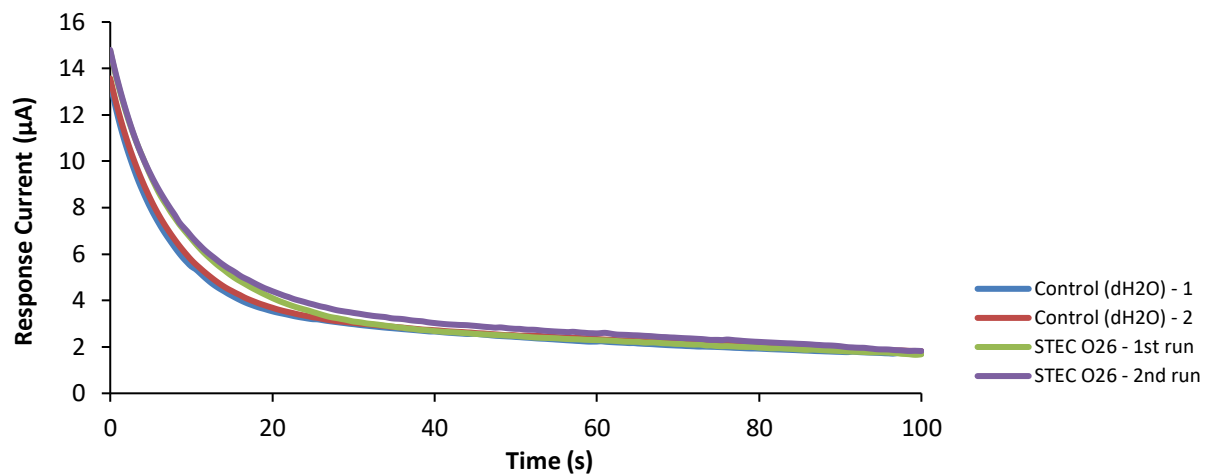


Figure 11.2. Response current of STEC O26 with 30% Casein and TBS-T20 washing buffer.

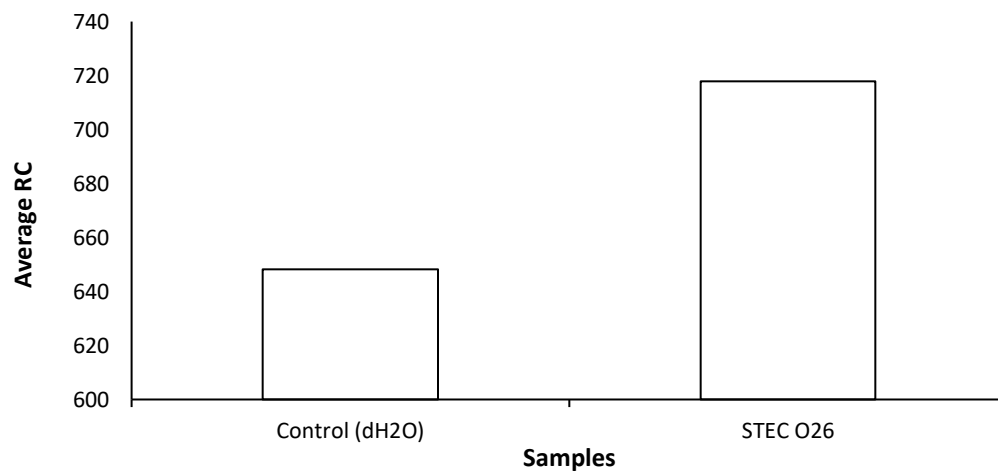


Figure 12.1. Amperometric test of STEC O179 and blocking reagent optimization using 30% Casein and TBS-T20 washing buffer.

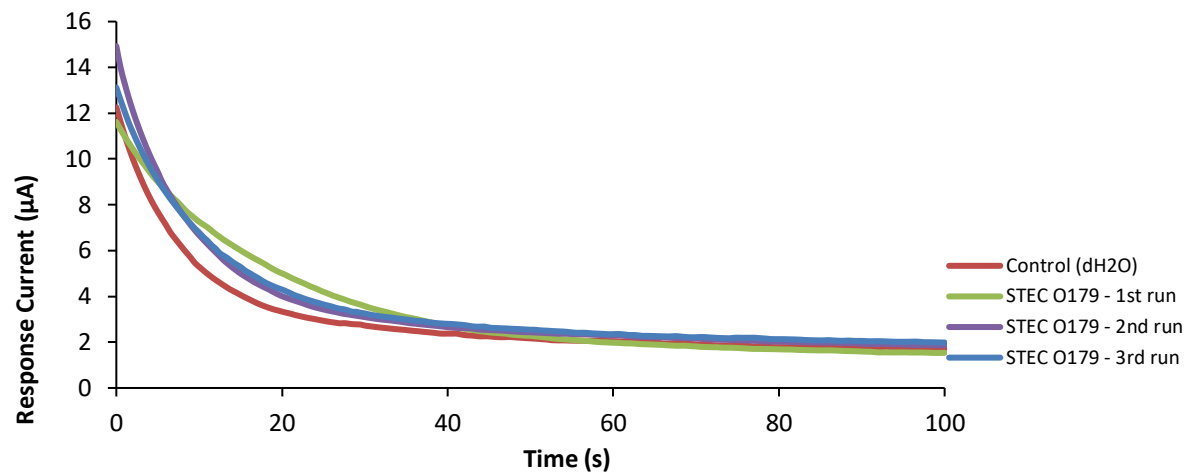


Figure 12.2. Response current of STEC O179 with 30% Casein and TBS-T20 washing buffer.

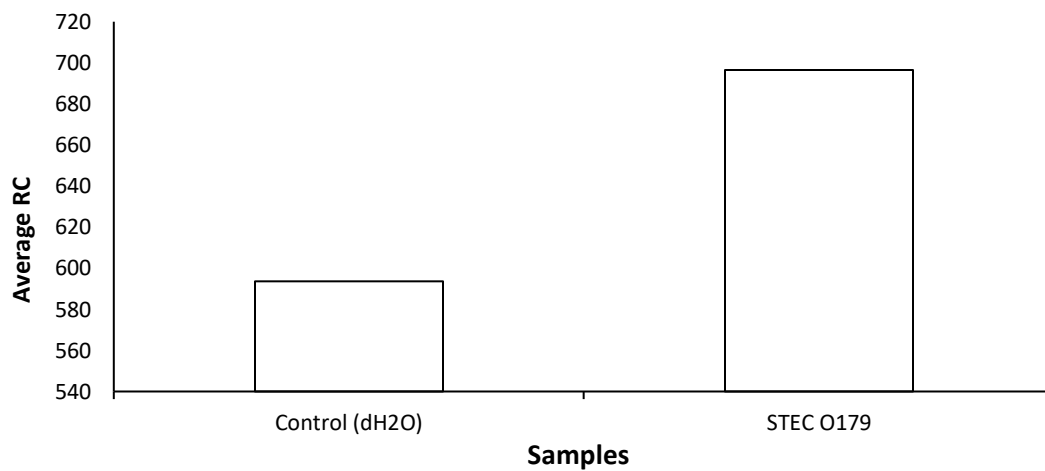


Table 7.1. Calculation for estimating Material Cost (C_{mt}) (all values are in USD₂₀₁₈).

Item		Volume	Material density	Unit price	C_{mt}	Current Price	Cost/item
SPCE	Metro-Ohm	1875	1	2.8	5250	\$210/75 pc	2.8
Palmsens device	PalmSens	1	1	5000	5000	\$5,000	
Android Phone	Amazon	1	1	150	150	\$150	
Reagents							
CMD-Dextran	Sigma Aldrich	25	1	5.05	126.25	\$252.50/50 g	5.05
EDC-NHS	Thermo-Fisher	75	1	13.04	978	\$326/25 g	13.04
Streptavidin	Thermo-Fisher	50	1	3.68	184	\$184/50 mg	3.68
Biotin	Thermo-Fisher	30	1	30	900	\$343	34.3
Streptavidin-HRP	Thermo-Fisher	4	1	398	1592	\$199/0.5ml	398
Hydrogen peroxide (30%)	Thermo-Fisher	30	1	0.35472	10.6416	\$177.36/500ml	0.35472
Others							
Miscellaneous	Lab suppliers				1500	\$100	
Total Material Cost (C_{mt})					15690.8916		

Table 7.2. Calculation for estimating Total Process Cost (P_c) (all values are in USD₂₀₁₈).

Process Cost (P_c)	Costing
Lc (per annum)	$20 \times 1920 = 38400$
Time consumed	$1920 / 960 = 0.5$
Tooling cost	$5250 + 900 + (100/1875) = 6150$
	$38400 \times 0.5 + 6150/1875$
Total P_c	\$ 25350.06

Table 7.3. Calculation for estimating Manufacturing Cost (M_t) (all values are in USD₂₀₁₈).

Manufacturing Cost	Total Manufacturing Cost (\$)
Process Cost (P _c)	25350.06
Material Cost (M _t)	15690.89
Total	\$41040.95

Table 7.4. Calculation for Estimating the Cost of functionalized-screen printed carbon electrode (SPCE) (all values are in USD₂₀₁₈).

Costing of functionalized-screen printed carbon electrode (SPCE)	Cost
Tooling cost	6150
Number of SPCE produced	1875
Cost/functionalized SPCE (\$)	3.28

BIOGRAPHY OF THE AUTHOR

Irwin Adame Quintela was born and raised in Batangas, Philippines. He attended the University of the Philippines Los Banos where he obtained his Biology (Microbiology) degree in 2003. In June 2012, he started his MS studies at the School of Food and Agriculture, The University of Maine. Since then, he has been involved with biosensor development for the detection of significant foodborne pathogens using gold nanoparticles at the Pathogenic Microbiology Laboratory. While doing his MS degree, he presented in both oral and poster sessions and competitions at the Institute of Food Technologists in Chicago and New Orleans, USA. He also gave a talk in San Diego, California for the Produce Marketing Association (PMA) Nanotechnology Symposium and had poster and oral presentation at Institute of Food Technologists (IFT) conferences.

He is a candidate for the Doctor of Philosophy degree in Food and Nutrition Sciences from The University of Maine in May 2018.